

ISTANBUL TECHNICAL UNIVERSITY ★ GRADUATE SCHOOL OF
SCIENCE ENGINEERING AND TECHNOLOGY

**COMPARATIVE EVALUATION OF RAMP CONTROL METHODS: A CASE
STUDY ON D-100 FREEWAY, ISTANBUL**



M.Sc. THESIS

ISMAIL M. A. ABUAMER

Department of Civil Engineering
Transportation Engineering Programme

JUNE 2017

ISTANBUL TECHNICAL UNIVERSITY ★ GRADUATE SCHOOL OF
SCIENCE ENGINEERING AND TECHNOLOGY

**COMPARATIVE EVALUATION OF RAMP CONTROL METHODS: A CASE
STUDY ON D-100 FREEWAY, ISTANBUL**

M.Sc. THESIS

**ISMAIL M. A. ABUAMER
(501141428)**

**Department of Civil Engineering
Transportation Engineering Programme**

Thesis Advisor: Prof. Dr. Hilmi Berk ÇELİKOĞLU

JUNE 2017

İSTANBUL TEKNİK ÜNİVERSİTESİ ★ FEN BİLİMLERİ ENSTİTÜSÜ

**OTOYOL KATILIM DENETİM YÖNTEMLERİNİN BAŞARIMININ
SINANMASI: D-100 OTOYOLU, İSTANBUL ÖRNEĞİ**

YÜKSEK LİSANS TEZİ

ISMAIL M. A. ABUAMER

İnşaat Mühendisliği Anabilim Dalı

Ulaştırma Mühendisliği Programı

Tez Danışmanı: Prof. Dr. Hilmi Berk ÇELİKOĞLU

HAZİRAN 2017

ISMAIL M. A. ABUAMER, a **M.Sc.** student of ITU **Graduate School of Science Engineering And Technology** student ID 501141428, successfully defended the thesis entitled “**COMPARATIVE EVALUATION OF RAMP CONTROL METHODS: A CASE STUDY ON D-100 FREEWAY, ISTANBUL**”, which he prepared after fulfilling the requirements specified in the associated legislations, before the jury whose signatures are below.

Thesis Advisor : **Prof. Dr. Hilmi Berk ÇELİKOĞLU**
İstanbul Technical University

Jury Members : **Prof. Dr. Abdullah Hilmi LAV**
İstanbul Technical University
Prof.Dr. Serhan TANYEL
Dokuz Eylül University

Date of Submission : 05 May 2017
Date of Defense : 08 June 2017





Dedicated to my family,



FOREWORD

Foremost, I would like to express my sincere gratefulness to my advisor Prof. Hilmi Berk Çelikoğlu for the continuous support of my M.Sc. study and research, for his precious guidance, patience, enthusiasm, motivation, immense knowledge, and “being a brother more than a teacher” throughout the completion of this study. Furthermore, my study experience with him enriched my knowledge to the point of becoming unforgettable stage in my life.

Besides my advisor, I would like to thank my colleagues Mehmet Ali SILGU and Mohd Sadat for their support and every advice they gave. I admit that they are really trust worthy partners, the days we have passed together will not be forgotten.

All my gritudes to the PTV GROUP Traffic Customer Service for providing us by a student version of VISSIM 7.00 which was an essential need for my research.

Last but not least, all my love and gritudes to my family, my mother, my father, and my brothers and sisters for their unutterable support and being patient waiting me to come back again to my country Palestine. Absolutely, neither this thesis nor my education would have been possible without their encouragements and "sacrifices".

JUNE 2017

ISMAIL M. A. ABUAMER
(Civil Engineer)

TABLE OF CONTENTS

	<u>Page</u>
FOREWORD	ix
TABLE OF CONTENTS	xi
ABBREVIATIONS	xv
LIST OF TABLES	xvii
LIST OF FIGURES	xix
SUMMARY	xxi
ÖZET	xxiii
1. INTRODUCTION	1
1.1 Motivation of Research	1
1.2 Research Objective	2
1.3 Organization of Thesis	2
2. FUNDAMENTALS OF FREEWAY TRAFFIC FLOW	5
2.1 Freeway Traffic Flow Variables	5
2.1.1 Flow rate	6
2.1.2 Time headway and space headway	6
2.1.3 Speed	6
2.1.4 Density and continuity equation	9
2.1.5 Time occupancy ratio	10
2.1.6 Traffic flow fundamental diagrams	11
2.2 Traffic Data Collection Methods	12
2.2.1 Measurement at a point	12
2.2.2 Measurements over a short section	13
2.2.3 Measurement along a length of road	13
2.2.4 Moving observer method	13
2.2.5 ITS wide-area measurements	14
2.3 Traffic Flow Modelling Approaches	14
2.3.1 Macroscopic approach	15
2.3.1.1 Greenshields models	16
2.3.1.2 Greenberg models	17
2.3.2 Microscopic approach	18
2.3.3 Mesoscopic approach	21
2.3.4 Limitations of simulation models	22
2.4 Freeway Traffic Management Strategies	23
2.4.1 Ramp metering	24
2.4.2 Variable speed limits	25
2.4.3 Route guidance	26
2.5 Summary	27
3. RELATED RESEARCH	29
3.1 Control Systems	30
3.1.1 Open-loop controller	31
3.1.2 Closed-loop controller	31

3.2 Ramp Demands	32
3.3 Ramp Metering Operation Modes	33
3.3.1 Pre-set mode	33
3.3.2 Adaptive mode	33
3.3.3 Predictive mode	34
3.4 Local Ramp Metering.....	34
3.4.1 Demand-capacity	34
3.4.2 Occupancy control	36
3.4.3 Zone.....	36
3.4.4 ALINEA	37
3.4.5 Extensions of ALINEA	38
3.4.5.1 PI-AINEA	38
3.4.5.2 MALINEA	39
3.4.5.3 FL-ALINEA.....	39
3.4.5.4 UP-ALINEA	40
3.4.5.5 UF-ALINEA	41
3.4.5.6 X-ALINEA/Q.....	41
3.4.6 AD-ALINEA	41
3.4.7 Model predictive control	43
3.5 Coordinated (Area-Wide) Ramp Metering.....	44
3.5.1 Optimal control approach.....	44
3.5.1.1 Static optimal control	44
3.5.1.2 Sequential optimal control	45
3.5.1.3 Dynamic optimal control	45
3.5.2 Feedback control approach.....	45
3.5.3 Heuristic approach	46
3.5.4 Hierarchical control approach.....	46
3.5.5 Cooperative algorithms	46
3.5.5.1 Helper	47
3.5.5.2 MILOS.....	47
3.5.5.3 Linked-ramp.....	48
3.5.6 Competitive algorithms	49
3.5.6.1 FLOW	49
3.5.6.2 Compass.....	51
3.5.6.3 SWARM	51
3.5.7 Integral algorithms	53
3.5.7.1 METALINE	53
3.5.7.2 Linear programming	54
3.5.7.3 Coordinated ramp metering using artificial neural networks	54
3.5.7.4 Fuzzy logic.....	55
3.5.7.5 Dynamic ramp metering	56
3.5.7.6 HERO	56
3.6 Evaluation Studies.....	57
3.6.1 Field operational evaluation	57
3.6.2 Simulation based evaluation	58
4. PROBLEM STATEMENT AND PROPOSED CONTROL STRATEGIES .61	
4.1 ALINEA	63
4.2 Parameters Calibration	63
4.3 PI-ALINEA	65
5. STUDY SITE AND DATA DESCRIPTION 67	

5.1 Congestion Periods	67
5.2 Data Description	68
6. MODELING AND SIMULATION	71
6.1 Software Description	71
6.1.1 Driving behavior model	72
6.1.2 Lane changing rules	73
6.2 Modeling and Calibration	74
6.2.1 Section modeling	75
6.2.2 System parameters	77
6.2.2.1 Vehicle inputs and compositions	77
6.2.2.2 Vehicle routes and relative flows	78
6.2.3 Operational parameters	79
6.2.4 Calibration trails and validation	80
6.3 Intervention via COM interface	84
6.3.1 The object model of VISSIM	84
6.3.2 Commands and methods	85
6.4 Experiment Set-Up	86
6.4.1 Downstream detector location	87
6.4.2 Downstream critical occupancy	89
6.5 Measures of Effectiveness	90
6.6 Simulation and Analysis	90
7. CONCLUSIONS	105
7.1 Findings	105
7.2 Further Research Directions	107
REFERENCES	109
CURRICULUM VITAE	119



ABBREVIATIONS

ACCEZZ	: Adaptive and Coordinated Control of Entrance Ramps with Fuzzy Logic
ADOT	: Arizona Department of Transportation
ALINEA	: Asservissement Lineaire d'Entrée Autoroutiere
ANN	: Artificial Neural Networks
CC0	: Standstill Distance
CC1	: Time Headway
CC2	: Following Variation
CCTV	: closed-circuit television
COF	: Centralized Optimization Framework
COM	: Component Object Model
DC	: Demand-Capacity
DOF	: Distributed Optimization Framework
DR	: Discharge Rate
DTM	: Dynamic Traffic Management
KFE	: Kalman Filter Estimation
LCMs	: Lane Changing Maneuvers
LMR	: Local Metering Rate
LQ	: linear quadratic
MBR	: Bottleneck Metering Rate
MILOS	: Multi-Objective, Integral, Large-Scale, Optimized System
MnDOT	: Minnesota Department of Transportation
MOE	: Measure of Effectiveness
MPC	: Model Predictive Control
OC	: Occupancy Control
O-D	: Origin-Destination
PI-ALINEA	: Proportional-Integral ALINEA
RTMS	: Remote Traffic Microwave Sensors
SD	: Standard Deviation
SG	: Slow-and-Go
SWARM	: System Wide Adaptive Ramp Metering
TTS	: Total Time Spent
TTT	: Total Travel Time
TWT	: Total Waiting Time at the Ramps
V/C	: Volume-Capacity Ratios
VMS	: Variable Message Signs
VMT	: Vehicle Miles Traveled



LIST OF TABLES

	<u>Page</u>
Table 5.1: Descriptive measures (summary-1).....	70
Table 5.2: Descriptive measures (summary-2).....	70
Table 5.3: Descriptive measures (summary-3).....	70
Table 6.1: Links modeling summary.	75
Table 6.2: GEH Statistic Measures (detector 301-main).	82
Table 6.3: GEH Statistic Measures (detector 533-main).	82
Table 6.4: GEH Statistic Measures (detector 534-main).	83
Table 6.5: Downstream Detectors Locations.	87
Table 6.6: Evaluation results (merge area-1).	91
Table 6.7: Evaluation results (merge area-2).	91
Table 6.8: Evaluation results (merge area-3).	92
Table 6.9: TTS reduction summary.	101
Table 6.10: Vehicles' emissions summary (merge area-1).	101
Table 6.11: Vehicles' emissions summary (merge area-2).	101
Table 6.12: Vehicles' emissions summary (merge area-3).	101
Table 6.13: Evaluation results (PI-ALINEA).	104



LIST OF FIGURES

	<u>Page</u>
Figure 2.1: Time-Space diagram of an individual vehicle.....	7
Figure 2.2: A simple derivation of the continuity equation.	9
Figure 2.3: Effective length detection zone scheme.....	10
Figure 2.4: Traffic flow fundamental diagrams.	11
Figure 2.5: Vehicular trajectories diagram (Silgu, 2015).	12
Figure 2.6: Follower-leader theory assumption (Garber and Hoel, 2014).....	18
Figure 2.7: Lane-changing models classification.	20
Figure 2.8: Ramp metering strategy presentation (Traffic Detector Handbook, 2006).	24
Figure 3.1: Plant representation.....	30
Figure 3.2: Open-loop/feedforward control system.....	31
Figure 3.3: Closed-loop feedback control system.	32
Figure 3.4: Demand-capacity ramp metering strategy presentation.	35
Figure 3.5: A presentation of ALINEA algorithm.	37
Figure 3.6: MILOS control architecture (Ciarallo and Mirchandani, 2002).....	48
Figure 3.7: SWARM forecast operation (Bogenberger and May, 1999).....	52
Figure 3.8: ANN based ramp control flow chart (Bogenberger and May, 1999).....	54
Figure 3.9: Conceptual operation of ANN (Bogenberger and May, 1999).	55
Figure 4.1: Problem formulation.	61
Figure 4.2: Problem formulation.	61
Figure 4.3: ALINEA controller layout.....	65
Figure 5.1: Section Sketch.	67
Figure 5.2: Congestion Observation.	68
Figure 5.3: Speed time-series profile for detector No. 301.....	68
Figure 5.4: Speed time-series profile for detector No. 533.....	69
Figure 5.5: Speed time-series profile for detector No. 534.....	69
Figure 6.1: Car following model (PTV AG, 2015).	72
Figure 6.2: Calibration methodology flow chart.	74
Figure 6.3: Section's links sketch.....	76
Figure 6.4: Section model part-1.....	76
Figure 6.5: Section model part-2.....	76
Figure 6.6: Section model part-3.....	77
Figure 6.7: Speed time-series profile.....	78
Figure 6.8: Volume time-series profile.....	78
Figure 6.9: Vehicle route choice phases.	79
Figure 6.10: Desired speed distribution (70:70 km/h).....	80
Figure 6.11: Speed time-series profiles for model validation (301-main).....	83
Figure 6.12: Speed time-series profiles for model validation (533-main).....	84
Figure 6.13: Speed time-series profiles for model validation (534-main).....	84
Figure 6.14: COM-VISSIM model object hierarchy (source: PTV AG, 2015).....	85
Figure 6.15: INet object properties.....	85

Figure 6.16: MATLAB-COM code for signal controller program.	86
Figure 6.17: a, b, and c occupancy time-series profile.	88
Figure 6.18: Time occupancy ratio vs volume.	89
Figure 6.19: a, b, and c Time-series speed profiles at downstream of merge area-1.	94
Figure 6.20: Time-series speed profiles, a and b at merge-2, and c at merge-3.	95
Figure 6.21: a, b, and c time-series speed profiles, at merge 1,2, and 3 respectively.	97
Figure 6.22: a, b, and c the occupancy 3D surface plot along the merge area-1.	98
Figure 6.23: a, b, and c the occupancy 3D surface plot along the merge area-2.	99
Figure 6.24: a, b, and c the occupancy 3D surface plot along the merge area-3. ...	100
Figure 6.25: Acceleration rates image plots in case of using ALINEA at merge-1.	102
Figure 6.26: Acceleration rates image plots in case of using PI-ALINEA at merge-1.	103



COMPARATIVE EVALUATION OF RAMP CONTROL METHODS: A CASE STUDY ON D-110 FREEWAY, ISTANBUL

SUMMARY

Freeway networks are designed to provide a flexible flow of vehicles and uninterrupted routes especially in the metropolitan areas where the traffic volumes are considerably high. However; when the traffic volumes reach the highway capacity, speed differentials occur leading to phenomenon of congestion which either can be recurrent in peak hours or nonrecurrent in case of having an incident on the highway. Congestions are considered a case of matter as the freeway network performance is adversely affected in terms of reducing the speed, increasing the travel time, and increasing the vehicle emissions due to increase the fuel consumption. Also the distraction during congestion period, can increase the probability of accidents occurrence, where all drivers try to pass the congested segment of the freeway. Different solutions were considered for solving or reducing the effect of congestion on freeways. The structural solutions for example by adding additional lanes in order to increase the system capacity are sufficient up to a certain time, later the congestion starts to form again. The reason is that the traffic volume in another word the demand is driven by increasing the capacity, rather than other environmental and economic considerations that do not allow to increase the system capacity. Thus, since 1960s the trend have been changed to control the link traffic and optimize its capacity by using coordinated and integrated surveillance and control strategies. Several control approaches and strategies are introduced including ramp metering, variable speed limits, and route guidance systems. For the recent decades ramp metering strategies are noticed to be an effective approach for controlling and managing the freeway traffic with the forms of local ramp metering such as ALINEA, PI-ALINEA, and Model Predictive Control, and coordinated ramp metering such as FLOW, HERO, and SWARM. In this thesis the feedback control based algorithms ALINEA and PI-ALINEA are evaluated by utilizing them under different scenarios on a section of the D-100 freeway, Istanbul. The evaluation process considers different measures of effectiveness such as the travel time reduction, speed increase, volume increase, and occupancy reduction. The algorithms are applied in a microscopic environment using VISSIM integrated with MATLAB via COM interface. The microscopic model is calibrated using a real data provided by the municipality of Istanbul and the control algorithm is conducted online through MATLAB via COM interface. According to the considered measures of effectiveness such as the increase in the speed, the occupancy reduction, and the improvement in the acceleration rates, PI-ALINEA outperformed ALINEA which agrees with the literature.



OTOYOL KATILIM DENETİM YÖNTEMLERİNİN BAŞARIMININ SINANMASI: D-100 OTOYOLU, İSTANBUL ÖRNEĞİ

ÖZET

Trafik taleplerinin doğru olarak tahmin edilmesi, herhangi bir otoyolun kapasitesinin belirlenmesinde belirleyici faktördür. Genellikle trafik talepleri otoyolun tasarım dönemi temel alınarak belirlenir. Ancak teknolojik gelişmeler, taşıt fiyatlarının düşmesi, arazi kullanımının artması, yeni cazibe merkezlerinin oluşması gibi durumlar taşıt sahipliğini artırır ve tasarım döneminde elde edilen değer ile gerçek talebin uyumsuzluğunu ortaya çıkarır. Özellikle sabah ve akşam zirve saatlerinde talebin kapasiteye yaklaşması ve ulaşması, tıkanıklık adı verilen bir fenomene sebep olur.

Tıkanıklık, trafik akımı içerisinde bulunan taşıtların, taşıt yoğunluğundan hareket edememeleri olarak adlandırılabilir. Tıkanıklık, gün boyunca zirve saatlerde yinelenen tipte veya yoldaki anlık olaylara bağlı olarak gerçekleşen ve yinelenmeyen tipte olabilir. Tıkanıklık ile otoyol ağ performansı arasında zıt bir ilişki vardır. Tıkanıklık olduğu durumda taşıt hızları azalır, yolculuk süresi artar. Bununla birlikte azalan taşıt hızları daha fazla yakıt tüketimine ve daha fazla emisyon ortaya çıkmasına neden olur. Tıkanıklık süresince ortaya çıkan dikkat dağınıklığı da trafik kazası gerçekleşme olasılığını da arttırmaktadır.

Tıkanıklığın önüne geçmek için yeni yollar ve ek şeritleri yapılması gibi yapısal çözümlerinin faydasız ve pahalı olduğu 1960'lı yıllardan beri bilinmektedir. Yeni yollar yapmak yerine kapasitenin etkin kullanımı “ talep yönetimi “ kavramının ortaya çıkmasına sebep olmuş ve 1960'lı yıllardan günümüze talep yönetimini destekleyici çalışmaların yapılmasına da ön ayak olmuştur.

Bu çalışma kapsamında, İstanbul D100 otoyolunun Zincirlikuyu- Okmeydanı arasında yer alan 3,96 km'lik bir kesimi ele alınmış, ilgili kesimde farklı otoyol katılım denetim yöntemleri uygulanarak toplam yolculuk süresinin azaltılması, taşıt hızlarının artırılması, emisyonların azaltılması amaçlanmış ve uygulanan denetim yöntemleri karşılaştırılmıştır.

Tez kapsamında birinci bölümde tezin amacından ve tezin katkılarından bahsedilmiştir.

İkinci bölümde trafik akımının temel ve türetilmiş değişkenleri ile bu değişkenlerin birbirleriyle olan ilişkileri tanımlanmıştır. Trafik verisi toplama yöntemleri, trafik akımı modelleme yaklaşımları, ince-boyut, orta-boyut ve kaba-boyut trafik akım modelleri, benzetim modellerinin kısıtları ve otoyol trafik yönetim stratejilerinden de yine ikinci bölüm içerisinde bahsedilmiştir.

Üçüncü bölümde denetim sistemlerinden, açık- çevrimli ileri beslemeli ve kapalı-çevrim geri beslemeli denetim sistemleri tanıtılmıştır. Ek olarak, otoyol katılım denetimi yöntemi ayrıntılı olarak ele alınmış ve bu kapsamda geliştirilen algoritmalar tanıtılmıştır. Katılım denetimi yersel ve eşgüdümlü katılım denetimi olarak sınıflandırılmış ve yersel katılım denetimi algoritmaları altında ALINEA, PI-ALINEA, MALINEA, FL-ALINEA, UP- ALINEA, UF- ALINEA, X-ALINEA/Q hakkında bilgiler verilmiştir.

Eşgüdümlü katılım denetimi alt başlığında ise en uygun (optimal) denetim yaklaşımı, geri-beslemeli denetim yaklaşımı, sezgisel denetim yaklaşımı, hiyerarşik denetim yaklaşımı ile Helper, MILOS, Linked-Ramp, Flow, Compass, SWARM, METALINE, HERO gibi algoritmalar hakkında bilgiler verilmiştir.

Dördüncü bölümde ise çalışma kapsamında kullanılan ALINEA ve PI- ALINEA algoritmalarının ince boyut benzetim yazılımına MATLAB [MATrix LABoratory] yazılımı kullanılarak entegre edilmesi irdelenmiş ve bir örneği sunulmuştur. Bununla birlikte dördüncü bölümde algoritmalarda yer alan parametrelerin kalibrasyonu irdelenmiş ve en uygun parametre seçiminden bahsedilmiştir.

Beşinci bölümde çalışma alanı ve benzetim yazılımına girdi olarak verilen veriye ait bilgiler verilmiştir. Çalışma alanı 3,96 km uzunluğunda, 3 otoyol katılım, 2 de otoyol ayrılma bölgesine sahiptir. Çalışmada kullanılan veriler, İstanbul Büyükşehir Belediyesi Trafik Müdürlüğü tarafından sağlanmış ve 2 dakikalık aralıklara toplulaştırılmış, 5 saatlik hız, taşıt sayısı ve işgal değerlerinden oluşmaktadır. Bu bölümde kullanılan veriye ait tanımlayıcı istatistiklere de yer verilmiştir.

Altıncı bölüm tez çalışmasının temelini oluşturmaktadır. Bu bölümde, ALINEA ve PI-ALINEA algoritmalarının farklı senaryolar altında ince- boyut benzetim yazılımı yardımıyla D100 otoyolu kesimlerinde verdiği sonuçlar incelenmiştir. Sonuçlar

sadece akım, hız ve işgal açısından değil, toplam yolculuk süresindeki azalma, taşıt emisyonları ve hızlanma ivmeleri açısından da irdelenmiştir.

Yedinci bölümde çalışmanın sonuçları ve gelecekte yapılması öngörülen çalışmalara ait öneriler sunulmuştur.



1. INTRODUCTION

Freeways are designed to provide a flexible movement of vehicles by providing uninterrupted flow. According to the Highway capacity manual (HCM): the freeways are “divided highway with full control of access and two or more lanes of the exclusive use of traffic in each direction, providing uninterrupted flow”. Opposing directions of the flow are continuously separated by a raised barrier, and at-grade median, or a continuous raised median. Vehicles access to and egress from the freeway using ramps, on-ramp for entering the freeway and off-ramp for leaving the freeway. However; the congestion problems came up to disturb the proposed task of freeways. Previously, structural solutions for example by adding more lanes to the highway were a traditional trend, yet these solutions were permanent as soon as congestion starts developing again. Accordingly, in order to prevent the traffic flow from breaking down on a highway, the necessity of traffic management systems has been raised. This chapter outlines the following: motivation of research, thesis contribution, and the structure of the whole work.

1.1 Motivation of Research

The proper estimation of the traffic demand is the ruling factor in determining the capacity of any highway. Typically, the estimated traffic demands are considered to cover the highway design period. Nevertheless; since traffic demand is driven, the unexpected changes in the land use; for example, new residential, industrial or business areas, will significantly increase the car ownership. At peak periods the demand reaches the capacity, speed differentials with a high density will produce flow disturbances which eventually lead to the phenomenon of congestion. In simple words, we can define *congestion* as a blocking in the flow stream path due to a high vehicles concentration on the road. There are two types of congestion, the first one is *recurrent congestion* which appears in peak hour during the day, and the second one is *nonrecurrent* congestion which is related to incidents on the freeway. This blocking decreases the speed of vehicles leading to increasing the travel time causing

delays. Furthermore; the increase of travel time consequently means the increase of fuel consumption and vehicle emissions to the atmosphere that have many adverse effects on the environment and our health. Also, the distraction during a congested segment can increase the probability of accident occurrence, where all drivers try to pass the congested segment of the freeway. Any incident's impact on a freeway network can be assessed by the cost dis-benefits resulted because of this incident. That means incidents that occur in the network including congestion's consequences cost the operator of the network significant amount of money every year. For instance, the structural solutions for relieving or avoiding congestions on freeways, for example by adding additional lanes, have become inefficient since the traffic demand is driven by increasing the capacity, rather than other environmental and economic considerations. For this reason, the trend has been moved to the freeway traffic management as an effective solution for congestion using coordinated and integrated surveillance and control strategies.

1.2 Research Objective

Istanbul/Turkey is considered one of the most worldwide metropolitan areas with huge transportation networks and different transport modes. Nevertheless, the city networks still suffering from severe congestions especially in the peak periods, meanwhile structural solutions are not applicable. The main contribution of this research is a comparative micro-simulation based evaluation study between different local ramp metering strategies considering various Measures of Effectiveness (MOEs) parameters. The control strategies are utilized on one of the most congested segments of D-100 freeway in Istanbul using the microscopic simulation software VISSIM integrated with MATLAB through the Component Object Model (COM).

1.3 Organization of Thesis

The rest of this research is organized as follows; chapter 2 briefly discusses the traffic flow elements in order to understand the nature of traffic flow and congestion formation, and a general review of freeway traffic management strategies. Chapter 3 provides an extended overview of ramp control strategies including a wide literature review for the most recent practical and simulation based reactive ramp metering evaluation studies. Chapter 4 is concerned with a brief description of the proposed

control strategies and problem formulation. Chapter 5 describes in details the chosen section for deploying the proposed control strategies and the used data. Chapter 6 is the core chapter of this research, it discusses the simulation environment, the implementation technique, the model calibration process, and MOEs which are considered for the evaluation process. Also, the simulation results and a comparative analysis is provided by this chapter. Finally, Chapter 7 presents the conclusion of this research and further research directions.





2. FUNDAMENTALS OF FREEWAY TRAFFIC FLOW

Freeway traffic flow modeling and control relies on understanding the fundamentals of traffic flow. When traffic flow fundamentals are mentioned, the first thing that comes to our minds is the basic traffic flow stream variables: speed, density, and flow. These variables are very important for giving indications and assessment about any traffic flow stream. However; there is still a need to understand how this stream acts, how the flow oscillations propagate, why the stream characteristics in the initial time are not the same after some time period, how we can propose a traffic flow model that reflects the real corresponding values. Seeking answers to all these questions, in this chapter, the primary variables of the traffic flow theory are explained briefly including the interrelationships among them and the flow fundamental diagrams. Ending up with introducing the principles of traffic modeling approaches: macroscopic, microscopic, and mesoscopic simulation models, and explaining some other flow variables are related to each of them.

2.1 Freeway Traffic Flow Variables

The traffic flow variables and the mathematical relationships between them, in other words, traffic flow theories are very important in designing and evaluating the effectiveness of traffic management and control strategies. Also, they are the base for understanding and analyzing the traffic stream characteristics since the traffic flow is not uniform over time. These elements or variables are the scientific indicators to assess and evaluate a traffic stream and tell if there is a congestion or not. Another important application of traffic flow theories is the simulation; where mathematical relationships are used to study the complex interrelationships that exist among the elements of a traffic stream or network and to estimate the effects of traffic flow changes on some parameters such as link capacity, crashes, travel time, air pollution, and fuel consumption.

2.1.1 Flow rate

The traffic flow rate (q) is the equivalent hourly rate at which vehicles passing a cross section of a highway over a unit time interval less than one hour. Normally the time interval defers according to the method used for counting the vehicles. However; as a final output, the flow rate is obtained for one hour time period (equivalent hourly rate), see the following relationship:

$$q(\text{veh}/h) = \frac{N \times 3600}{T} \quad (2.1)$$

Where N and T denote respectively the number of vehicles passing the cross section within a time period and the unit time period in seconds.

2.1.2 Time headway and space headway

The time headway (h) is the time in seconds required by two successive vehicles' front bumper to reach a specific point on the highway. The space headway (d) is the distance in meters between the front bumpers of two successive vehicles. Since the elapsed time (time interval) between the first and the last counted vehicle equals to the sum of all vehicles time headways, equation (2.1) can be rewritten to get the flow rate:

$$q = \frac{N \times 3600}{\sum_i h_i} = \frac{N/N \times 3600}{\sum_i h_i/N} \rightarrow q(\text{veh}/h) = \frac{3600}{\bar{h}} \quad (2.2)$$

Same procedure for space headway,

$$q(\text{veh}/h) = \frac{\bar{u} \cdot 3600}{\bar{d}} \quad (2.3)$$

Where h_i , \bar{h} , \bar{d} , and \bar{u} denote respectively time headway of the i th vehicle, average time headway, average headway, and average speed.

2.1.3 Speed

The term speed (u) is the traveled distance by a vehicle during a given time period t , it can be expressed in kilometers per hour (km/h), miles per hour (mph), or meters

per second (m/s). It is very important to differentiate between the instantaneous (spot, time) speed (u_t) and the space speed (u_s) of an individual vehicle. Considering the time-space diagram in Figure 2.1, the time speed is the slope of the time space line at given point for example point A where the speed is recorded, this approximately equals to the slope of the tangent at this point. On the other hand, the space speed is the slope of the time space line that connects between the start and end points (A and B) of the traveled distance.

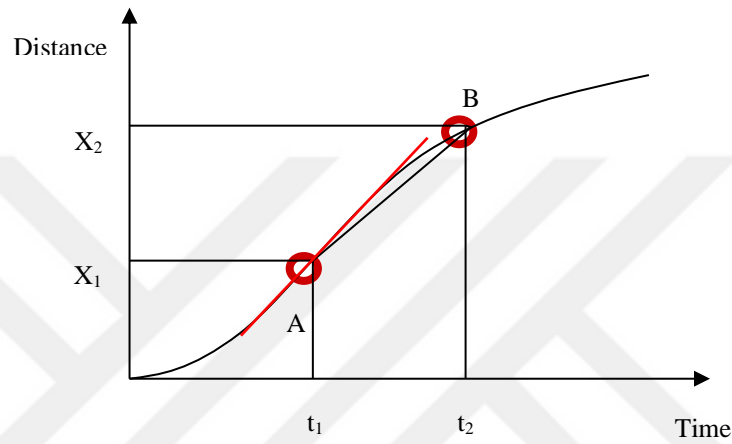


Figure 2.1: Time-Space diagram of an individual vehicle.

So, the previous explanation can be formulated as the following:

$$\text{Space speed } (u_s) = \frac{X_2 - X_1}{t_2 - t_1} \quad (2.4)$$

$$\text{Time speed } (u_t) = \frac{dx}{dt} = \lim_{(t_2-t_1) \rightarrow 0} \frac{X_2 - X_1}{t_2 - t_1} \quad (2.5)$$

Now for all vehicles passing a certain point on a highway during a given time interval: time mean speed is the arithmetic mean of vehicles' speed that passing a certain point on a highway during a given time interval.

$$\text{Time mean speed } (\bar{u}_t) = \frac{1}{N} \sum_{i=1}^N u_i \quad (2.6)$$

Where u_i and N are the speed of the i th vehicle and the number of vehicles passing the point on the highway respectively.

On the other hand, space mean speed is the harmonic mean of vehicles' speed that passing a certain point on a highway during a given time interval. In other words, it is the total distance traveled by vehicles divided by the average total time spent by these vehicles to travel this distance.

$$\text{Space mean speed } (\bar{u}_s) = \frac{D}{\frac{1}{N} \sum_i t_i} \quad (2.7)$$

Where D and t_i denote respectively total distance traveled by vehicles on a highway segment and the time spent by the i th vehicle to travel distance D .

Since,

$$t_i = \frac{D}{u_i} \quad (2.8)$$

If the traveled distance D is constant, then equation (2.7) can be arranged to get:

$$\text{Space mean speed } (\bar{u}_s) = \frac{1}{\frac{1}{N} \sum_i (1/u_i)} \quad (2.9)$$

Where u_i denotes the speed of the i th vehicle.

Wardrop (1952) shows that both speeds differ by the proportion of the variance to the mean of space mean speed:

$$\bar{u}_t = \bar{u}_s + \frac{\sigma_s^2}{\bar{u}_s} \quad (2.10)$$

$$\sigma_s^2 = \frac{\sum k_i (u_i - \bar{u}_s)^2}{k} \quad (2.11)$$

Where σ_s^2 , k_i , and k denote respectively standard deviation of the spot speed, the density of sub-stream i , and the density of the total stream.

2.1.4 Density and continuity equation

The density (k) is the vehicles' concentration measurement over space as it refers to the number of vehicles traveling along a unit length (usually 1 mile or km) of a highway at an instant in time. For example, if a screen shot is taken for a unit length of a highway, the number of vehicles showing in the screen shot presents the density. If only point measurements are available, density can be estimated either by using continuity equation which will be explained in this subsection or the time occupancy ratio that will be explained in the next subsection. For any stable traffic conditions, the continuity equation ($q=k \times u$) relates the three traffic flow variables density, flow, and speed.

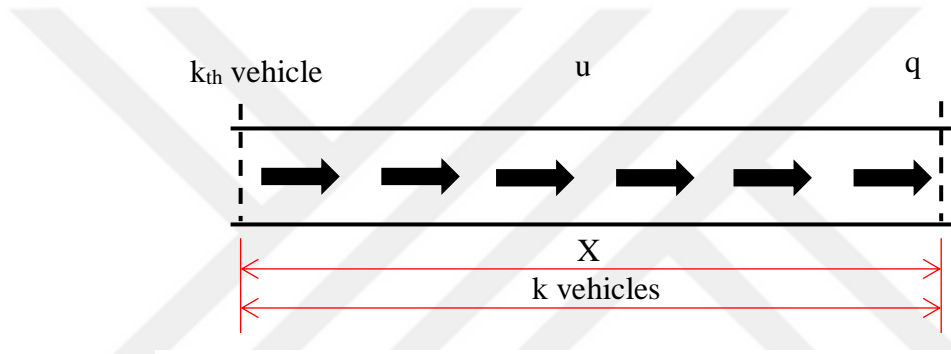


Figure 2.2: A simple derivation of the continuity equation.

By definition, as in Figure 2.2 consider a road segment with length X , the number of vehicles k moving at constant speed u , at the end of this segment q vehicles pass to exist. Under steady state condition, for the time period ($T=X/u$), at $t=0$ the number of vehicles in this segment will be equal to the number of vehicles that will pass the exist during the time interval $[0, T]$. The above statement can be formulated at the following:

$$kX = qT \quad (2.12)$$

Since $u=X/T$, equation (2.12) can be rewritten to get:

$$q = \bar{u}_s \times k \quad (2.13)$$

Intuitively, one can understand why space mean speed is considered in this equation as follows (mathematical proof can be found in (May, 1990)): A detector lies at location x_{det} we reconstruct which vehicles will pass in the time of one aggregation

period. For this, the vehicle must be closer to the detector than the distance it travels in the aggregation time t_{agg} :

$$x_{det} - x_j \leq t_{agg} v_i \quad (2.14)$$

In this formula, x is the position on the road. For faster vehicles, this distance is larger. Therefore, if one takes the local arithmetic mean, one overestimates the influence of the faster vehicles. If the influence of the faster vehicles on speeds is overestimated, the average speed u is overestimated (compared to the space-mean speed u_m).

2.1.5 Time occupancy ratio

Time occupancy ratio or occupancy is the measurement vehicles concentration over time. It is the fraction of the time that a detector is occupied by a vehicle for a specific time interval (T).

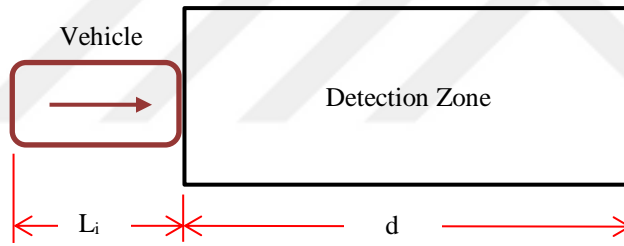


Figure 2.3: Effective length detection zone scheme.

Referring to Figure 2.3 the detector is occupied by the vehicle when the front bumper enters the detection zone until the rear bumper leaves the end of the detection zone. According to Althol (1965), if L_i is the vehicle length, u_i the vehicle speed, and d is the detector length (this length is constant), the occupancy is calculated as the following:

$$\text{Occupancy} = \frac{\sum_i (L_i + d)/u_i}{T} = \frac{1}{T} \sum_i \frac{L_i}{u_i} + \frac{d}{T} \sum_i \frac{1}{u_i} \quad (2.15)$$

Althol simplified the previous equation assuming a uniform vehicle length L ,

$$\text{Occupancy} = (L + d) \times k = C_k \times k \quad (2.16)$$

2.1.6 Traffic flow fundamental diagrams

The fundamental diagrams of traffic flow depicting the traffic stream behavior depending on the macroscopic traffic flow variables: flow, density, and speed. These diagrams are very important in order to determine the flow breakdown point to distinguish between the congested and uncongested regimes. Figure 2.4 a, b, and c depicts a one-dimensional fundamental diagram of the traffic stream, showing the curves of space-mean speed vs density, space-mean speed vs flow, and density vs flow respectively. Starting with Figure 2.4a when there are no vehicles on the highway (density (k) = 0) the mean speed takes its maximum value referred as free-flow speed (u_f). The term free flow speed means that the flow at this point is free to act since there are no vehicles to produce interaction and limit the driver behavior to other vehicles behavior. Now as Figure 2.4b Illustrates, when the flow starts increasing the density also increases and at the same time the speed is reduced.

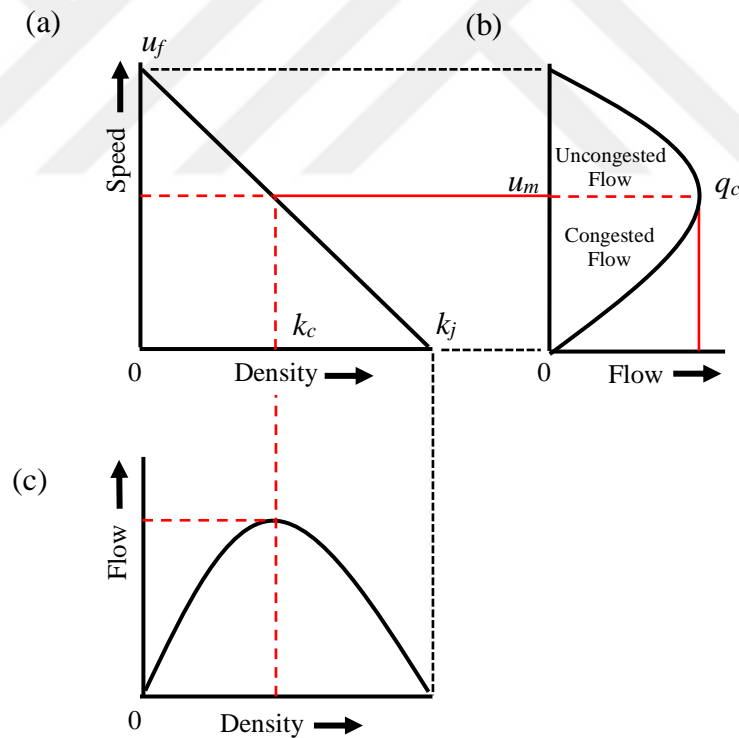


Figure 2.4: Traffic flow fundamental diagrams.

The relationship between the flow and density keeps proportional until it reaches the breakdown point q_c , the corresponding density k_c is the critical density for that highway segment and the optimum speed u_m . After the breakdown point, the

relationship becomes inversely where the flow and speed reach 0 and the density takes its maximum value, jam density k_j . This critical density is the split point between two flow regimes, uncongested and congested flow.

2.2 Traffic Data Collection Methods

The Traffic control strategies and the development of Intelligent Transportation Systems require high-quality real-time traffic information. For several years, under growing pressure for improving traffic management, collecting traffic data methods have been evolving considerably and the access to real-time traffic information is becoming routine worldwide. In this subsection, five different traffic variables measurement approaches are discussed by focusing on the variables that can be measured by each approach.

2.2.1 Measurement at a point

Measurement at a point was the first procedure used for traffic data collection. As shown in Figure 2.5 it presents a horizontal line crosses the vehicular trajectories, the location is constant but the time varies.

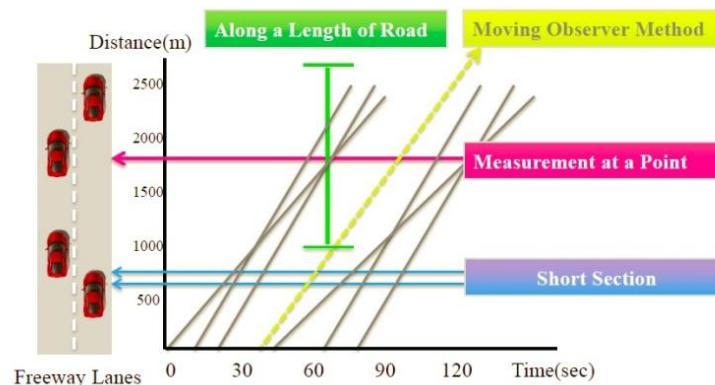


Figure 2.5: Vehicular trajectories diagram (Silgu, 2015).

There are many techniques for making traffic measurement at a point, starting from using pneumatic tubes placed across the roadway to the use of point detectors (May et al., 1963; Athol 1965). The most commonly used point detectors are based on inductive loop technology, but other methods in use include microwave, radar,

photocells, ultrasonics, and television cameras. Volume, headways, and speed are the only traffic flow variables that can be directly measured at a point since density and occupancy require a detection length, they cannot be measured at a point. Speeds can be obtained only by radar or microwave detectors while in the absence of such instruments the second location for observation is required to obtain speed.

2.2.2 Measurements over a short section

Measurements over a short section employ two point measurements, as presented in Figure 2.5 by two parallel horizontal lines spaced by a very short distance (less than 10 m). Most of the currently used point detectors, such as inductive loops or microwave beams are considered a short section measurement since they take up space over the road. These loops give a continuous reading usually at 50 or 60 Hz. Thus, the variable occupancy which was not available from earlier technologies such as pneumatic tubes or manual counts can be obtained. The measurement of occupancy depends on the instrument's detection zone size, so that the measured occupancy, for identical traffic may differ from site to site depending on the nature and construction of the detector.

2.2.3 Measurement along a length of road

This approach bases on measurements captured either from aerial photography or from cameras installed on tall buildings or poles. Referring to Figure 2.5, this approach presents a vertical line at one instant of time, for example, a single snapshot taken from above the road. It is recommended that at least 0.5 km of the road be detected. On the basis of a single frame from such sources, only density can be measured. The single frame gives no sense of time, so neither volumes nor speed can be measured.

2.2.4 Moving observer method

Moving observer method can be presented by one of the vehicle's trajectories as shown in Figure 2.5. There are two approaches to this method, the simple floating car approach where the speeds and travel times are recorded as a function of time and location along the road. There are two forms of this approach, the first one uses a

second person in the car for recording speeds and travel times. The second form uses a modified recording speedometer of the type regularly used in long-distance trucks or buses. The other approach was introduced by Wardrop and Charlesworth (1954) for urban traffic measurements obtains both speed and volume simultaneously. The floating car approach cannot give precise average speed data because of the floating car behavior as same as an average vehicle within the traffic stream. However; this approach is effective for qualitative information about freeway operations without the need for elaborate equipment or procedures.

2.2.5 ITS wide-area measurements

Traditional on-road sensors (e.g. inductive loops) are necessary but not sufficient due to their limited coverage and their high cost. In the last years, we have been witnessing the emergence of alternative data sources. This is, for example, the case for methods based on the vehicle location (Floating Car Data) which are a promising cost-effective solution to cope with some limitations from fixed detectors. The ITS Wide-Area measurements use different technologies for detecting vehicles' speeds, for example, it can use the communication between specially-equipped vehicles and ITS technologies. Other technologies are based on a vehicle identifier, which allows the system to measure the journey time between two locations. A third type is based on receiving speed and location information back from the vehicles regardless of their location.

2.3 Traffic Flow Modelling Approaches

Traffic flow models have become an essential need for understanding and analyzing traffic flow streams. These models must be simple but not simpler with intuitive and easy to calibrate parameters and be able to describe the flow stream by reflecting the real characteristics of this stream under several conditions. Stands to reason, the model has to give realistic corresponding values for all traffic phases starting from free flow phase, stop-and-go traffic ending up with congested traffic flow.

Traffic flow models can be deterministic or stochastic, continuous or discrete, and analytical or simulation. Stochastic and deterministic model address the processes represented by the model, where deterministic models have no random variables

(exact relationships), however stochastic models include probability functions (Jillella and Hobeika, 2001). Continuous models describe how the traffic flow changes state continuously over time by responding to continuous stimuli, whereas discrete models represent real-world systems that are either continuous or discrete by asserting their states change abruptly at points in time.

According to the level of details, traffic flow modeling falls within three general approaches: macroscopic (low fidelity), microscopic (high fidelity), and mesoscopic (mixed fidelity) approach. A simple comparison between the three approaches is that microscopic models describe both system entities and their interactions at a high level of details. On the other hand, macroscopic models describe the system entities, their activities, and their interactions at the low level of details. The macroscopic approach considers flow density relationships, literally, it concerns with macroscopic flow characteristics, where attention is given to temporal, spatial and modal flows”, meanwhile Microscopic approach is concerned with individual time and space headway between vehicles (May, 1990). For mesoscopic models, they represent the system entities at a high level of details but describe their activities and interactions at a much lower level of details. In this section, these approaches are discussed including the most used models and the baseline parameters.

2.3.1 Macroscopic approach

Macroscopic models were introduced by scientists in the 1950's since traffic flow initially appeared to be similar to the fluid flow. The macroscopic modeling approach is based on the continuity equation where it describes the vehicle's dynamic from overall or average perspective at a specific location (x) and time (t) in terms of density and average velocity. Typically, macroscopic models are performed using partial differential equations, nevertheless; modern macroscopic models utilize hyperbolic partial differential equations (May, 1990). The first step in this approach was taken by Lighthill and Whitham (1955), by indexing the comparability of traffic flow on long crowded roads with flood movements in long rivers.

2.3.1.1 Greenshields models

Greenshields (1935) was among the first to investigate the relationship between the speed and density, where he suggested a linear model basing on data derived from an aerial photographic study. Considering constraints posted in Figure 2.4 a, he used the linear regression to propose his model as the following:

$$\bar{u}_s = b + mk \quad (2.17)$$

Where \bar{u}_s , b, m, and k denote respectively, average space mean speed, y-intercept = u_f , the slope = $(\Delta y/\Delta x)$, the corresponding density.

The slope can be found using the two limit points (0, u_f) and (k_j , 0).

$$m = \frac{u_f - 0}{0 - k_j} \rightarrow m = -\frac{u_f}{k_j} \quad (2.18)$$

Substituting b and m values in equation (2.17) we can get Greenshields, model:

$$\bar{u}_s = u_f - \frac{u_f}{k_j} k \quad (2.19)$$

Since $k = q/\bar{u}_s$ from equation (2.19) flow and speed relationship can be derived:

$$\bar{u}_s = u_f - \frac{u_f}{k_j} \times \frac{q}{\bar{u}_s} \rightarrow \bar{u}_s^2 = \bar{u}_s u_f - \frac{u_f}{k_j} q \quad (2.20)$$

Also, for $\bar{u}_s = q/k$ flow and density relationship can be derived:

$$\frac{q}{k} = u_f - \frac{u_f}{k_j} k \rightarrow q = u_f k - \frac{u_f}{k_j} k^2 \quad (2.21)$$

To determine the corresponding speed for maximum flow, by differentiating Equation (2.20) with respect to \bar{u}_s :

$$2\bar{u}_s = u_f - \frac{u_f}{k_j} \frac{dq}{d\bar{u}_s} \rightarrow \frac{dq}{d\bar{u}_s} = k_j - 2\bar{u}_s \frac{k_j}{u_f} \quad (2.22)$$

For maximum flow $\rightarrow dq/d\bar{u}_s=0$,

$$\bar{u}_m = \frac{u_f}{2} \quad (2.23)$$

Same procedure to find the corresponding density for maximum flow, by differentiating equation (2.20) with respect to k :

$$k_c = \frac{k_j}{2} \quad (2.24)$$

Now, the maximum flow equal to:

$$q_c = \frac{k_j u_f}{4} \quad (2.25)$$

Equations (2.19) and (2.20) indicate that if we assume a linear relationship between speed and density, then parabolic relationships will be obtained between flow and density and between flow and speed, thus we can say that Figures 2.4 b and 2.4 c have parabolic relationships.

2.3.1.2 Greenberg models

Greenberg used the analogy of fluid flow to develop a macroscopic model in describing the relationships between traffic flow variables.

$$\bar{u}_s = c \ln \frac{k_j}{k} \quad (2.26)$$

Multiplying each side of equation (2.26) by k , we obtain:

$$\bar{u}_s k = q = c k \ln \frac{k_j}{k} \quad (2.27)$$

Differentiating q with respect to k , we obtain:

$$\frac{dq}{dk} = c \ln \frac{k_j}{k} - c \quad (2.28)$$

For maximum flow $\rightarrow dq/dk=0$, giving:

$$\ln \frac{k_j}{k} = 1 \quad (2.29)$$

Substituting 1 for (k_j/k) in equation (2.26) gives:

$$\bar{u}_m = c \quad (2.30)$$

That evolves, the value of c is the speed of maximum flow.

2.3.2 Microscopic approach

Microscopic traffic models describe traffic behavior at the level of individual vehicles by delineating the positions $x(t)$ and velocities $v(t)$ of all interacting vehicles between themselves and the infrastructure. Typically each vehicle has its differential equations as functions of the position, velocity, and acceleration. The behavior of these models is usually dictated by a lead vehicle thus they are termed “car-following” models. The traffic behavior is described by determining when a vehicle accelerates, decelerates, changes lane, and how vehicles change their routes. Thus, to govern the vehicle’s behavior there are three general models, car-following model, lane-change model, and route choice model. The route choice models describe how drivers choose their routes to reach their destination, and how they react to traffic and route information along the way.

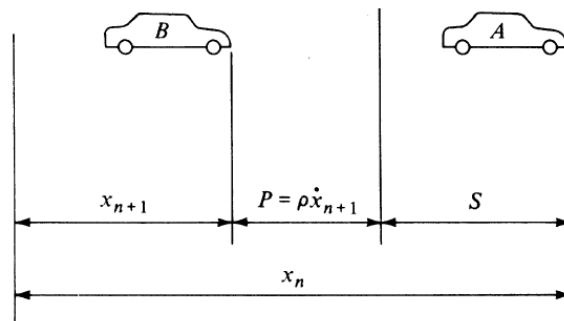


Figure 2.6: Follower-leader theory assumption (Garber and Hoel, 2014).

The car-following models describe the acceleration and deceleration patterns as a response to vehicles interaction as well as other objects such as speed limits, road curvature, etc. Reuschel (1950) and Pipes (1953) were pioneers in the development of car following theories. Three parallel efforts were undertaken in the late 1950s and continued to the mid-1960s. There were a series of the car following theories proposed by (May, 1990). The basic form of these theories was:

$$\text{Response} = f\{\text{sensitivity, Stimuli}\}$$

Where response, sensitivity, and stimuli mean respectively, acceleration or deceleration of the vehicle which is dependent on the sensitivity of the automobile and the driver himself, the ability of the driver to perceive and react to the stimuli, visual and auditory inputs that influence driver's decision.

Considering two executive vehicles A and B on a single-lane as depicted in Figure 2.6, if the leading vehicle is considered to be the n th vehicle and the following vehicle is considered to be the $(n+1)$ th vehicle. At rest condition, the spacing between the two vehicles (front bumper to front bumper) from a fixed section is defined as S , and the follower driver maintains an additional distance P that is proportional to his/her speed ($P = \rho \dot{x}_{n+1}$), the bumper to bumper distance can be obtained in the form (Garber and Hoel, 2014):

$$x_n - x_{n+1} = \rho \dot{x}_{n+1} + S \quad (2.31)$$

Where ρ and \dot{x}_{n+1} denote respectively, the factor of proportionality with units time, and the speed of the $(n+1)$ th vehicle.

The case of there is no lane-changing, follower driver will try to maintain a specific distance between the leader vehicle by accelerating or decelerating as stimulus response to the disturbance. By differentiating equation (2.31) it gives the value of the required acceleration/deceleration:

$$\ddot{x}_{n+1} = \frac{\dot{x}_n - \dot{x}_{n+1}}{\rho} \quad (2.32)$$

The driver response cannot be immediate where there is a delay in response called the stimulus response time referred as T , thus equation (2.32) can be rewritten to give the driver's reaction as:

$$\ddot{x}_{n+1}(t + T) = \lambda [\dot{x}_n(t) - \dot{x}_{n+1}(t)] \quad (2.33)$$

Where T and λ are the response time and sensitivity parameter ($1/\rho$) respectively.

A general expression for λ is given by:

$$\lambda = a \frac{\dot{x}_{n+1}^m(t + T)}{[x_n(t) - x_{n+1}(t)]^l} \quad (2.34)$$

Thus, the basic expression for the microscopic models (Car-Following models) can be written as:

$$\dot{x}_{n+1}(t + T) = a \frac{\dot{x}_{n+1}^m(t + T)}{[x_n(t) - x_{n+1}(t)]^l} [\dot{x}_n(t) - \dot{x}_{n+1}(t)] \quad (2.35)$$

Where a , l , and m are constants.

The lane-changing model simulates the driver behavior when to change lanes based on the driver's preferences and the situation in both the current lane and other lanes (speed of vehicle in front, sufficiently large gap in adjacent lane, etc.) Lane-changing maneuvers play a major role in traffic flow oscillations, where during heavy traffic conditions the oscillations appear as a result of lane-changing rather than car following (Mauch and Cassidy, 2002; Laval and Daganzo, 2006). Frequent lane-changing maneuvers such as merging, diverging, and weaving can create bottleneck points in freeways. As a result of that, the traffic flows breakdown especially in the case of heavy traffic conditions (Hoogendoorn and Bovy, 2001; Daganzo, 2002; Banks et al., 2003; Wall and Hounsell, 2005).

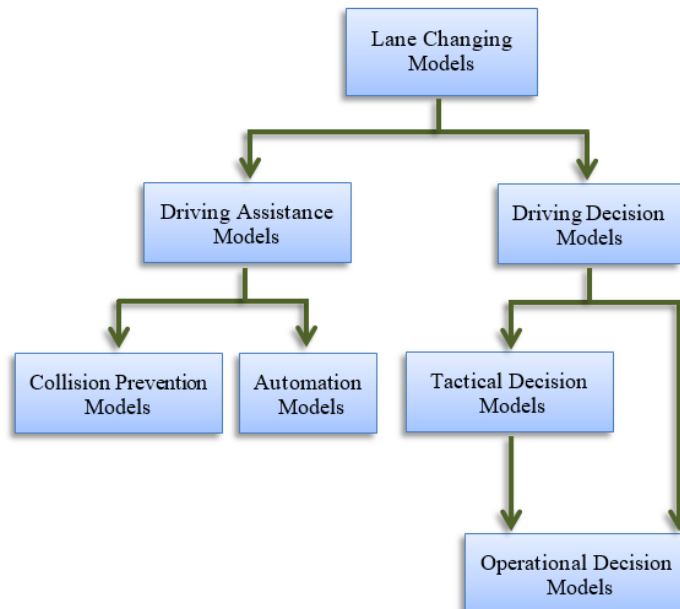


Figure 2.7: Lane-changing models classification.

Lane-changing modeling approaches can be classified as shown in Figure 2.7. Driving assistance models are categorized into collision prevention models or automation models, where both models consider the steering wheel angle and lateral motions for controlling the lane-changing performance of a vehicle. Based on the time required for executing the decision, driving decision models are classified into tactical or operational levels (Sukthankar et al., 1997). At the tactical level, lane-changing maneuvers are performed to achieve short time objectives such as decisions to pass slowly the moving vehicle or maintain the desired speed. At the operational level, drivers decide to perform maneuvers in order to control their vehicles (Alexiadis et al., 2004).

2.3.3 Mesoscopic approach

Mesoscopic approach fills the gap between the aggregate level of macroscopic approach and the individual level of microscopic approach. This approach based on describing traffic entities at a high level of elaborating, yet their behavior and interactions are described at a lower level of details. There are many forms of this approach, for example, vehicles grouped into packets, which are routed through the network e.g. CONTRAM (Leonard, D.R. et al., 1989). A single packet acts as one entity where its speed on each link is derived according to a speed-density function defined for that link. Once the link density is high, the speed-density function assigns low speed values to vehicles in order to regulate the traffic flow on that link. Contrary the function will assign high-speed values to vehicles in case of low density. The lane changing and Car-Following (acceleration/deceleration) are not modeled in this approach. Another form is that individual vehicles are grouped into cells which control their behavior. The cells traverse the link and vehicles can enter and leave the cells when needed, but not overtake them. The speed of the vehicles is determined by the cell, not the individual drivers' decisions (Ben-Akiva, 1996). Jayakrishnan, et al. (1994), Gawron (1998) and Mahut (2001) they used in their models a queue-server approach, where the link is modeled as a queueing and a running part. The level of entities details that the lanes can be modeled individually, vehicles and their speeds are also represented individually, nevertheless; their behavior is not. The vehicles speed to traverse the running part is determined by a macroscopic speed-density function, once vehicles reach the downstream end a queue-server transfers the vehicles to connecting roads. This form of mesoscopic approach combines the advantages of individual vehicle modeling and

the ease of calibration by using macroscopic speed-density relationship. Also, the individual representation of vehicles allows the possibility of disaggregated routechoice modeling.

The capacities at the node servers follow from saturation flows and their variance (measured or calculated). Signal controlled intersections can be modeled by replacing the queue servers with gates that open and close according to the states of the signal control (green/amber/red). Adaptive signal control is harder to model since the positions of the vehicles on the link are not known, and therefore it is difficult to know when they pass detectors connected to the signal control. Another type of mesoscopic model uses cellular automata (there is a paper about that in mini-study), where the link is discretized into cells with two phases either empty or occupied by a vehicle. The vehicles follow a minimalist set of behavior rules, most notably the Nagel- Schreckenberg rules (Nagel and Schreckenberg, 1992), which determine for each time step the number of cells that are traversed by the vehicle (Bush, 2000).

2.3.4 Limitations of simulation models

As a main advantage of macroscopic and mesoscopic models, they are easy to calibrate due to their few and directly measurable parameters, still they are more applicable to cases where the interaction between vehicles is not crucial for obtaining the simulation results. For example, with the purpose of analyzing merging areas (such as on-ramps), it requires an explicit simulation of the vehicle's gap acceptance behavior, besides a precise coding of the geometrical features of the ramp and freeway. Also, macroscopic models do not consider the individual vehicle modelling, in the same time the positions and behavior of the vehicles are approximated in mesoscopic models. Thus, when these vehicle positions are not known, or are imprecise, it is tough to simulate the initiations of detectors that are used in the adaptive control systems. This leads us to improper comparison between results from macroscopic models with the detector data. Microscopic models have proven their value in detecting, analyzing, and understanding a lot of problems related to traffic, still, they are very difficult to calibrate, where their calibration requires a lot of effort and computations.

2.4 Freeway Traffic Management Strategies

Freeway traffic control systems help the network operators to sustain the traffic flow within the capacity to avoid congestion and its consequences. This can be done by controlling the flow stream in the carriageways and the flow entering to the freeway to maintain a smooth flow below the breakdown point. The importance of these control systems has taken a place since adding roads or increasing the number of lanes is limited to many environmental, practical, and economic aspects. Newman et al. (1969), Moscovitz (1973) and Klijnhout (1985) state that, an efficient cost-effective amelioration can be achieved if the control measures are conducted properly on congested traffic. The control system includes a combination of sub-systems: traffic monitoring sub-system (surveillance tools) and lane traffic control sign sub-system. The criteria of traffic control system involve three main functions:

- I. Information collection: In order to control a network we need real time measurements of the flow variables (speed, the rate of flow, density), or a full image of the traffic flow state so that the traffic control center response with the appropriate action. Can be done using roadside equipment, (Vehicle detectors such as inductive loops, image detector, closed-circuit television (CCTV) cameras, traffic control center, GPS,)
- II. Action or response derivation: Information evaluation and processing in the traffic control center, then applying appropriate action. The applied action related to the type of incident on the freeway.
- III. Information dissemination: or implementation of control actions, provided by the traffic control center using (Ramp metering light, lane control sign, speed limit sign, message sign, guidance sign, etc.).

As mentioned before the freeway traffic control methods are spread between lane control, variable speed limits, driver guidance system and ramp metering. The most effective and investigated strategies for freeway traffic management are:

- I. Metering traffic entering the freeway using on-ramp metering. Various on-ramp metering strategies such as ALINEA, FLOW, METALINE, demand-capacity strategy and occupancy strategy.
- II. Using surveillance and control systems, such as inductive loop detectors and overhead mounted lane control signs along the length of the freeway, can

detect the near capacity flows and present advisory speed information along the freeway (variable speed limits).

III. Route guidance.

Papageorgiou (1983) classifies the control measures into two classes:

- I. Control measures affecting density: Congestion can be avoided if density is maintained below the critical value. This can be accomplished by metering the on-ramps' traffic and/or diverting the traffic upstream of the merging area.
- II. Control measures affecting the fundamental diagram: Variable message signs such as speed limit signs, "keep your lane" signs etc., are known to increase the capacity in the fundamental diagram, if applied appropriately.

2.4.1 Ramp metering

Ramp meters are traffic signals placed on freeway entrance ramps or freeway connectors to control the flow of vehicles entering the freeway or moving from one freeway to another. They are designed to improve the average speed of all vehicles traveling on a freeway mainline by decreasing congestion that can result when too many cars enter at certain points. The concept behind ramp metering is simple: by using a signal at on-ramps it can regulate the rate at which vehicles enter the freeway, see Figure 2.8. Vehicles entering at short intervals are less likely to slow down existing mainline traffic and can merge onto the freeway with less potential for accidents. Otherwise, they will experience bottlenecks generated by non-metered on-ramps.

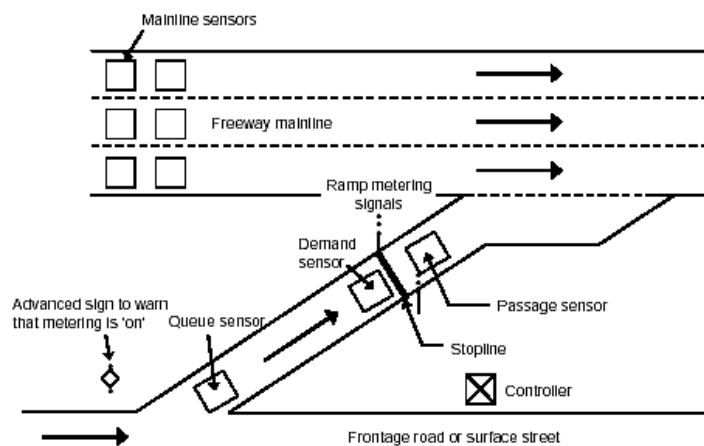


Figure 2.8: Ramp metering strategy presentation (Traffic Detector Handbook, 2006).

Generally, we can identify three ramp control algorithms that can be used for calculating the metering rates, fixed time (pre-set) algorithm, responsive (reactive) algorithm, and proactive strategies. Wattleworth (1965) firstly suggested fixed time ramp metering algorithms, where the metering rates are derived off-line basing on a historical traffic conditions data. However; the absence of real-time measurements, the flow can be disturbed in case of non-recurrent incidents. On the other hand, responsive ramp metering algorithms derive the metering rates online basing on a real time measurements of the traffic variables (Papamichail and Papageorgiou, 2008). Proactive ramp metering strategies work as a whole system to specify optimal traffic conditions for a whole freeway or a network based on demand and model predictions of the traffic over a time horizon. Using the hierarchical control structure reactive and proactive strategies can combine to predict the optimal traffic conditions and using it a set value for the controller respectively. Reactive ramp metering strategies with respect to the implemented section can be classified to local and coordinated (system wide adaptive) ramp metering. Local ramp metering strategies are suitable for a single ramp by taking into account traffic conditions with a vicinity of this ramp to compute the metering rates. However, coordinated ramp metering strategies determine the metering rates basing on the traffic conditions for a more extended section of the network (Chu et al., 2009). Local ramp metering strategies are easy to implement, less cost and more adequate when the ramp generally has no impact on or from other ramps along the route. As the contribution of this research is an evaluation case study of different ramp metering strategies, chapter 3 will explain briefly the most investigated and well-known ramp control algorithms within research-related literature review.

2.4.2 Variable speed limits

Variable speed limits regulate the mainstream traffic flow by assigning different speed limits in the purpose of relieving shockwaves, improving the traffic safety, or considering environmental aspects. The working principle of speed limit systems can be categorized based on their intended effects: improving safety, improving traffic flow, or their environmental effects, such as reducing noise or air pollution. Considering traffic flow improvement, dynamic speed limits follows two approaches, the first one is instigating the homogenization effect, while the second approach is

more focused on avoiding traffic breakdown by tumbling the flow by means of speed limits.

The homogenization approach bases on the idea that speed limits reduce the speed differences to achieve a more stable flow. This approach assumes speed limits that are above the critical speed (i.e. the speed that corresponds to the maximum flow). Thus, the speed limits do not limit the traffic flow, yet they only slightly reduce the average, as well as the density, is slightly increased. In theory, this approach can increase the time to break down slightly (Smulders, 1990), but it cannot suppress or resolve shock waves. An extended overview of speed limit systems that aim at reducing speed differentials is given by (Wilkie, 1997).

The traffic breakdown prevention approach concentrates more on avoiding high densities, where it considers speed limits that are lower than the critical speed in terms of limiting the incoming flow to these areas. In contrary with the homogenization approach, higher flow is achieved by resolving bottlenecks (Hegyi et al., 2005). Presently, speed limit systems mainly are used to increase traffic safety by lowering the speed limits in potentially dangerous situations especially upstream of on-ramps or during adverse weather conditions (National Research Council 1998; Sisiopiku and Virginia, 2001; Wilkie, 1997). Lenz et al. (2001) used a pseudo-anticipative scheme in the form of shifting between speed limits based on the neighboring downstream section density.

2.4.3 Route guidance

Route guidance systems help the drivers to choose their routes when other routes exist to their destination. The systems typically display traffic information such as the length of congested segments, the delays on the alternative routes, or the travel time to the next destination on the alternative routes. Route guidance has two approaches; system optimum and user equilibrium (or user optimum). In the system optimum approach is based on minimizing the costs of all drivers (the travel time), on the other hand; the user equilibrium approach considers individual drivers where a driver may select another route that has a shorter individual travel time. The user equilibrium system is triggered when on each utilized route the cost (travel time) are equal and on the not utilized routes when the cost is higher than the one on the utilized routes. The objective variable in the cost function is the travel time which

either can be the predicted travel time or the instantaneous travel time. The predicted travel time considers the time that the driver will spend on the route based on their experience, however; the instantaneous travel time is estimated based on the current speed of the driver on the route. The instantaneous travel time is dynamically changed according to the instantaneous speed of the vehicle, thus it may be different than the predicted travel time.

2.5 Summary

Freeways congestion problems are still the big challenge that engineers are researchers trying to find suitable and environment friendly solutions for them. In the past, congestion problem is used to be solved by increasing the capacity of the road system, however, it has been noticed that the system capacity is only one factor of many factors that lead to congestion formation. The changes in land use, individual income, social aspects, .etc. all of them are affecting the rate of car ownership increase, thus increasing the road system capacity is not enough, also it can make it worse. Accordingly, in the early 1960s traffic management systems have been arisen as an effective solution for relieving congestions on freeways. These management strategies are totally based on the deep understanding of the traffic flow theories, seeking the congestion triggers and the most rolling parameters which can be controlled in order to avoid to relief it. Congestion can be presented by the increase of vehicles concentration over the road section, this increase is related with two parameters speed and flow. Three of them (density, speed, flow) continue to increase until they reach the balance point, after that density continues to increase while the other two parameters decrease gradually until they reach the jam phase. So, the concept here it to maintain the traffic flow within the balance point, (maximum flow and no congestion). Different approaches have been developed focusing on the most effective and investigated ones, ramp metering and variable speed limits. All of the control strategies rely two ways for traffic control, either maintaining the section density under a certain critical value or changing the behavior of the fundamental diagram in order to avoid the congestion formation. Traffic flow models took their position in the field by making testing and implementing these control strategies less time and cost consumer. Still, it is very important to calibrate these models and allocate all their requirements in order to describe the real-life situation.



3. RELATED RESEARCH

Ramp metering considered one of the most effective Dynamic Traffic Management (DTM) measures in the utilization of the freeways traffic conditions. Practically, ramp metering is a traffic light installed at the entrance of an on-ramp to regulate the flow of vehicles entering the freeway according to a specific control algorithm and system. The target control variable is the signal cycle time, where the computed metering rates are translated to green phase times, in other words, the duration of the green phase is vehicle actuated. The role of ramp metering is spreading dense groups of vehicles or platoons on the on-ramp in order to utilize the downstream capacity and avoid the traffic flow breakdown. Thus, the extent and the duration of recurrent congestion, and the occurrence of non-recurrent congestion are reduced. As an indirect effect of ramp metering is that, increasing the waiting time on the on-ramps can instigate drivers to choose a different on-ramp, or not entering the freeway at all. This impact on route choice can have positive or negative consequences that may cause problems with e.g. traffic safety and rat running. Also, ramp metering can one of the incidents management system's components. According to the Minnesota Department of Transportation (MnDOT), "the use of ramp metering is an ITS development which provides the single greatest boost to freeway capacity and safety" (ITS International, 1997, p. 39-41).

For the last decades, different ramp metering strategies have been introduced considering different implementation approaches and control systems. Typically, two main types of ramp metering can be identified according to the implemented area: local ramp metering (considers only a single ramp) and coordinated ramp metering (considers a set of ramps). Also, ramp metering strategies can be classified according to the control system/algorithm type into fixed-time ramp metering, responsive ramp metering and predictive. Generally, fixed-time ramp metering algorithms derive the metering rates basing on historical data (offline derivation), however; responsive ramp metering derives the metering rates online as a dynamic response to traffic states. Predictive ramp metering strategies estimate the traffic conditions over a time

horizon in order to adapt the current system parameters for the next control step. Implementing any of these algorithms depends on many factors such as traffic conditions, freeway and ramp structure, environmental aspects, and political decisions.

The rest of this chapter is organized as the following: section 3.1 is a concise introduction to control theory and different control systems are used in DTM. Section 3.2 outlines the boundary conditions of the calculated metering rates considering different system aspects. Section 3.3 introduce the working modes of a ramp metering which can be applied to any ramp control approach. The rest of this chapter discusses the most investigated and implemented ramp metering strategies with a brief literature review.

3.1 Control Systems

Designing a traffic controller such as ramp metering requires a brief knowledge of control systems' basics and elements. Chiefly, control systems are designed to alter the functioning of a plant in order to reach the needed plant performance (Ioannou and Sun, 2012). There are different control system types and approaches, still before discussing them, it is very important to define the term *plant* where understanding this term is very crucial to determine the control system elements and parameters. A plant can be any process characterized by one or more inputs u and outputs y , where y are the measure of the plant response to the inputs u , see Figure 3.1.

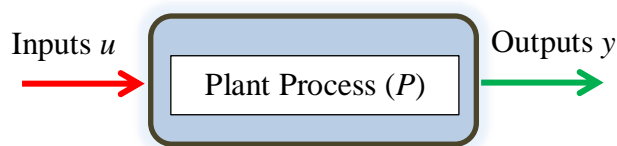


Figure 3.1: Plant representation.

Consequently, the control system modifies the input u in terms of that the output y meet the set of performance requirements, in other words, for whatever reason, if the system input is changed the system output must respond consequently and adapt itself to imitate the new input value. Generally, control systems have three types: open-loop feedforward controllers, closed-loop feedback controllers and adaptive

controllers (Dorf and Bishop, 1998), more explanation is provided in the following sub-sections.

3.1.1 Open-loop controller

Open-loop feed-forward or non-feedback control system depicts a continuous control system whereas the output y has no stimulus or consequence on the control action over the input u . Literarily in the case of an open-loop control system, the system output is neither measured nor fed back for comparison with the system input. Referring to Figure 3.2 the observed input u is modified to give the plant input u^* .

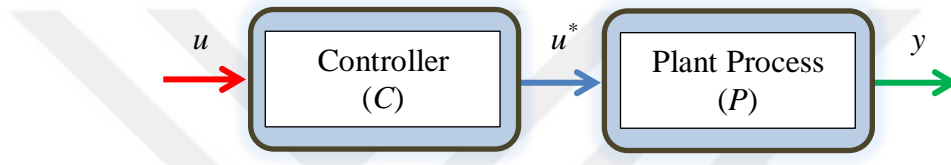


Figure 3.2: Open-loop/feedforward control system.

The open-loop system has many disadvantages, for example, the system cannot adapt and self-correct the preset values since there is no feedback about the output conditions. Also, open-loop systems are not sufficient to handle disturbances or condition changes which may restrict its ability to the desired level of the task.

3.1.2 Closed-loop controller

On the other hand, the closed-loop control system has one or more feedback control loops or paths between the output and input. The feedback term indicates that some portion of the output is returned back as input as a part of the system excitation. Rather than an open-loop system, a closed-loop system automatically compares the output and the actual conditions (the difference between output and reference input) in order to accomplish and sustain the desired output conditions. The term feedback is the main distinct between open-loop and closed-loop controllers, whereby using this action, the errors within the system are reduced. Referring to Figure 3.3 the observed input u is modified to give the plant input u^* .

Closed-loop systems outperform open-loop systems that they have the ability to reduce the system sensitivity to external disturbances. The adaptive control system is

a special type of feedback controllers where measures are explicitly taken to simultaneously compensate uncertain system parameters in order to maintain optimal system performance (Ioannou and Sun, 2012). This control system will be explained clearly accordingly with adaptive ramp metering strategies.

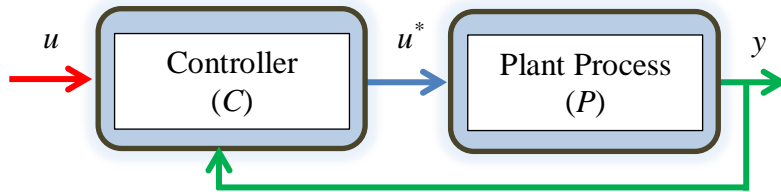


Figure 3.3: Closed-loop feedback control system.

3.2 Ramp Demands

Ramp demands can be satisfied when the flows that enter the ramp can be metered into the freeway with acceptable delay. Because of this delay, a residual queuing may form but without extending back into the ramp intersection, that's why a minimum value of the metering rate (r_{min}) must be considered. If the ramp demand exceeds the ramp capacity, limiting the entry flow maybe be the only solution to sustain free-flow conditions on the freeway. However; this metering rate will result in residual queuing on the ramp with high delays and also the queues will extend back onto the arterial road. With coordinated ramp metering, this problem can be managed because of the coordination between ramps for balancing queues.

For a ramp control, it is very important to choose an effective control algorithm to maximize the efficiency of the ramp. This requires a brief analysis and understanding of freeway flow characteristics and geometry as well as appropriately designed entry ramp to provide adequate capacity and storage. Elefteriadou et al. (1995); Lorenz and Elefteriadou (2001) demonstrated that under similar environmental conditions e.g., weather, lighting, however; the traffic breakdown at merge areas may occur at different flow capacity values q_{cap} on different days. In contrast, the critical occupancy (O_{cr}) at which capacity flow occurs, it was found to be fairly stable. Owens et al. (1988) showed that O_{cr} remain stable even under adverse weather conditions.

3.3 Ramp Metering Operation Modes

Ramp metering algorithms or ramp control system can response to the input influences in three different actions or operation modes. The first type is the static mode or pre-set based algorithm which based on historic data without considering the current traffic conditions. A second type is a real-time input data responsive (adaptive) mode which reacts directly to the system environment using the real-time gathered data and traffic conditions. The last action type is predictive action, where the algorithm uses a forecast model with computed reaction to predict the traffic conditions for the next control step in order to solve any capacity breakdown cases before it occurs. Both responsive and predictive actions overcome static action because static response fails in case of any sudden change in traffic conditions. Still, responsive and predictive actions performance depends on the quality of the real-time data and the system complexity. In the following three of these actions are explain briefly.

3.3.1 Pre-set mode

In fixed-time or pre-set ramp metering operation mode, the metering rates pattern is computed basing on historical data with a vicinity with the target ramp. This data are gathered and accumulated over time and merged into a common recurrent driver behavior pattern. This means the control algorithm works under the statement that is the current traffic conditions present its general average data. Practically, this technique is more suitable for well-defined recurrent congestion periods e.g. morning and evening peak hours.

3.3.2 Adaptive mode

Adaptive ramp metering operation mode reacts simultaneously to the actual traffic measurements on the mainline and ramp. One of the basic requirements of this mode is providing a real-time traffic data with a good quality including speed, traffic volumes, and occupancy.

3.3.3 Predictive mode

Predictive ramp metering uses the current real-time traffic data for predicting the traffic condition changes over a predefined horizon so that the control algorithm computes a metering rate to keep the capacity below the critical value over the whole control period. That means predictive ramp metering operation mode reacts on the predicted data, not on the current-real data.

3.4 Local Ramp Metering

Local ramp metering strategies are concerned only with a single ramp, where the metering rates are computed with a vicinity with the traffic conditions related to the ramp so they are not affected by the traffic conditions elsewhere. Initially coordinated ramp metering algorithms are more dominant than local ones, however, always there is a local algorithm included for solving the local level of coordinated strategies. In this sub-section variety of local ramp metering strategies are mentioned and discussed supported by a brief literature review related to every strategy.

3.4.1 Demand-capacity

Demand-Capacity (DC) ramp metering strategy is an adaptive algorithm based control strategy was used in the United States (Masher et al., 1975; Koble et al., 1980). DC algorithm measures the downstream or upstream (related to the availability of data) occupancy and if it is above the critical occupancy congestion is assumed to develop, and the metering rate is set to the minimum value. Otherwise, the volume is measured upstream of the merging area, and the metering rate is set to the difference between the downstream capacity and the upstream volume, see Figure 3.4. For a freeway segment with a time index k , the metering rate $r(k)$ can be computed by:

$$r(k) = \begin{cases} q_{cap} - q_{in}(k-1), & \text{if } O_{out}(k-1) \leq O_{cr} \\ r_{min}, & \text{else} \end{cases} \quad (3.1)$$

Where q_{cap} , $q_{in}(k-1)$, $O_{out}(k)$, O_{cr} , and r_{min} denote respectively, capacity of the merging area (veh/h), previous time step capacity of the merge area (veh/h),

downstream or upstream Occupancy for the current time step, critical occupancy downstream of the merging area, and minimum metering rate of the ramp.

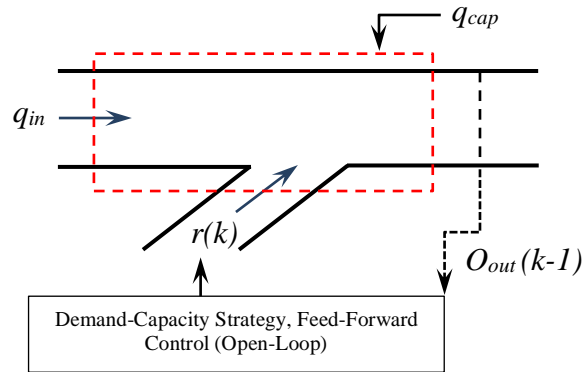


Figure 3.4: Demand-capacity ramp metering strategy presentation.

However; for some reason the downstream measured occupancy becomes overcritical (i.e., a congestion may form), $r(k)$ is reduced to r_{min} to avoid or to relieve the congestion. Clearly, this strategy does not represent a closed-loop control system but an open-loop disturbance-rejection controller which is generally known to be quite sensitive to various non-measurable disturbances. If the actual capacity of the freeway section is higher than the proposed one, then the freeway section will be fully utilized and the vehicles needlessly will be waiting on the on-ramp. On the other hand, if the actual capacity is lower, then the congestion will increase and propagate backward.

Another form of Demand-Capacity strategy is the Percent-Occupancy controller (Masher et al., 1975; Koble et al., 1980). The percent-occupancy strategy does not require calculations of the freeway capacity so that potentially it has lower implementation cost. This strategy uses only upstream sensor occupancy measurements and uses the occupancy as the sole means to identify and measure congestion. The critical occupancy is measured using historical data (Hadj Salem et al., 1988). This algorithm involves 2 constants: K_1 is the capacity flow, and K_2 is a constant based on the slope of a straight line approximation of the uncongested part of the fundamental diagram. The metering rate is determined by:

$$r(k) = k_1 - k_2 O_{in}(k - 1) \quad (3.2)$$

3.4.2 Occupancy control

Occupancy Control (OC) ramp metering strategy presents an adaptive control system where it compares the actually computed solutions with the pre-defined metering rates corresponding to the measured mainline upstream occupancy values. These pre-determined metering rates are derived basing on the assumption of a relationship between the actual mainline traffic volumes and the mainline upstream measured occupancy. The control type is this strategy is a feed-forward control approach, thereby the previous metering rate is not included in the current calculations. Stands to the reason for the inconsistency of the metering rates (Chu et al., 2004). OC approach is a basic key that used on the local level of coordinated ramp metering strategies such as bottleneck algorithm, nevertheless, in some simulation based coordinated ramp metering evaluation studies, it was compared with ALINEA algorithm as a local controller where ALINEA showed better time improvement than OC (Zhang et al., 2001).

3.4.3 Zone

Before to be updated to an adaptive control system, Zone algorithm was first used in Minneapolis, Minnesota, the USA as a static ramp metering algorithm. The Zone approach divides the mainline into zones with a variable length (usually 3 to 6 miles). The zones are determined so that the upstream part of a zone must have free flow traffic conditions, on the other hand, the downstream part is should present a bottleneck area with a relatively high demand-capacity ratio (Zhang et al., 2001). For each zone, Zone algorithm works on balancing the entering and leaving traffic. For a 30-second metering interval, the following equation can be used to compute the metering rate:

$$A + U + M + F = X + B + S \quad (3.3)$$

Where A , U , M , F , X , B , and S denote respectively, the mainline upstream volume (measured), the sum of the non-metered ramps' volumes (measured), the sum of the metered ramps' volumes (to be calculated), the sum of metered ramp volumes from freeway to freeway (to be calculated), the sum of off-ramps' volumes (measured), the capacity of the downstream bottleneck, and available space within the zone.

If $S=0$ the maximum number of vehicles that can enter the zone through the metered ramp is:

$$M + F = (X + B) - (A + U) \quad (3.4)$$

Now, if each ramp is weighted and a ramp factor (f_i) is obtained, the i th ramp metering rate is:

$$R_i = f_i(M + F) \quad (3.5)$$

3.4.4 ALINEA

Both Demand-Capacity and Percent-Occupancy are examples of open-loop or feedforward control. These strategies do not use the system output as input for the next iteration. In contrast, ALINEA (Asservissement Lineaire d'Entrée Autoroutiere) is a classical feedback based control algorithm suggested by (Papageorgiou et al, 1991). Referring to Figure 3.5, ALINEA presents a closed-loop ramp metering concept, where the control algorithm task is to maximize the corridor flow by sustaining the desired occupancy value on the downstream of the merging area.

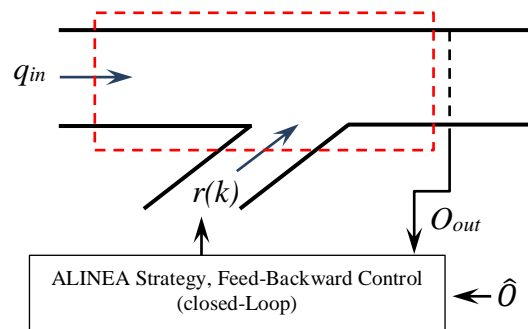


Figure 3.5: A presentation of ALINEA algorithm.

ALINEA is based on the linear quadratic (LQ) feedback law. The LQ regulator relies on minimizing a quadratic performance index related to a system contains linear equations which represent the traffic dynamics. Considering the freeway segment that depicted in Figure 3.5 with time index k , the metering rates can be simply calculated by the following equation:

$$r(k) = r(k - 1) + K_R[\hat{O} - O_{out}(k)] \quad (3.6)$$

Where k , $r(k)$, $O_{out}(k)$, \hat{O} , and K_R denote respectively, a discrete time index (1,2,..), the entering flow at time step k , the measured downstream occupancy (%), a desired downstream occupancy value, and a regulator parameter used for adjusting the constant disturbances of the feedback control in order to utilize the downstream capacity (>0).

Note that $r(k)$ is a function of the metering rate for the previous iteration, $r(k-1)$, therefore ALINEA is a closed loop algorithm. The metering rate is also a function of the difference between the measured occupancy O_{out} and for the downstream a target set point occupancy \hat{O} which can be O_{cr} . The reason of using occupancy rather than the flow measurements such as traffic volume is that the critical occupancy when congestion starts to form tends to be less sensitive to traffic and weather changes than capacity (Papageorgiou et al, 1991). Also, traffic volumes cannot be an indicator for characterizing traffic states, stands to reason that the same traffic volume can present a congested and non-congested traffic due to the inverse U-shape of the volume and occupancy fundamental diagram. ALINEA will be explained in details in the proposed algorithms section.

3.4.5 Extensions of ALINEA

Still, ALINEA has some disadvantages, for example, ALINEA considers the downstream occupancy, however, congestion can still occur upstream of the ramp. In addition, the problem determining the optimal detector location is another challenge or in some cases, the downstream detectors are not available. Researchers have developed enhanced versions of ALINEA by addressing solutions for these disadvantages. In the following are some different extensions of ALINEA where each of them trying to cover one or more of ALINEA pitfalls or to improve ALINEA performance in special conditions.

3.4.5.1 PI-AINEA

In the case of a bottleneck existence downstream of the ramp nose, congestion is first instigated at this bottleneck rather than in the merge area. The Proportional-Integral

ALINEA (PI-ALINEA) ramp metering is the full version of ALINEA where it relies on a proportional-integral feedback regulator which provide a better performance in case of a bottleneck existing further downstream of the merging area. An extended structure of ALINEA is used to compute the metering rate (Wang et al. (2014):

$$r(k) = r(k-1) - K_P [O_{out}(k) - O_{out}(k-1)] + K_R [\hat{O} - O_{out}(k)] \quad (3.7)$$

Where K_P is a regulator parameter for the additional proportional term (>0).

This version of ALINEA will be explained briefly in the proposed ramp metering strategies for this study, since understanding the reasons for using the PI-regulator requires the full identification of ALINEA parameters especially the detector location and the activation control time interval.

3.4.5.2 MALINEA

Oh and Sisiopiku (2001) proposed a modified version known as MALINEA. In this version of ALINEA, the upstream occupancy is also considered for the section capacity optimization and the time lag between the upstream and downstream measurements. With a time index (t), the metering rate for the next step $Q^r(t+1)$ is:

$$Q^r(t+1) = [O_u(t+n+1)O_u(t)](K/A) + Q^r(t-n) \quad (3.8)$$

Where O_u , K , A , and n denote respectively, the upstream occupancy, a regulator factor, the downstream and upstream occupancy based relationship derivation, and the time lag between the upstream and downstream measurements.

3.4.5.3 FL-ALINEA

ALINEA is based on the downstream occupancy measurements which cannot be available in all cases and directly related to the basic traffic flow variables (density, volume, and speed) because of the measurement device sensitivity to the traffic composition and variant installation conditions which lead to uncertainties in the g -factor. For the mentioned reasons, Smaragdis and Papageorgiou (2003) expanded the application of ALINEA to Flow-Based ALINEA (FL-ALINEA) algorithm that uses flow measurements from downstream detectors rather than occupancy measurements. FL-ALINEA algorithm has the same formula that used in ALINEA,

however, it considers the flow measurements to reach the desired flow value rather than desired occupancy value, the formula as the following:

$$r(k) = \begin{cases} r(k-1) + K_F[\hat{q} - q_{out}(k-1)] & \text{if } O_{out} \leq O_{cr} \\ r_{min} & \text{Otherwise} \end{cases} \quad (3.9)$$

Where K_F , \hat{q} , and q_{out} denote respectively, a positive regulator factor for damped control behavior (equal to or slightly less than 1), the desired downstream flow value, and the measured downstream flow.

Same principle, FL-ALINEA algorithm will try to sustain q_{out} around \hat{q} as long as $O_{out} \leq O_{cr}$. Contrary, if $O_{out} \geq O_{cr}$, $r(k)$ is set to the minimum value r_{min} to recover the uncritical occupancy level. Still, it should be noticed that if the lower part of equation 3.8 is activated within a very short time period (sudden switches from $r(k)$ to r_{min}) this may lead to burst traffic volume trajectories rather than smooth traffic. Therefore, FL-ALINEA is only suggested if \hat{q} is sufficiently less than capacity.

3.4.5.4 UP-ALINEA

Another version of ALINEA is Upstream-Occupancy Based ALINEA (UP-ALINEA) that uses the upstream occupancy measurements and estimates the downstream occupancy. The downstream occupancy (\tilde{O}_{out}) is estimated in terms of upstream occupancy and incorporating the effects of the ramp traffic volume, see the following equation (Smaragdis and Papageorgiou, 2003):

$$\tilde{O}_{out}(k) = O_{in}(k) \left[1 + \frac{q_{ramp}(k)}{q_{in}(k)} \right] \frac{\lambda_{in}}{\lambda_{out}} \quad (3.10)$$

Where O_{in} , q_{ramp} , q_{in} , λ_{in} , and λ_{out} denote respectively, the measured upstream occupancy, the ramp flow entering the freeway (measured), the mainline traffic volume, the number of lanes upstream, the number of lanes downstream.

The metering algorithm is identical to the traditional ALINEA, where $r(k)$ is:

$$r(k) = r(k-1) + K_R[\hat{O} - \tilde{O}_{out}(k-1)] \quad (3.11)$$

3.4.5.5 UF-ALINEA

Upstream-Flow Based ALINEA (UF-ALINEA) estimates the downstream flow by taking the sum of the upstream flow and downstream flow:

$$\tilde{q}_{out}(k) = q_{in} + q_{ramp} \quad (3.12)$$

Accordingly, the metering rate:

$$r(k) = \begin{cases} r(k-1) + K_F[\hat{q} - \tilde{q}_{out}(k-1)] & \text{if } O_{out} \leq O_{cr} \\ r_{min} & \text{Otherwise} \end{cases} \quad (3.13)$$

3.4.5.6 X-ALINEA/Q

Smaragdis and Papageorgiou (2003) introduced a sophisticated queue control based ramp metering control strategy ALINEA/Q. ALINEA/Q computes two metering rates and taking the maximum one. First one is computed using traditional ALINEA algorithm, and the other rate is computed so that the ramp queue is at or below the maximum allowable queue length. The second metering rate derived by:

$$r'(k) = \frac{1}{T} [\hat{w} + w(k)] + d(k-1) \quad (3.14)$$

Where $r'(k)$, \hat{w} , $w(k)$, T , and $d(k-1)$ denote respectively, a minimum rate to avoid queue buildup, the maximum allowable queue length (as number of vehicles), number of vehicles in the ramp queue for the current time step, cycle update time, and the number of vehicles entering ramp.

This simple on/off queue override method gives smoother metering rate and the traffic oscillations are avoided. Also, considering the queue length at each time interval, the ramp metering rate is sufficiently increased since vehicles are no longer waiting on the ramp.

3.4.6 AD-ALINEA

The ramp metering algorithm AD-ALINEA was developed by Kosmatopoulos et al. (2006) as an adaptive version of ALINEA. The control concept of ALINEA remains the same, the only change is that an estimation module of \hat{O} has been added. In each

time step k , the measured O_{out} and q_{out} are compared with various thresholds. Accordingly, if \hat{O} is not reached the critical estimated occupancy (\hat{O}_{est}) is increased, otherwise, \hat{O}_{est} is decreased. The system is instigated to update \hat{O}_{est} if the difference between O_{cr} and \hat{O}_{est} is at least 5%, else \hat{O} remains the same. In addition, updating \hat{O} depends on the estimation of the following derivative:

$$D = \frac{\delta q_{out}}{\delta O_{out}} \quad (3.15)$$

The value of \hat{O} is updated according to the following algorithm:

$$\hat{O}(k) = \begin{cases} \hat{O}(k-1) + 1\% & D > D_{max} \\ \hat{O}(k-1) & D_{max} < D < D_{min} \\ \hat{O}(k-1) - 1\% & D < D_{min} \end{cases} \quad (3.16)$$

The values of the boundary conditions $D_{max} = 40$ and $D_{min} = -15$ are assumed to consider that \hat{O} always remains in the top of the occupancy-flow diagram.

There are two methods suggested by Zhang and Levinson (2004); Barto (2007) for the estimation of D where both of them have been developed and tested basing on historic data. The first method is a simple derivation process by using the measurements of the previous and the current time step as the following:

$$\delta q_{out} = q_{out}(k) - q_{out}(k-1) \quad (3.17)$$

$$\delta O_{out} = O_{out}(k) - O_{out}(k-1) \quad (3.18)$$

The second method of estimation is based on Kalman Filter which presents an online mathematical tool that filters the noise of data (e.g. traffic measurements) and estimates statistically the real system properly. The system is described as “the calibration problem: least squared errors and maximum likelihood.” (Treiber and Kesting, 2013). The base assumption in Kalman Filter that is the failures are Gaussian-Distributed. The D value is estimated in within two steps: Firstly, to obtain the new value for the next time step, the current estimated D value is projected forward in time. Secondly, the current traffic measurements are used to improve the estimated D value. In Gaffney and Burley (2010) they compared both estimation

methods and it was concluded that Kalman Filter Estimation (KFE) outperformed the first method.

3.4.7 Model predictive control

Proactive or model predictive control (MPC) ramp metering strategies are traffic conditions predictive models aim to specify the optimal traffic conditions for a whole freeway or a network based on the demand and prediction model over a time horizon. The metering rate $r(k)$ is determined every time step k by the optimization of a cost function restricted by the input and output constraints. The objective variables that can be incorporated into the cost function include total delay, average speed, and the number of signals control changes.

Two prediction horizons N_p and N_c ($N_c < N_p$) are assumed in order to reduce the complexity and the size of computations. The horizon N_p presents the maximum number of intervals for which MPC will forecast the future state. The horizon N_c presents the number of intervals so that, the MPC is allowed to change. MPC is considered to remain constant if the intervals are beyond the control horizon. MPC uses a receding horizon framework in which a new optimal control strategy is calculated and implemented each interval.

Using the hierarchical control structure, proactive and reactive strategies can be combined to predict the optimal traffic conditions and using them as a set values for the controller respectively. In Bellemans et al. (2006), a model predictive control based ramp metering is utilized on 9 km stretch of E17 motorway Ghent–Antwerp / Belgium, where the stretch is simulated using real-life measurements by METANET traffic flow model. The performance of the model predictive control based ramp metering is compared with ALINEA based controller where the on-ramps maximum allowable queuing lengths are imposed. The MPC ramp metering performed better than ALINEA in terms of the total time spent in the network, the maximum allowable queuing length, and the smoothness of traffic flow. Still, the optimization problem is a challenge since it is computationally intractable for online applications since the system has a wide application. In Ghods et al. (2010), a game-theory-based approach to address the computational complexity of MPC by employing distributed controllers, in other words, distributed optimization framework (DOF), is introduced. Based on the simulated results DOF outperformed the conventional non-decomposed

optimization, namely centralized optimization framework (COF), in terms of both solution quality and computation time.

3.5 Coordinated (Area-Wide) Ramp Metering

Coordinated ramp metering strategies consider the traffic conditions at more than one ramp for computing the ramp metering rates by the achievement of a system-level objective. The local systems are connected to present the system-level objective in order to optimize the ramps' space for storing vehicles to increase the system efficiency. Generally, based on the problem formulation area-wide ramp metering control is divided into three approaches: optimal control strategies, feedback control strategies, heuristic control strategies, and hierarchical control strategies. Further, in terms of the used algorithm coordinated ramp metering can be classified into three classes: bottleneck or competitive algorithms, cooperative or incremental algorithms, and integral algorithms (Kwon et al, 2001; Zhang et al, 2001). Both of problem formulation approaches and control algorithms are discussed briefly in the following sub-sections.

3.5.1 Optimal control approach

Optimal control approach was first postulated by Wattleworth (1967), as a linear programming problem. Accordingly, researchers have used optimization tools for designing efficient ramp control strategies. The optimization problem solution includes control variables, an objective function, and traffic flow model. In this approach, three models can be defined: static, sequential and dynamic models.

3.5.1.1 Static optimal control

Static optimal control relies on historic traffic data to perform a fixed time control policies. Wattleworth (1967) were the pioneers by proposing a mathematical formulation of a static control strategy. In that strategy, a freeway is divided into several homogeneous segments, considering that each segment contains only one on-ramp and one off-ramp. The optimization problem is to maximize the performance index (objective function) e.g. the sum of output or input flows constrained by the capacity.

3.5.1.2 Sequential optimal control

Sequential optimal control remedies the faintness of the static control approach by using real-time traffic and ramp queue data (Papageorgiou, 1980 and 1983; Chang, et al., 1994). The time horizon is structured into equal time intervals, where the metering rate of each interval is computed by the linear programming approach to the static model. Follows the same in the static control approach, the performance index as an objective function is maximized, taking into account the demand and ramp queues as constraints. In each time step, the ramp demand is modified by adding the queue in the previous time step to the current demand.

3.5.1.3 Dynamic optimal control

Still, in sequential models, the traffic flow representation is static, wherein each time interval the main corridor flow is assumed to have a steady-state condition. Thus, the propagation of flow from one segment to the next one is ignored. Accordingly, dynamic optimal control models have been developed based on mathematical programming approach (Stephanedes and Chang, 1993; Chang, et al., 1994), by presenting the flow propagation. Dynamic control models are based on macroscopic dynamic traffic flow model that combines the conservation equation of flow, the flow and density relationship, and the kinematic wave propagation theory which developed by Lighthill and Whitham (1955) and Richards (1956). The performance index or objective function in the optimization problem considers different variables e.g. total travel distance, total input volumes, total output volumes, total delays, total travel time, ramp queue, etc. These variables are subjected to dynamic traffic flow model, capacity, and ramp queue constraints. The resulting problem can be formulated either as a linear program (Chang, et al., 1994) or a non-linear one (Stephanedes and Chang, 1993), depending on the whether the traffic flow relationship is linearized or not.

3.5.2 Feedback control approach

Feedback control approach follows the same methodology used in local feedback control ramp metering (linear-quadratic organization), however, the control law in coordinated ramp metering case has more than one variable. LQ optimization theory

is considered as a strong tool for designing multi-variable feed-back control laws. Papageorgiou, et al. (1990) used a quadratic performance criterion as an objective function to penalize deviations of the problem variables from their steady states.

3.5.3 Heuristic approach

A good example of heuristic ramp metering approach is FLOW ramp metering algorithm. FLOW was developed by Jacobson, et al. (1989). This strategy is a real-time coordinated responsive ramp metering algorithm. FLOW algorithm is formed of two components: local metering rate (LMR) which based on local conditions, and a bottleneck metering rate (MBR) constrained by the system capacity.

3.5.4 Hierarchical control approach

Coordinated and local ramp metering can be combined in the form of *hierarchical control*. Hierarchical control approach has two feedback loops depicted on two levels: major level that uses a system-wide model to calculate the desired states, on the other hand, a minor level uses a local controller in order to adjust the metering rates to eliminate the differences among the actual and desired network states (Chen et al.1997). Four models can be identified in hierarchical control approach: state estimation, (origin-destination) OD prediction, local control, and area-wide control. The first model estimates the best current state of the network depending on the surveillance data. This data are used by the OD prediction module in order to predict the future OD demand, after that the control values are optimized by the area-wide module in order to obtain a system objective. The metering rate values provided by the area-wide controller is adjusted locally by the local module to compensate for the system errors e.g. errors in state estimation and OD prediction.

3.5.5 Cooperative algorithms

Cooperative or incremental ramp metering algorithms provides a communication between ramps. The Cooperation process takes the form when upstream ramps response to downstream ramps when they are metered very restrictively by reducing their metering rates to support the following ramp.

3.5.5.1 Helper

Firstly was introduced in Denver, Colorado, the USA in early 1981. Helper strategy takes the control algorithm at two levels; local ramp metering algorithm and a superior coordinated algorithm. Accordingly, the freeway is divided into control zones where each zone includes from one to seven ramp. The local algorithm considers the upstream occupancy and the queue override data. If the queue override detector is occupied, the metering rate is increased by one step per cycle time. Next to the local control, the coordinated algorithm with the linked-ramp approach, the current ramp load is distributed on the upstream ramps in order to assist the target ramp in avoiding the arterial spillback that is where the name Helper come from. Helper algorithm differs from the Linked-ramp algorithm that separates between the local solution and the coordinated solution (Bogenberger and May, 1999).

3.5.5.2 MILOS

The Multi-Objective, Integral, Large-Scale, Optimized System (MILOS) algorithm was developed by the Arizona Department of Transportation (ADOT) during the RHODES-ITMS project in 1999. MILOS presents a hierarchical ramp control system. This strategy is adopted for large-scale freeway networks where the metering rates computation problem is decomposed into a series of optimization problems (are solved with quadratic programming) of different temporal and spatial resolutions. Since the system parameters and conditions change, the optimization problems are resolved to constantly adjust the control strategy to the system real-time behavior. Also, to avoid the unpredictable changes in the future state of the system, a macroscopic model is used for the estimation of the traffic state to prepare the system at the local level for the next short-term stochastic disturbance. The hierarchical system has two levels: area-wide coordinator, and a predictive-cooperative real-time (PC-RT) rate regulator with a vicinity to each single ramp (Ciarallo and Mirchandani, 2002), see Figure 3.6.

The area-wide coordinator operates on the tactical level for decision making and feeds the lower level by the desired metering rates for the medium-term (10-20 minutes) for the following goals: maximizing the freeway throughput, balancing the queues growth rate, and minimizing queue spillback. These tasks are performed

basing on a rolling horizon application of a multiple-criteria, and optimization of quadratic programming problem. After that, the area-wide coordinator delivers to PC-RT controller a set of metering rates and preferred freeway states. Accordingly, in order to describe the mainstream flow response to given ramp metering rates, PC-TR controller over a time horizon of minutes, and with a vicinity of a single ramp and a small freeway section solves optimization problems based on a linearized description. The optimization problem objective variable is to minimize the travel time beyond the area-wide coordinator, where PC-TR tries to be proactive in adjusting the nominal rates supplied by the area-wide coordinator (Ciarallo and Mirchandani, 2002).

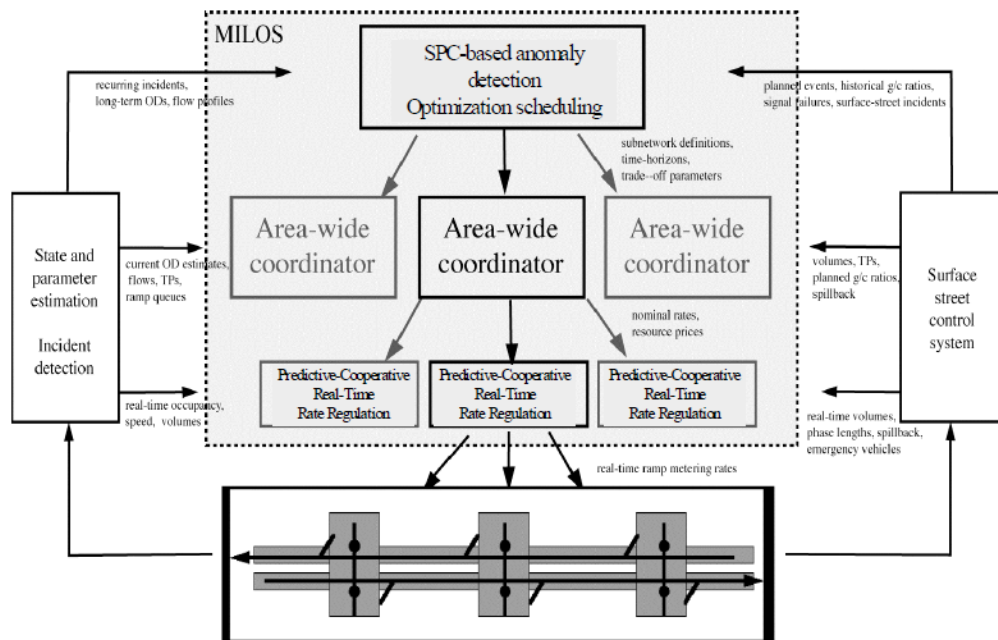


Figure 3.6: MILOS control architecture (Ciarallo and Mirchandani, 2002).

3.5.5.3 Linked-ramp

Responsive linked-ramp algorithm (Banks, 1993) presents a set of local traffic responsive controllers, where the metering rate is computed basing on the flow measurement upstream of each ramp:

$$\text{metering rate} = \text{target flow rate} - \text{measured upstream flow rate} \quad (3.19)$$

If the metering rate of one ramp is one of its lowest three metering rates, similar to the concept in the Helper, the upstream ramps should use the same metering rate

value or lower. Most of the advantages and disadvantages are shared between linked-ramp and helper algorithms, still, the linked-ramp local controller is inappropriate for congested traffic, since lower upstream traffic (can be in the free flow phase or congested phase) will instigate the controller to allow more vehicles to enter the freeway.

3.5.6 Competitive algorithms

Competitive or bottleneck ramp metering algorithms are based on a comparison between local and bottleneck metering rates. The most dominant rate is applied and other rate has to bow to it. The bottleneck metering rate is used to maintain the traffic flow under the bottleneck capacity especially in case if a single on-ramp would collapse the whole system.

3.5.6.1 FLOW

A good example of heuristic ramp metering approach is FLOW ramp metering algorithm. FLOW was developed by Jacobson, et al. (1989), is a real-time coordinated responsive ramp metering algorithm. FLOW algorithm is formed of two components: local metering rate (LMR) which based on local conditions, and a bottleneck metering rate (MBR) constrained by the system capacity. Predetermined metering rates are selected basing on the upstream occupancy level. LMR uses a percent-occupancy algorithm, where a lookup table relates the occupancies upstream with the ramp metering rates. This table is developed using historical volume-occupancy relationships. The metering rates that derived from the lookup table determine the number of vehicles that allowed to merge with the mainline associated with each upstream occupancy value. These rates are the difference between the capacity and the volume associated with the occupancy on the fundamental diagram. For BMRs the locations of the bottlenecks on the freeway have to be determined, considering the influence zone with one or more on-ramps affected by each bottleneck. Accordingly, basing on the distance between the ramp and the bottleneck and the historical volumes of the ramp, a weighting factor is developed for each ramp. Loop detectors have to be installed upstream and downstream of the influence zone, all the on-ramps, and all the off-ramps.

The bottleneck algorithm is invoked under two conditions: the freeway is operating above the capacity (the downstream occupancy $>$ the critical value), and the vehicles are storing in the freeway section, in other words, the section inflow (mainline inflow and ramp flow) is greater than the section outflow. For section i the total metering rate reduction for the next time interval $(t+1)$ is determined as follows:

$$U_{i(t+1)} = (q_{in,it} + q_{on,it}) - (q_{out,it} + q_{off,it}) \quad (3.20)$$

Where $U_{i(t+1)}$, $q_{in,it}$, $q_{on,it}$, $q_{out,it}$, and $q_{off,it}$ denote respectively, the total required reduction in the metering rates for section i for the time step $(t+1)$, the mainstream inflow for section i at time step t , the on-ramps' volumes that associated with the influence zone of section i at time step t , the mainstream outflow for section i at time step t , and the off-ramps' volumes that associated with the influence zone of section i at time step t .

The total reduction and the weighting factors are used to compute the reduction in each ramp j metering rate within the influence zone i as the following:

$$BMRR_{ji(t+1)} = U_{i(t+1)} \frac{WF_j}{\sum_j^n (WF_j)_i} \quad (3.21)$$

Where $BMRR_{ji(t+1)}$, and WF_j are the reduction in the ramp j metering rate for the next time step and the weighting factor of ramp j respectively.

Thus, the ramp metering rate for the next time step is:

$$BMR_{ji(t+1)} = q_{on,jt} + BMRR_{ji(t+1)} \quad (3.22)$$

In case if the influence zones overlap, each ramp will have more than one MBR value, accordingly, the most restrictive MBR value is considered. Finally, the most restrictive of LMR and BMR is chosen. The queue control criteria take two steps, once the queue length reaches the critical values the ramp metering rate is increased. The second step is queue override as an advance controller as the queue length reach its maximum, hence the ramp meter is totally shut off.

3.5.6.2 Compass

Compass algorithm was first introduced in Toronto, Canada 1975 with the following control elements: local and the system-wide level competitive algorithms, vehicle detector stations, closed circuit television (CCTV) cameras, variable message signs (VMS), and operator control access at the traffic control center. The used data include the mainline occupancy near to the ramp, the downstream occupancy, the upstream volume. At the local level, these detected traffic parameters are combined with preset thresholds, downstream occupancies, and upstream volume in order to be compared with a look-up table. The lookup table will provide the most dominant metering rate with a 17 steps resolution basing on the downstream occupancy and upstream volume. On the system-wide level, an additional off-line optimized metering rate is also compared with the metering rates resulted from the local level, where the most restrictive metering rate is considered. Seeking the queue control, the calculated metering rate is set up one level higher than computed, this higher obstructive decision shall lead to a ramp approval to a value under the on-ramp occupancy threshold (Bogenberger and May, 1999). Still, Compass algorithm is not robust as other reactive ramp control algorithms since it is based on a pre-defined look-up tables, therefore, it was replaced by responsive algorithms e.g. ALINEA in 2012 in Ontario.

3.5.6.3 SWARM

The System Wide Adaptive Ramp Metering (SWARM) algorithm had been developed in 1996 and was implemented in Orange County, California, USA. SWARM presents a heuristic coordinated control approach with two separated algorithm, system-wide algorithm and local level algorithm. In the general form of implementing this algorithm, the freeway is divided into zones where each zone locates between two bottlenecks (Monsere et al., 2008; Bogenberger and May, 1999). The local algorithm can take any isolated responsive ramp metering algorithm where the metering rate is computed based on the local density. On the global level, the system-wide algorithm provides the total volume reduction of the ramps upstream from a critical bottleneck. This total reduction is distributed on ramps (upstream ramps) following a predefined fraction computed based on the weight of each ramp. Later, the most restrictive rate (locally computed or provided by system-wide

algorithm) is chosen. For each zone, the system-wide algorithm acts proactively using the measured traffic data (density and predefined critical density) in order to predict the traffic demands, therefore, it has the potential to nail congestion before propagation. For a pre-determined prediction horizon period, if the computed density is higher than the critical one, vehicles reduction is distributed over the ramps so that the threshold density will not be topped after the computed time T_{crit} , (Zhang, et al., 2001). Referring to Figure 3.7, the required vehicles reduction can be computed as the following:

$$d_{tar} = d_{curr} - \frac{d_{exc}}{d_{crit}} \quad (3.23)$$

Where d_{tar} , d_{curr} , d_{exc} , and d_{crit} denote respectively, the required density to stay under the saturation level, the measured mainline density, the excess computed density, and the computed critical time required to exceed the critical density.

$$V_{red} = (d_{loc} - d_{tar}) \times n \times l \quad (3.24)$$

Where V_{red} , d_{loc} , n , and l denote respectively, the number of vehicles to be reduced from the mainline volume, the measured local density on the mainline, the number of lanes within the target section, and the distance to the next ramp.

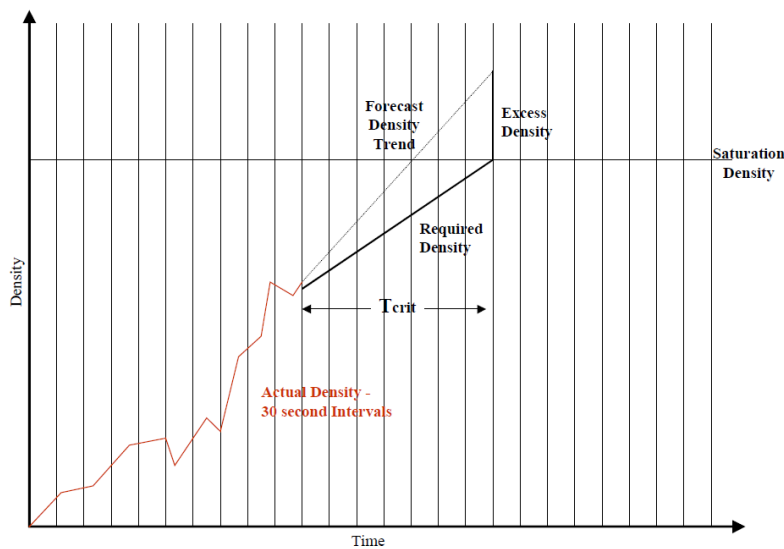


Figure 3.7: SWARM forecast operation (Bogenberger and May, 1999).

The most dominant metering rate (system-wide or local metering rate) is deployed. For adequate prediction, an internal algorithm is used in order to exclude any inappropriate data which come from defected detectors.

3.5.7 Integral algorithms

Integral ramp metering algorithms follow a well-defined objective function in order to optimize the system. The metering rates are computed separately at the local level and then results are compared from an open standpoint. Zhang et al (2001) stated that integral algorithms are potentially the most robust and the most theoretically sound, nevertheless, they are the most complex to operate and calibrate.

3.5.7.1 METALINE

METALINE is a coordinated ramp metering algorithm was developed in Paris, France in 1991 by Papegeorgiou et al. (1990) as an extension to ALINEA by transferring it from scalar values based equation into a vectors and matrix based equation. The control principle is the same as in ALINEA, however, the algorithm uses the measured occupancies and compare them with defined capacities where the ramp storage is used to keep the mainline volume under the critical capacity. METALINE equation contains occupancy vectors and two control matrices in order to develop the metering rates vector:

$$\vec{r}(k) = \vec{r}(k-1) - K_1(\vec{o}(k) - \vec{o}(k-1)) - K_2(\vec{O}(k) - \vec{O}_{cr}) \quad (3.25)$$

Where $\vec{r}(k)$, $\vec{r}(k-1)$, $\vec{o}(k)$, $\vec{O}(k)$, \vec{O}_{cr} , and K_1 , K_2 denote respectively, the metering rates vector of several ramps at time step k , the metering rates vector of several ramps at time step $(k-1)$, the measured occupancies vector at time step k , the downstream measured occupancies vector for each ramp, the critical occupancies vector corresponding to each value, and the matrix weighting factors.

The factors K_1 and K_2 determine how much is the impact of a detector on the metering rate of a certain ramp. The first matrix with a weighting factor K_1 presents the impact of the measured occupancy by any detector along the mainline on the metering rate, and K_2 measures the impact of the critical detectors on the metering rate of a certain ramp (Scariza, 2003; Bogenberger and May, 1999).

3.5.7.2 Linear programming

Before the use of dynamic control algorithms, linear programming based ramp metering algorithms were widely deployed in developing time of day ramp metering rates (Yoshino et al., 1995). Linear programming based ramp metering firstly was deployed on Hanshin Expressway, Kobe, Japan in 1970 where the control algorithm uses the mainline occupancy and demand values to solve the optimization problem simultaneously. With the defined constraints a maximization or minimization equations are defined to represents the ramps, for further details about the used algorithm check (Bogenberger and May, 1999). The noticed drawbacks of this algorithm that it is totally based on the accurate O-D data and it has a static form by neglecting the travel time variation during the ramp rates computation.

3.5.7.3 Coordinated ramp metering using artificial neural networks

This volume-capacity ratio (V/C) based algorithm was first suggested by Wei and Wu (1996) where a metering plans are generated by a traffic simulation model (FREEQ10PC) and a ramp control expert system. The metering rates are evolved by using Artificial Neural Networks (ANN), see Figure 3.8. The algorithm suggested by Wei and Wu (1996) it does not has adaptive form, therefore the algorithm suggested by (Zhang 1995, scholarship) presents an adaptive algorithm since the neural network controllers adapt themselves online. Accordingly, V/C ratios must be calculated upstream and downstream of the ramp with ramp queue detectors (Bogenberger and May, 1999).

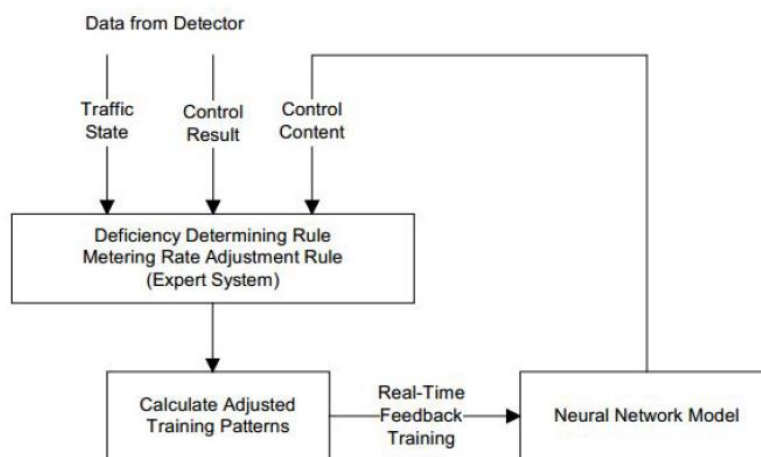


Figure 3.8: ANN based ramp control flow chart (Bogenberger and May, 1999).

The metering rate is determined basing on the pre-defined pattern by matching this information on the local level. The computed metering rate is considered by this local ramp, in the same time is used an input data via the hidden layer for other ramps so that all ramps are coordinated widely in an integral way. In order to maintain V/C under 1, the system receives the new data and combine them with the previous time step output. The process is visualized in Figure 3.9.

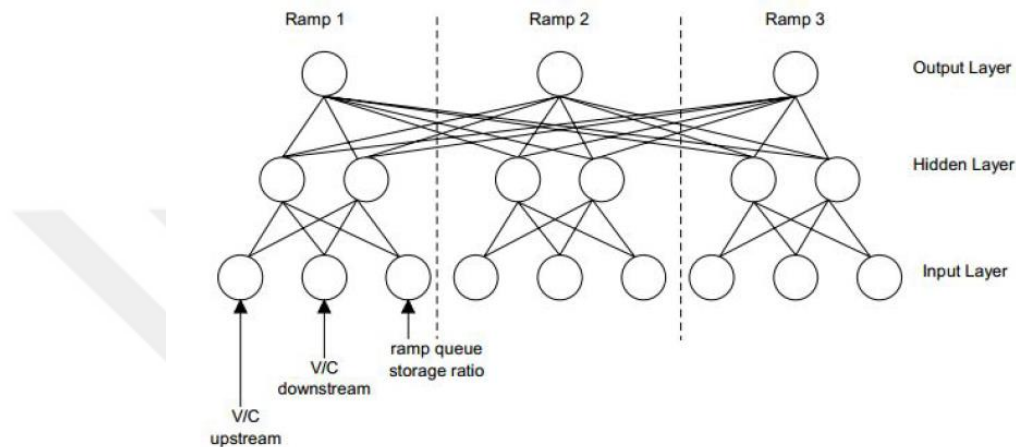


Figure 3.9: Conceptual operation of ANN (Bogenberger and May, 1999).

3.5.7.4 Fuzzy logic

The fuzzy logic algorithm was first introduced in 1989 in the Netherlands, and in 1999 in Seattle, USA. Fuzzy logic based algorithms are sophisticated algorithms divide measurements into classes using qualitative measurements and human reasoning to react properly to the upcoming traffic. With different weighting factors and a set of fuzzy rules, this algorithm is able to convert the fuzzy measurements to metering rates. Fuzzy logic algorithms can avoid congestion formation before it occurs and efficiently use imprecise detector data. Another, more recent example of an integral algorithm is the fuzzy logic algorithm (Meldurm and Taylor 1995), used today in Seattle, Washington. The general operation of the algorithm follows (Bogenberger and May, 1999):

- 1) Fuzzification: the measured traffic data (occupancy) is transferred into classes (textual description) to a certain degree, for example, 35% small, 70% medium, and 0% high.
- 2) Inference: plausible {IF}-{THEN}-{ELSE} rules process the data.

3) Defuzzification: the results are transferred into metering rates.

The interpretation of data as multiple states makes of this type of algorithms more plausible and robust. However, using the plausible rules demands a high knowledge of the operator and they must be adjusted to the real conditions especially if they change along the freeway. (Zhang et al., 2001) developed an Adaptive and Coordinated Control of Entrance Ramps with Fuzzy Logic (ACCEZZ) where the plausible rules adjust themselves to the mainline conditions. The mainline upstream occupancy and the V/C ratio are used for computing the metering rates.

3.5.7.5 Dynamic ramp metering

Dynamic control algorithm was developed by Chen et al. (1997) as a system-wide, adaptive, and predictive algorithm where it has four layers:

- 1) State estimation.
- 2) O-D prediction.
- 3) Local control.
- 4) Area-wide control.

The algorithm attempts locally to maintain the traffic conditions close to the provided conditions by the area-wide controller that presents a dynamic predictive optimal control model. The system-wide control model derives the metering rates by minimizing the system travel time including delays on ramps subjected to demand and queue capacity constraints. Also, the state estimation and O-D models are used for traffic conditions prediction. Both local and area-wide controllers are combined as the following:

$$r_t = \bar{r}_k - K(o_t - \bar{o}_k) \quad (3.26)$$

Where r_t , o_t , \bar{r}_k , \bar{o}_k , and K denote respectively, the local ramp metering rate, occupancy, the ramp metering rate set by the area-wide control algorithm, the occupancy set by the area-wide control system, and a regulator parameter.

3.5.7.6 HERO

HEuristic Ramp metering coOrdination (HERO) algorithm was discussed in (Papageorgiou et al. 2006; Papamichail and Papageorgiou, 2008) uses the real-time

measurements without performing real-time calculations or external disturbance prediction. The control strategy is based on two algorithms, local control algorithm which is originally ALINEA and a coordinated algorithm called HERO. The control algorithm is instigated in case if at one of the ramps the critical queue length is reached and this ramp is activated as a master-ramp so that the other upstream ramps are recruited as slaves (Yuan, 2008). Same as other coordinated control strategies, the algorithm uses the ramps' storage capacity to relieve the critical ramp. HERO controls the queue length by using gradually up to 6 upstream ramps to relieve the burden as the following (Papamichail et al., 2010):

$$queue_{min}(k) = \frac{queue_{max}(k) \times \sum_{i=1}^n queue_i}{\sum_{i=1}^n queue_{i,max}} \quad (3.27)$$

Where $queue_{min}(k)$, $queue_{max}(k)$, $queue_i$, and $queue_{i,max}$ denote respectively, the required minimum queue length at the slave ramp k , the maximum queue length at the slave ramp k , the actual queue length at master and slave ramps in the coordinated control, and the maximum queue length at master and slave ramps in the coordinated control.

The desired minimum queue length is reached by the local level controller as the local algorithm will reduce the cycle time at slave-ramps meanwhile the master ramp controller will act independently from the coordinated system.

3.6 Evaluation Studies

Various types of ramp metering control strategies have been introduced and developed, however, a few of them was used in the real life. The evaluation of ramp metering system can take two paths, either by real-filed implementation or simulation-based evaluation. Simulation based evaluation studies can use real freeway sections with real data or hypothetical section with assumed demand data. In this subsection, different evaluation studies are presented.

3.6.1 Field operational evaluation

Papageorgiou et al. (1997) provided comparative field trials conducted in various countries to assess and compare the efficiency of local ramp metering strategies,

whereby ALINEA outperformed feedforward-based strategies with respect to all evaluation criteria. Some examples of these field trials a number of local ramp metering strategies were applied in the field at a single ramp of Boulevard Peripherique in Paris it was found that ALINEA led to a maximum improvement in all measures (total travel time (TTT), total waiting time at the ramps (TWT), total time spent (TTS), vehicle miles traveled (VMT), etc.) compared to the other strategies namely demand–capacity and fixed timing. Similar results were found for A10 West Motorway in Amsterdam. ALINEA and METALINE were also tested at multiple on-ramps of the clockwise Boulevard Peripherique, where the results mostly are the same. (Jacobson, et al., 1989) measured the effectiveness of FLOW ramp metering strategy in the Seattle metropolitan area. The waiting of individual vehicles on the metered on-ramps was reduced from 5-8 minutes to 2 minutes per vehicle. The mainline traffic volumes in the morning peak period have increased up to 49%. (Papamichail et al., 2010) evaluated the performance of HERO at 6 consecutive inbound on-ramps on the Monash Freeway in Melbourne, where the utilized strategy showed improvement on the traffic throughput and travel time reduction. Bhourri et al. (2013) performed an evaluation study on A6W motorway in Paris, France to compare the improvement in the travel time reliability and traffic impact considering coordinated and isolated ramp metering ALINEA. With respect to the travel time reliability, both strategies showed improvement with similar results. Wu et al. (2007) carried out an investigation study to monitor the potential impacts of ramp metering strategy ALINEA on driving behavior. The driving behavior parameters that considered are speed, headway, acceleration and deceleration, the size of accepted gaps, merge distance..., etc. ALINEA showed a considerable improvement on the merge conditions of traffic, nevertheless; it caused minor speed reductions on the corridor during the metering time.

3.6.2 Simulation based evaluation

Some other simulation-based evaluation studies have been mentioned by Papageorgiou et al. (1990 & 1991) where ALINEA and coordinated feedback control algorithm (METALINE) were tested in simulation for Boulevard Peripherique in Paris using the macroscopic traffic simulator. Both strategies were found to decrease the total travel time under normal conditions. Chu et al. (2004) considered three well-

known adaptive ramp metering algorithms: ALINEA, BOTTLENECK, and ZONE in an evaluation study using a capability-enhanced PARAMICS simulation model. The evaluation has been conducted over a stretch of I-405 freeway in California under both recurrent and non-recurrent congestion scenarios. According to the results, ALINEA showed a good performance under both scenarios, however; BOTTLENECK and ZONE strategies are found more efficient using ALINEA as the native local occupancy control local algorithm than ALINEA alone. Abdel-Aty et al. (2007) used micro-simulator PARAMICS to evaluate the performance of ALINEA for real-time safety improvement. The study has utilized on 9 miles section of Interstate-4 freeway in metropolitan Orlando area where the results showed that using the feedback ramp metering algorithm ALINEA at multiple locations provided a significant decrease in the risk of crashes without any adverse effects on the freeway operation. Demiral and Celikoglu (2011) utilized ALINEA for a single lane merging ramp to Bosphorus strait crossing the bridge in Istanbul using real and theoretical data where the evaluation results showed that ALINEA has performed effectively in all scenarios. Abuamer et al. (2016), and Abuamer and Celikoglu (2017) evaluated the improvement in traffic volume, speed, TTS reduction, occupancy reduction, and vehicle emissions reduction considering ALINEA as a ramp meter utilized on a section of D-100 freeway, in Istanbul.



4. PROBLEM STATEMENT AND PROPOSED CONTROL STRATEGIES

The main contribution of this research is a comparative evaluation and analysis study considering the utilization of different ramp metering control strategies on Istanbul freeways. According to the previously conducted studies on Istanbul freeways, (Demiral and Celikoglu, 2011; Abuamer et al., 2016, Sadat and Celikoglu, 2017), the local ramp metering strategy ALINEA showed a noteworthy improvement in traffic conditions over the considered evaluation criteria. In this research, a comparative performance evaluation case-study of ALINEA with its full version PI-ALINEA considering different measures of effectiveness (MOEs) aspects which will be explained in chapter 6. Figure 4.1 gives a general view of the problem formulation.

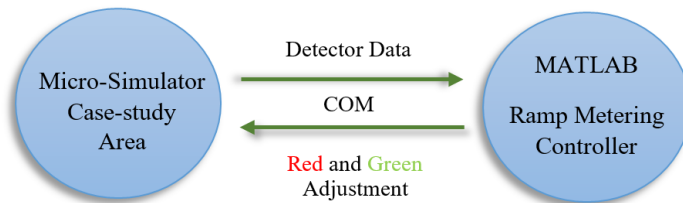


Figure 4.1: Problem formulation.

The following pseudocode gives a general description of the problem formulation in MATLAB.

Step1: Create a new COM server.
Step2: Load the network.
Step3: Load the layout.
Step4: Set the simulation period as a variable *time*.
Step5: Get all detector groups, 1,2, and 3. “each group contains 3 detectors, each cover 1 lane”
Step6: Get the occupancy values of each group, group1: oc1, oc2, oc3 group 3: oc7, oc8,
and oc9. “the downstream occupancy that will be used in the control algorithm”
Step7: Initialization of a1=0, a3=0; as variables for the average occupancy.
Step8: FOR the time interval [1 *time*] with a time step *i*
Run a single time step simulation

“ call the necessary parameters for the proposed control algorithm”

The average of the 1st group’s occupancies as $\rightarrow a1 = (oc1+oc2+oc3)/3$.

The average of the 2nd group’s occupancy values as $\rightarrow a2 = (oc4+oc5+oc6)/3$

The average of the 3rd group’s occupancy values as $\rightarrow a3 = (oc7+oc8+oc9)/3$

Verify every 90 seconds “update cycle” as \rightarrow

IF rem (i/90)==0;

Get the 1st on-ramp flow output as $\rightarrow flow1$

Get the 2nd on-ramp flow output as $\rightarrow flow2$

Get the 3rd on-ramp flow output as $\rightarrow flow3$

Define the control algorithm using the above defined parameters, for example define

ALINEA as \rightarrow

meteringRate1 = $flow1 + K_R(O_{cr}-a1)$;

meteringRate2 = $flow2 + K_R(O_{cr}-a2)$;

meteringRate3 = $flow3 + K_R(O_{cr}-a3)$;

CHECK

IF meteringRate1 $\leq r_{min}$ “ minimum metering rate)..... THEN.....

The green time = $(r_{min} / 2000)*90$ “ 2000 is the saturation flow of the ramp and 90 is the cycle time”

ELSEIF meteringRate1 $> r_{min}$ and $< r_{max}$ THEN.....

The green time = $(meteringRate1 / 2000)*90$

ELSE

The green time = $(r_{max} / 2000)*90$

END

IF meteringRate2 $\leq r_{min}$ “ minimum metering rate)..... THEN.....

The green time = $(r_{min} / 2000)*90$

ELSEIF meteringRate2 $> r_{min}$ and $< r_{max}$ THEN.....

The green time = $(meteringRate1 / 2000)*90$

ELSE

The green time = $(r_{max} / 2000)*90$

END

IF meteringRate2 $\leq r_{min}$ “ minimum metering rate).... THEN.....

The green time = $(r_{min} / 2000)*90$

ELSEIF meteringRate2 $> r_{min}$ and $< r_{max}$ THEN.....

The green time = $(meteringRate1 / 2000)*90$

ELSE

The green time = $(r_{max} / 2000)*90$

END

END “ first conditional statement end”

AGAIN Initialization of $a1=0$, $a3=0$;

END

The following sections provide a brief literature on the proposed control strategies with full parameters definitions.

4.1 ALINEA

ALINEA is a classical feedback based control algorithm suggested by Papageorgiou et al. (1991), therefore the metering rate is a function of the previous time interval metering rate, referring to equation (3.6) $O_{out}(k)$ is the collected measured average occupancy during the control time interval $[(k-1)T, (k)T]$, same $r(k)$ is the metering rate will be assigned for the time interval $[(k)T, (k+1)T]$ (Wang et al., 2014). The term T is the activation time period of ALINEA, it will be discussed later in this section.

From a heuristic approach for the current control step, if the measured occupancy $O_{out}(k)$ is smaller (greater) than \hat{D} , then the second part of the right-hand term will be positive (negative) and the new metering rate is increased (decreased) compared with $(k-1)$. This presents a dynamic response to any changes in the traffic, even slight ones (Papageorgiou et al., 1991). As postulated in (Wang et al., 2014), the inflow $r(k)$ resulted from equation (3.6) must fall within the range $[r_{min}, rr_{max}(k)]$, since r_{min} to avoid the ramp closure and $rr_{max}(k)$ is determined by:

$$rr_{max}(k) = \min\{r_{max}, q_r(k-1) + 400\} \quad (4.1)$$

Where r_{max} and $q_r(k-1)$ are the saturation flow of the ramp, the measured ramp flow for the time interval $[(k-1)T, (k)T]$, and 400 vehicles/h is an empirical value.

Otherwise $r(k)$ is curtailed and replaced by r_{min} or r_{max} , still it must enter as $r(k-1)$ in the next time step to avoid the well-known wind-up effect of such Integral (I) type regulators as ALINEA. For single-lane ramps Papageorgiou et al. (1991) and Papamichail and Papageorgiou (2008) suggest typical values of 200-400 (veh/h) and 1800 (veh/h) be used for r_{min} and r_{max} respectively.

4.2 Parameters Calibration

ALINEA is a case-dependent control algorithm with four parameters need to be calibrated as mentioned in (Abdel-Aty et al., 2007; Wu et al., 2007; Papageorgiou et al., 2008). The parameters are:

- 1) The first parameter is the downstream detector location which should be at the congestion originated point that is usually 40 to 500 m downstream from the

ramp nose. The approximated location of the congestion originated point can be determined using the occupancy-distance profile for the merging area, starting from the downstream side.

- 2) The second parameter is \hat{O} that could be equal or slightly less than the occupancy at capacity (O_{cr}). Papageorgiou et al. (2008), suggests two ranges (either from 19% to 21% or from 30% to 31%) for \hat{O} based on the volume and occupancy relationship. The second range indicates that ALINEA can also perform well in case of heavy traffic conditions. Abuamer et al. (2016) used three values 18, 25 and 30% as the desired occupancy, where ALINEA gave the best results at 25%. Also, \hat{O} can be determined using the occupancy profile by obtaining the inflection point value, which can be used the same or factorized to the purpose of section utilization.
- 3) The third parameter is K_R , Papageorgiou et al. (2008) and Papageorgiou et al. (1991) state that ALINEA performed well for $K_R=70$ (veh/h/%) in real life experiments, where it can vary between 70 and 120 without any significant effect on the metering rates. Increasing K_R value can lead to stronger regulator reactions with a short time, contrary; decreasing it lead to smoother reactions of the regulator with a longer time.
- 4) The fourth parameter is the cycle updating time, where it ranges from 40 seconds to 5 minutes, however; in the case of a very small updating time, the detector location should be close enough to the ramp entrance. If not, congestion may build-up in the stretch between the ramp nose and the detector.

ALINEA is based on the assumption that vehicles will reach the downstream detector within a time period T , which refers to the activation time of the controller. The determination of T is very important since the new entering vehicles have to reach the downstream detector thus the new value of $O_{out}(k)$ can be updated. Referring to Figure 4.2, assuming that the traffic signal is setup at the entrance of the acceleration lane, Δx_1 is the distance between the entrance of the acceleration lane and the downstream detector, and \bar{u}_{merg} is the average speed of merging vehicles. In order to hold the assumption mentioned above, the condition $T > \frac{\Delta x_1}{\bar{u}_{merg}}$ must be satisfied (Wang et al., 2014).

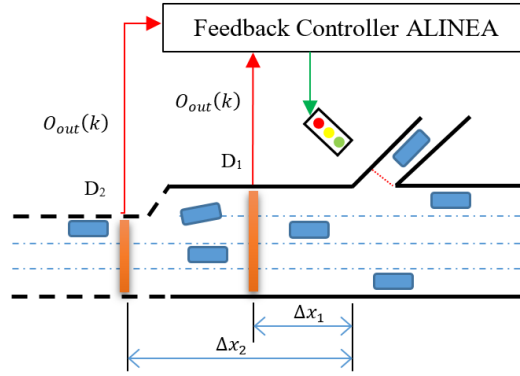


Figure 4.3: ALINEA controller layout.

4.3 PI-ALINEA

In the case of bottlenecks exist further downstream from the merging area, it is more perspective that congestion appears firstly at the downstream of the bottlenecks. In this case, the detector measurements must be from the bottleneck area rather than from the merging area otherwise the above-mentioned assumption cannot be held. In such cases, Wang et al. (2014) extended ALINEA by adding a proportional term, since PI-regulator is more appropriate in the case of slow dynamics. According to equation 3.7:

$$r(k) = r(k - 1) - K_P [O_{out}(k) - O_{out}(k - 1)] + K_R [\hat{O} - O_{out}(k)]$$

The second part of the right-hand term in the equation presents the instant change in the occupancy which can be significant in the case of bottlenecks exist further downstream from the merging area, where T will be increased compared with Δx_2 . For a brief explanation, see the linearized system analysis section in (Wang et al., 2014).



5. STUDY SITE AND DATA DESCRIPTION

The geographical and historical place of Istanbul made it one of the most metropolitan areas in the world, where it is the connector between Europe and Asia. Istanbul is characterized by its huge transportation network and increasing urban expanding. The state road D-100 and the European E-80 route are the two main freeways connect Europe and Turkey, where they lead east to Ankara and west to Edirne. Many segments along these freeways suffer from recurrent congestions, however, for utilizing ALINEA we have chosen a congested segment from D-100 freeway starts from Zincirlikuyu and ends at Okmeydani within 3.96 km length and consists of two links (link-1 and link-2) each link has 3 lanes. This segment is considered one of the most congested sections of D-100 freeway since it is connected by three on-ramps along a short length. Nevertheless, link-1 was considered for the evaluation study since there are enough Remote Traffic Microwave Sensors (RTMS) to hold the flow conservation principle. Figure 5.1 presents a sketch of link-1 including three on-ramps (ON-1, ON-2, and ON-3), off-ramps (OFF1 and OFF2) and the RTMS detectors (301, 533, and 534).

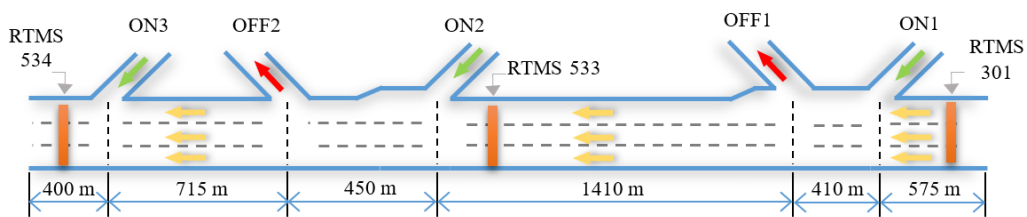


Figure 5.1: Section Sketch.

5.1 Congestion Periods

Data were provided by the municipality of Istanbul including traffic volumes, speed, and occupancy. The data has been extracted from RTMS detectors number 301, 533 and 534. The congestion has been measured using the speed as a direct indicator where the traffic volumes cannot be used since low volumes can occur in congested

and uncongested phases. Occupancy and density can be also used, but still using the occupancy requires a relatively accurate estimation of the capacity as same as for density. By initial observation, the chosen section shows a severe congestion along 5 hours' time period (6:30 to 11:30 am) at merges ON1 and ON2. Figure 5.2 presents the speed profiles captured by the detectors from the mainstream line. Because of the software calculations, the first 3 hours are considered for this study.

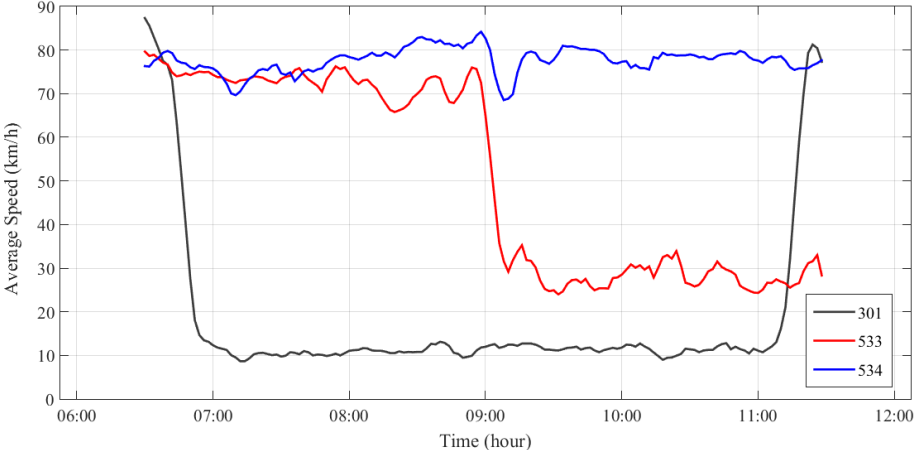


Figure 5.2: Congestion Observation.

5.2 Data Description

The provided data present 2 minutes data for each lane of the freeway, so it is considered as a population, not a sample. All lanes show the relatively similar speed values as the Figures 5.3, 5.4, and 5.5 depict.

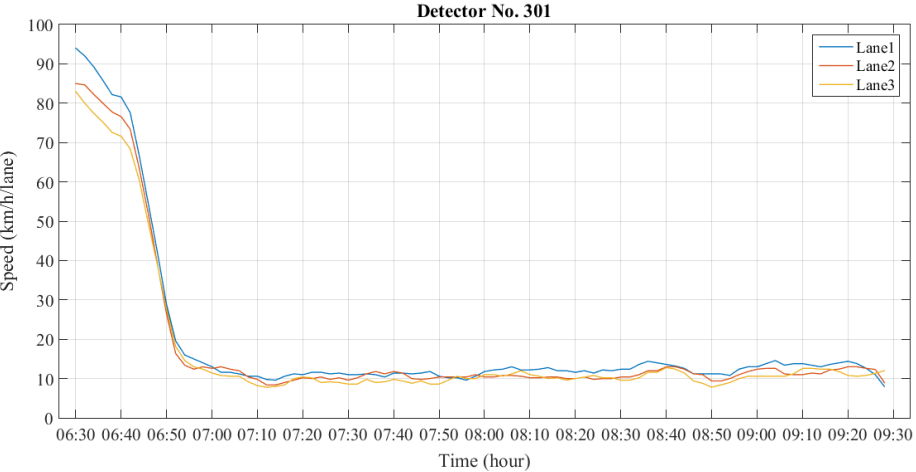


Figure 5.3: Speed time-series profile for detector No. 301.

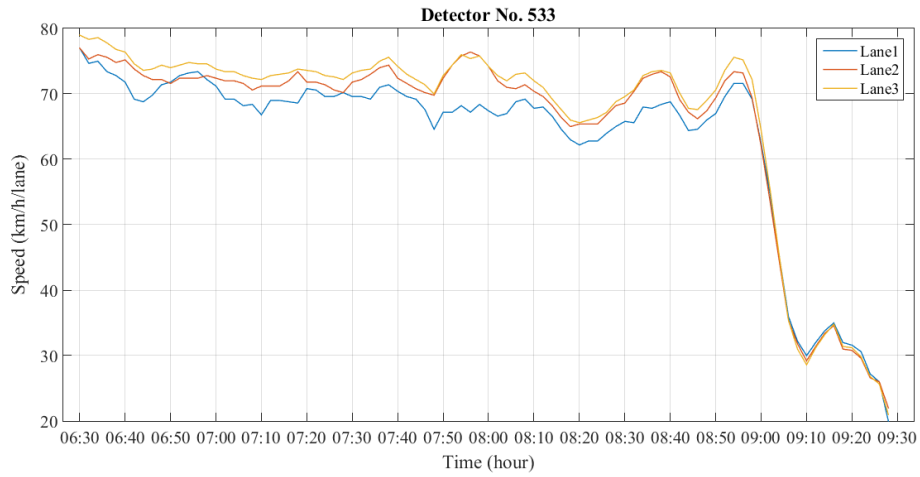


Figure 5.4: Speed time-series profile for detector No. 533.

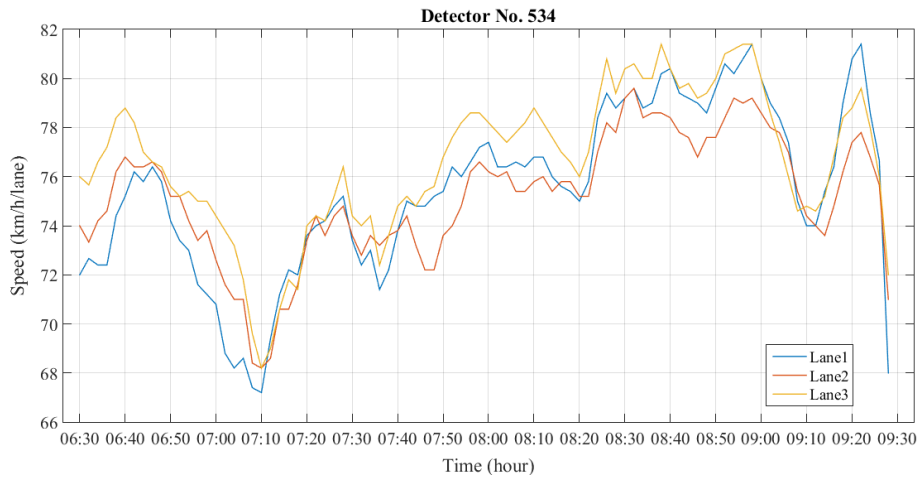


Figure 5.5: Speed time-series profile for detector No. 534.

For the purpose of the traffic model calibration, it is very important to identify the nature of this data (first 3 hours of the congestion period), for example, the mean value of each set, variation including the upper and lower boundaries, and the Standard Deviation (SD). Tables 5.1, 5.2, and 5.3 provides some descriptive measures on the captured traffic parameters data including volume, speed, and occupancy respectively.

Table 5.1: Descriptive measures (summary-1).

Parameter	Unit	Data Type	Detector	Mean	SD	Upper Limit	Lower Limit
			301-main	1955	679	4380	1050
			301-ON1	3853	361	4740	2850
Volume	Veh/h	discrete	533-main	3773	357	4650	2730
			533-ON2	840	360	1830	360
			534	3950	464	5040	2850

Table 5.2: Descriptive measures (summary-2).

Parameter	Unit	Data Type	Detector	Mean	SD	Upper Limit	Lower Limit
			301-main	18.12	20.28	87.33	6.000
			301-ON1	68.98	2.750	75.75	60.75
Speed	km/h	continuous	533-main	66.84	15.68	82.00	21.33
			533-ON2	22.28	19.68	80.00	6.000
			534	78.28	4.877	90.00	54.33

Table 5.3: Descriptive measures (summary-3).

Parameter	Unit	Data Type	Detector	Mean	SD	Upper Limit	Lower Limit
			301-main	37.95	9.880	65.0	8.333
			301-ON1	10.97	1.780	16.76	7.500
Occupancy	-	continuous	533-main	13.84	3.607	37.66	7.000
			533-ON2	26.32	7.638	50.00	13.00
			534	11.70	3.415	25.00	6.000

6. MODELING AND SIMULATION

The success or failure of traffic management strategies is case-dependent. While a measure like a ramp meter, is successfully implemented in a number of cases, it may cause severe issues for some other cases. Ramp metering strategies are different in operation and implantation, not all of them are effective measures for all cases. Generally, traffic management policies are tested through either limited implementation or simulation. Traffic simulation is less time to consume and more economical compared to the real-world implementation for the purpose of assessing various traffic management measures. As mentioned in the second chapter, traffic simulation models can be divided into microscopic, mesoscopic, and macroscopic models.

Microscopic traffic models describe the traffic behavior at the level of individual vehicles by delineating the positions and velocities of all interacting vehicles between themselves and the infrastructure. Due to this detailed level of description, microscopic traffic simulators have become progressively more famous and common in recent years in freeway traffic operations analysis. These tools use stochastic approaches in modeling traffic conditions by giving a set of geometry, traffic demands, vehicles' routing, and drivers' behavior as inputs. Available stochastic microsimulation models are FLEXTYT-II-, FOSIM, PARAMICS and VISSIM. In this study, VISSIM is chosen because of the ability to integrate the model with MATLAB via COM which allows us to utilize the proposed control strategies online.

6.1 Software Description

VISSIM is a microscopic/stochastic traffic simulator based on Wiedemann (1974 and 1991) models which combines a perceptual model of the driver with a vehicle model. VISSIM is based on a discrete, stochastic, time step based microscopic traffic flow model, with driver-vehicle-units as single entities (PTV AG, 2015). This model includes a psycho-physical car-following model for longitudinal vehicle movements and a rule-based algorithm for lateral movements.

6.1.1 Driving behavior model

The driving behavior model involves a classification of reactions in response to the perceived relative speed and distance with respect to the preceding vehicles. According to Wiedemann model, four driving modes are: free driving, approaching, following, and braking, see Figure 6.1.

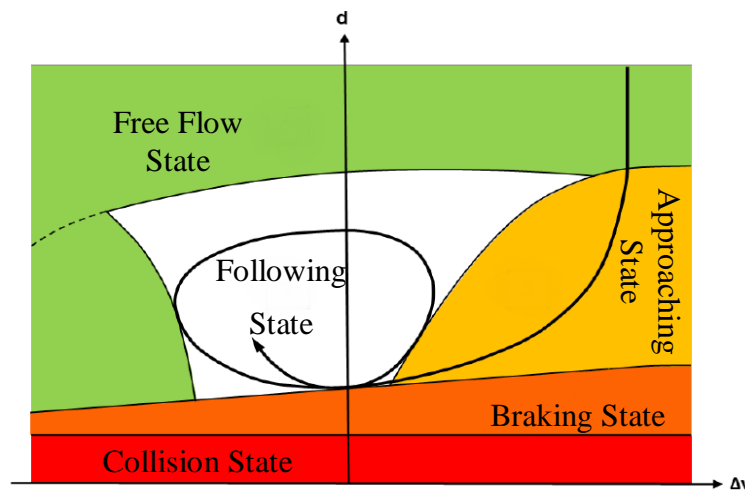


Figure 6.1: Car following model (PTV AG, 2015).

- I. Free driving: no interaction between vehicles, where driver tries to reach a certain desired speed. The speed in free driving behavior state is not stable; however, it oscillates around the desired speed because of the flawed throttle control.
- II. Approaching: the first phase of vehicles interaction, where the driver decelerates in order to maintain zero speed difference with the preceding vehicle once the desired safety distance is reached.
- III. Following: the driver maintains a relatively constant safety distance with the preceding vehicle.
- IV. Braking: applying high deceleration rates in case if the safety distance is lower the critical value.

For each mode, driver reacts differently as a result of distance, speed, speed difference, and the individual characteristics of driver and vehicle. The switching between modes happens once the driver reaches a certain threshold combination of speed difference and distance. The ability to identify speed differences and estimate the distance differs according to the driver characteristics such as desired speed and

desired safety distance. Accordingly, the expression psycho-physical car-following model comes from the combination of psychological characteristics and physiological restraints of the driver's perception.

VISSIM provides the ability for assigning stochastic variations of several parameters such as desired speed distribution, accelerations, occupancy distributions, etc. Also, it supports stochastic sources of flow rates and compositions. The model introduces the randomness ability of drivers to distinguish changes in relative speeds and distances and to determine their mode of driving (Fellendorf and Vortisch, 2001; PTV AG, 2015).

6.1.2 Lane changing rules

Lane changing occurs in case if a driver has to drive slower than the desired speed because of the leading vehicle or diverging from the mainstream to reach an upcoming exist such as an off-ramp. Therefore, VISSIM distinguishes between two lane changes (PTV AG, 2015):

- I. Necessary Lane change: a driver seeks to reach the next connector for his/her destination. For this lane change considers the maximum allowable deceleration of the vehicle and its trailing vehicle on the new lane. The deceleration rate relies on the emergency stop location of the next route connector.
- II. Free lane change: there is an enough distance for performing the maneuver and a higher speed is required. This free lane change depends on the safety distance to the trailing vehicle on the new lane which related to the speed of the vehicle seeking lane change and on the speed of the preceding one. The aggressiveness degree of free lane change cannot be changed, however free lane change can be influenced by changing the safety distance.

In both cases, the lane change maneuver depends on finding a suitable gap in the proceeded direction, where the gap size relies on two speeds: the speed of the vehicle performing the maneuver and the speed of the vehicle approaching from behind on the new lane. More comprehensive descriptions of the VISSIM model and software can be found in (Fellendorf and Vortisch, 2001; PTV AG, 2015).

6.2 Modeling and Calibration

The crucial step in using any simulation model generally and microscopic models especially is the calibration and validation stage, where the model results, as much as possible have to reflect the measured field results. VISSIM calibration and validation process for freeway traffic are associated with two elements: *micro-simulation traffic models*, and adjustment of *calibration parameters for freeway models*.

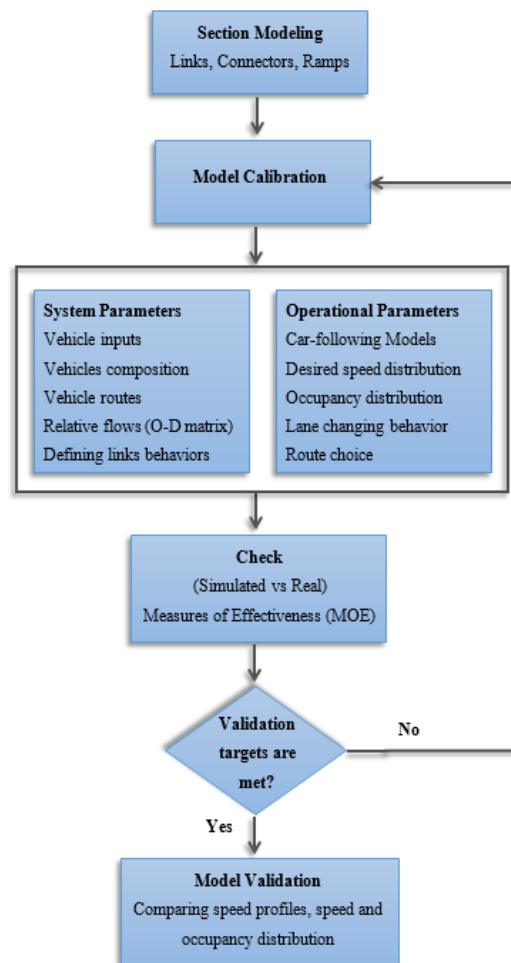


Figure 6.2: Calibration methodology flow chart.

Freeways parameters include system parameters and operational parameters. System parameters calibration process implicates investigation criteria of model input assumptions such as route choice, traffic demand inputs, vehicles composition, speed and occupancy distributions, study area geometric elements, seeding period .., etc. On the other hand, the calibration process of operational parameters focuses on a

detailed adjustment (or sensitivity analysis) of the driver behavior characteristics which control the overall traffic operations in the model.

Figure 6.2 depicts the methodology followed in order to calibrate the case-study model in VISSIM, where it follows three steps: network modeling, system parameters input and calibration, and operational parameters calibration.

6.2.1 Section modeling

As a first step, the section elements' (links, ramps, traffic signals ...etc.) are modeled based on a high-resolution map. Three types of links (mainline, connectors and ramps links) have been defined with the number of lanes, lane width, and driving behavior, see Table 6.1 and Figure 6.3.

Table 6.1: Links modeling summary.

Link	Lanes Number	Lane Width (m)	Driving behavior
Link-1	3	3.3	Freeway (free lane selection)
		3.3	
		3.3	
Link-2	3	5	Freeway (free lane selection)
		3.3	
		3.3	
Link-3	3	3.3	Freeway (free lane selection)
		3.3	
		3.3	
Link-4	3	5	Freeway (free lane selection)
		3.3	
		3.3	
Link-5	3	3.3	Freeway (free lane selection)
		3.3	
		3.3	
ON1	1	6	Urban (motorized)
ON2	1	4	Urban (motorized)
ON3	1	6	Urban (motorized)
OFF1	1	6	Urban (motorized)
OFF2	1	6	Urban (motorized)

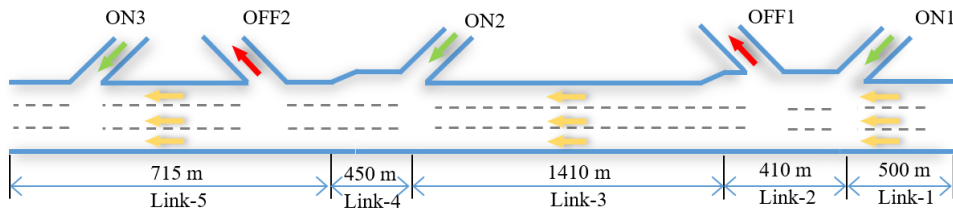


Figure 6.3: Section's links sketch.

After that, the section is divided into sub-sections in the purpose of providing weaving, merging, and diverging areas. The trigger of this is to provide a flexibility to use COM to change driving behavior and lane changing selection behavior over the congested sections once the traffic reaches its equilibrium phase, see Figure 6.4, 6.5, and 6.6.

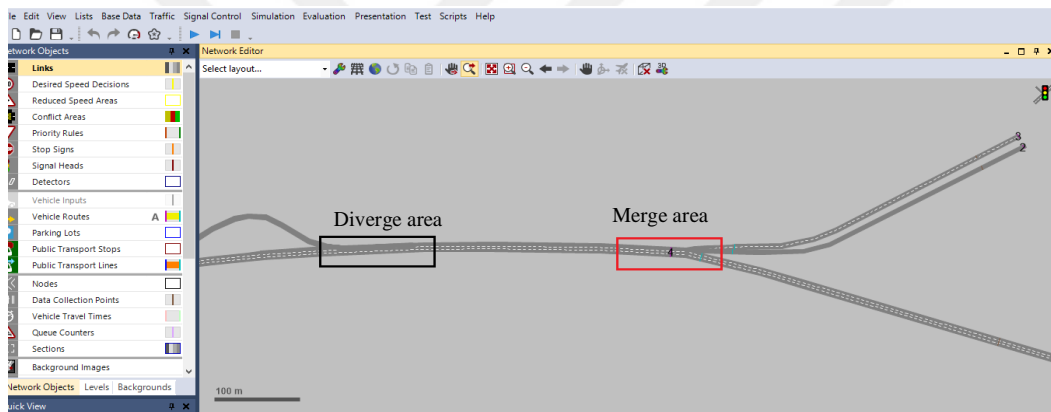


Figure 6.4: Section model part-1.

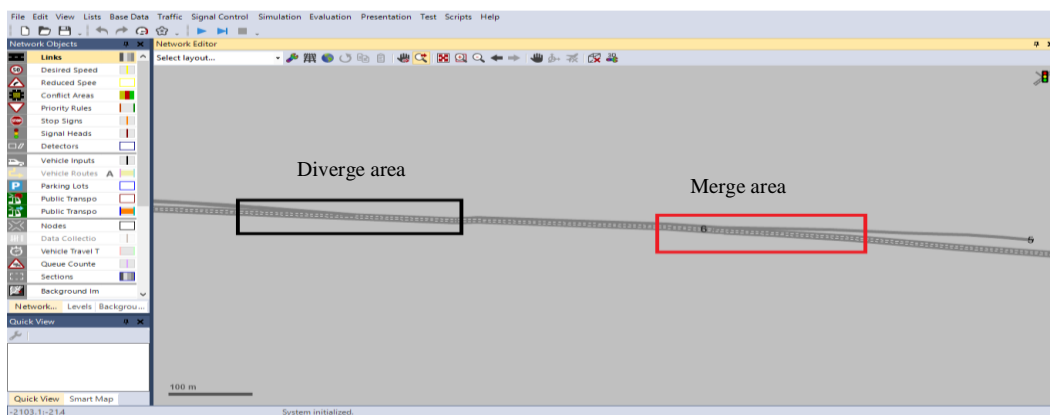


Figure 6.5: Section model part-2.

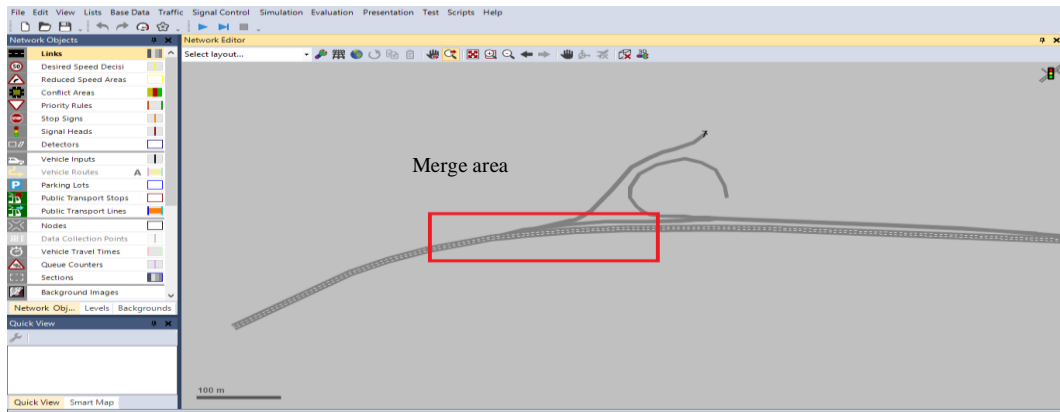


Figure 6.6: Section model part-3.

6.2.2 System parameters

System parameters base on how much variables the data contain, where more variables make the calibration process easier. The most dominant system parameters for the process of freeway model calibration are vehicle inputs, vehicles compositions, vehicles routes, and relative flows (O-D matrix).

6.2.2.1 Vehicle inputs and compositions

Essentially, vehicle inputs, speed, and occupancy distributions must be loaded from the nearest detector to the jam upstream. Referring to Figure 6.7 and 6.8, the traffic breaks at the first merging area (ON1), while approximately after two hours at the second merging area (ON2) the speed breaks slightly while the volumes remain the same manner. According to the above statement, it can be concluded that the exact traffic volumes captured from detector-301 cannot be used as vehicle inputs.

Moreover, as noticed on Figure 6.7, the volume breaks badly from 6:52 am until 11:10 am, so using any of these low volume values for the assumed simulation period (6:30 to 9:30 am) congestion will develop for the first few minutes then it will stop developing. In addition, the traffic volumes at detector-533 will be lower than the observed ones. Therefore, the actual traffic volumes based on the O-D matrix must be loaded as vehicle inputs, this can be done either by using a detector which captures the traffic before the jam (not available) or using the same values from detector-301 before the breaking point and repeats them over the simulation period.

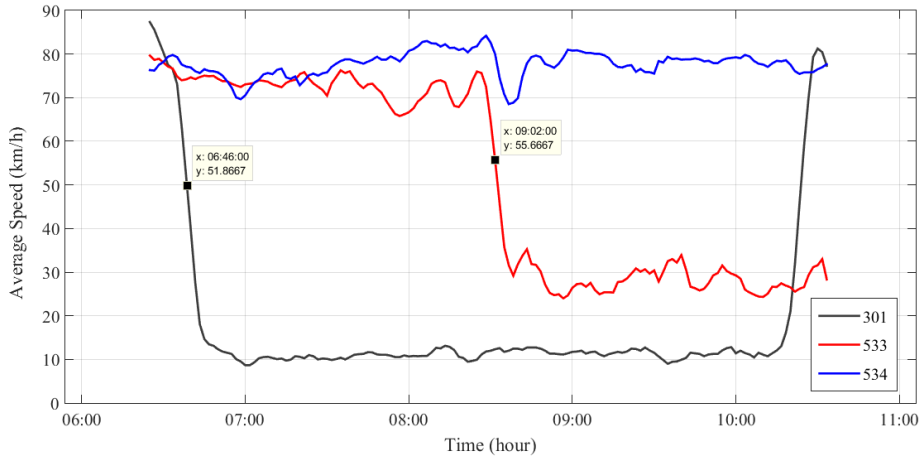


Figure 6.7: Speed time-series profile.

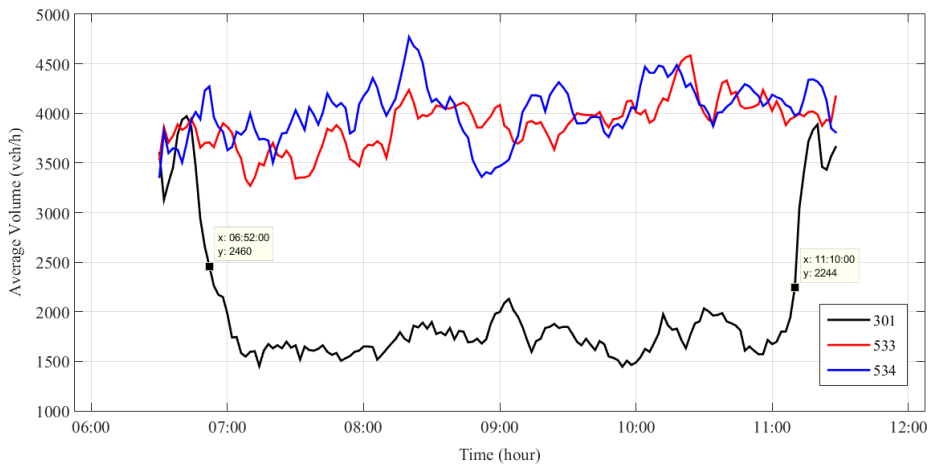


Figure 6.8: Volume time-series profile.

The first 14 volumes from detector 301 are repeated over the simulation period, where other ramps' volumes are loaded same as provided by the detectors. The provided data are equivalent for cars so no heavy vehicles or busses volumes included. Accordingly, one vehicle composition (car) is defined for all vehicle inputs. An initial seeding period (6 minutes is used) with the first volume value should be considered to load the network with vehicles.

6.2.2.2 Vehicle routes and relative flows

Defining vehicle routes is another crucial parameter considered for the calibration process. The first assumption in section modeling that is the vehicles come from the origin can take any arbitrary direction as a final destination. The section is divided into two route choice phases as depicted in Figure 6.9.

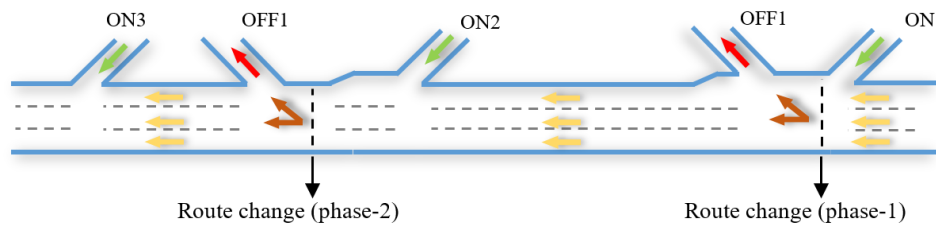


Figure 6.9: Vehicle route choice phases.

For each phase, the relative flow is the ruler which that determines the flow percent will take each route. The volume difference between the detector 301 and 533 cannot be considered the flow that will take the route OFF1 in the first phase. The reason is that the flow of a traffic stream cannot be considered as similar to the fluid stream flow because the fluid stream particles have the same speed which called steady-state flow conditions. The traffic volumes in our case do not show a steady-state flow condition between the detectors 301 and 533 which is clear in Figure 6.7, but still, this can only happen in the equilibrium phase. Still, the volume differences can be used to give an initial value for the relative flows in each phase. For phase-1, the relative flows are assumed 15%, 20%, and 25%. On the other hand, the volume difference between the detectors 533 and 534 can be used because steady-state flow conditions can be noticed as in Figures 6.7 and 7.8.

6.2.3 Operational parameters

VISSIM has many adjustable operational parameters that can be considered during the calibration process of freeway traffic. Freeway driving behavior parameter set which includes: car-following behavior (Wiedemann 74 suitable for urban traffic and merging areas and Wiedemann 99 for freeway traffic with no merging areas), lane-change behavior, gap acceptance, route choice, link occupancy distribution, and vehicle's speed and acceleration distributions. Rompis et al. (2014) state that CC0 (standstill distance), CC1 (time headway), and CC2 (following variation) are the most influential car-following parameters for calibrating freeway models in VISSIM. (Rrecaj and Bombol, 2015) presents a calibration study for freeway models in VISSIM, it postulates that freeway merging section depends on necessary lane changing and Wiedemann 99 car following parameters. Considering merging and

trailing vehicles' deceleration rates as well as the CC1 parameter will allow giving the priority to the ramp section or the mainline section. Diverging vehicles are most influenced by the necessary lane changing and lane change distance parameters.

The parameters are considered for calibration: relative flows, CC1, and desired speed distribution. For CC1 five values are set to (0.7, 0.8, 0.9, 1, and 1.1) considering the links in merge areas, where for others (diverging and waving areas) 0.9 seconds is used. By comparing the speed upper and lower limits before the traffic breaks down, the desired speed distribution (70:70 km/h) is used for each scenario with adding some changes so it can provide the maximum values as mentioned in the data description section, see Figure 6.10.



Figure 6.10: Desired speed distribution (70:70 km/h).

6.2.4 Calibration trails and validation

The last step in the calibration process includes checking if the model meets the required targets or not. According to the above-mentioned parameters assumptions (relative flow for route change in the first phase, desired speed, and time headways) 15 scenarios are run wherein each scenario data collection measurements are placed at the same location of the RTMS detectors in real life in order to detect the flow, speed, and occupancy measurements and compare them with the real data.

Geoffrey E. Heavers (GEH) statistic provides a performance indicator of the calibration process considering both relative and absolute difference between the observed and simulated values. GEH is given by:

$$GEH = \sqrt{\frac{2(M_{obs}(n) - M_{sim}(n))^2}{(M_{obs}(n) + M_{sim}(n))}} \quad (6.1)$$

Where $M_{obs}(n)$ and $M_{sim}(n)$ are the real-time volume and the simulated volumes respectively.

According to the Federal Highway Administration (FHWA) ‘if more than 85% of the measurement locations’ GEH values are less than 5, then the simulated flow would accurately reflect the real-field traffic flow characteristics (UK Highways Agency, 1996; Lyles et al., 2004). Tables 6.2, 6.3, and 6.4 summarize the GEH statistic measure for each scenario considering the mainstream traffic characteristics. Table 6.2 declares that for detector 301-main, the best scenario is a relative flow value of 15% for route change (phase-1) and headway time of 0.7 second for the first merging area. Table 6.3 declares that for detector 533-main, the best scenario is a relative flow value of 15% for route change (phase-1) and headway time of 1.0 second for the second merging area. Table 6.4 declares that for detector 534, the best scenario is a relative flow value of 20% for route change (phase-1) and headway time of 0.8 second for the third merging area, however, since the relative flow value can only be one value, the second best scenario (15% relative flow and 1 second headway time) is chosen.

As final model parameters, the desired speed of (70:70 km/h), a relative flow of 15%, and headway times of 0.7, 1.0, and 1.0 are used for the merges 1, 2, and 3 respectively. Figures 6.11, 6.12, and 6.13 depict the speed time-series profiles for the model validation.

Table 6.2: GEH Statistic Measures (detector 301-main).

Detector No.	Relative Flow (%)	Time Headway (s)	GEH Statistic Measures				
			GEH <5	Mean	S.D	Max.	Min.
301-main	15	0.7	90	0.95	0.78	3.57	0.00
		0.8	90	1.06	0.86	3.40	0.00
		0.9	90	1.11	0.88	4.73	0.00
		1	89	1.14	1.19	8.49	0.00
		1.1	90	1.12	0.96	4.71	0.00
	20	0.7	90	1.27	0.96	3.73	0.00
		0.8	89	1.26	1.07	5.86	0.00
		0.9	88	1.39	1.31	9.21	0.00
		1	89	1.45	1.17	7.52	0.00
		1.1	90	1.49	1.09	4.87	0.06
	25	0.7	89	1.50	1.06	6.08	0.00
		0.8	88	1.58	1.18	6.33	0.00
		0.9	88	1.60	1.28	7.43	0.00
		1	86	1.81	1.44	9.03	0.00
		1.1	89	1.63	1.11	5.59	0.00

Table 6.3: GEH Statistic Measures (detector 533-main).

Detector No.	Relative Flow (%)	Time Headway (s)	GEH Statistic Measures				
			GEH <5	Mean	S.D	Max.	Min.
533-main	15	0.7	88	1.80	1.27	5.51	0.00
		0.8	90	1.49	1.08	4.84	0.00
		0.9	90	1.56	1.11	4.67	0.00
		1	90	1.47	1.08	4.69	0.00
		1.1	89	1.64	1.24	5.37	0.00
	20	0.7	87	1.80	1.46	6.28	0.00
		0.8	88	1.85	1.33	6.01	0.00
		0.9	85	1.92	1.56	7.18	0.00
		1	85	2.09	1.47	5.63	0.00
		1.1	86	2.08	1.42	5.77	0.00
	25	0.7	87	2.61	1.38	6.89	0.09
		0.8	85	2.66	1.47	5.64	0.09
		0.9	83	2.79	1.61	7.28	0.10
		1	76	3.12	1.79	7.84	0.00
		1.1	82	2.92	1.44	6.27	0.48

Table 6.4: GEH Statistic Measures (detector 534-main).

Detector No.	Relative Flow (%)	Time Headway (s)	GEH Statistic Measures				
			GEH <5	Mean	S.D	Max.	Min.
534	15	0.7	87	2.14	1.35	5.37	0.00
		0.8	85	1.80	1.49	6.78	0.00
		0.9	87	2.07	1.32	5.69	0.00
		1	89	1.82	1.34	7.08	0.00
		1.1	88	1.77	1.25	5.66	0.17
	20	0.7	90	1.74	1.26	4.61	0.00
		0.8	90	1.59	1.14	4.32	0.00
		0.9	87	1.64	1.29	6.17	0.08
		1	87	1.69	1.31	6.08	0.00
		1.1	89	1.72	1.30	6.45	0.00
	25	0.7	90	1.77	1.14	4.99	0.00
		0.8	87	2.01	1.31	6.02	0.00
		0.9	88	2.02	1.42	6.01	0.09
		1	87	2.15	1.44	5.61	0.00
		1.1	88	1.87	1.37	5.61	0.00

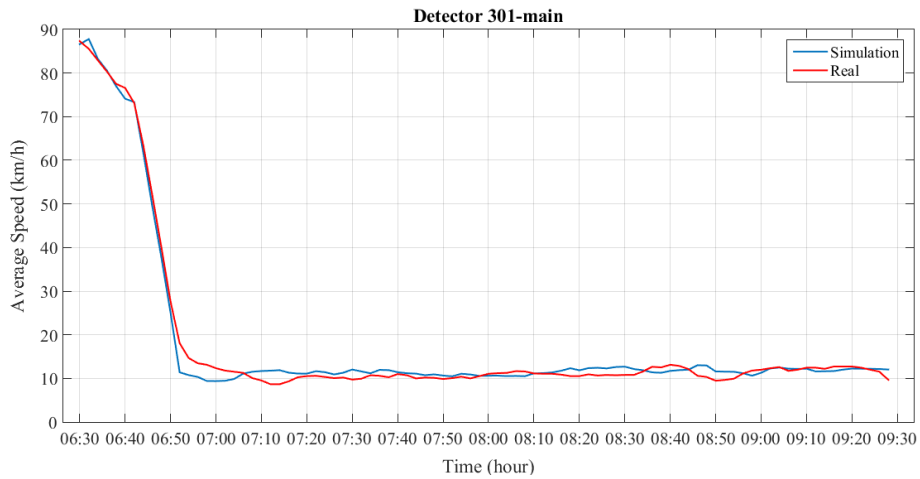


Figure 6.11: Speed time-series profiles for model validation (301-main).

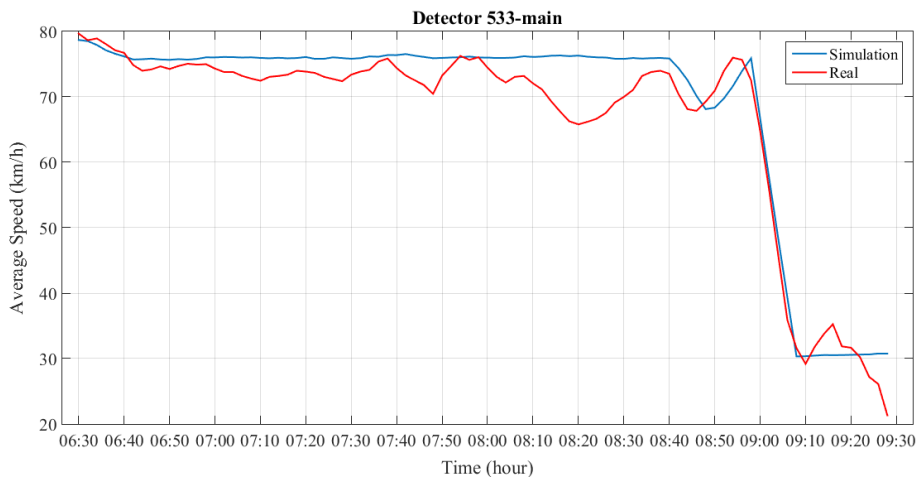


Figure 6.12: Speed time-series profiles for model validation (533-main).

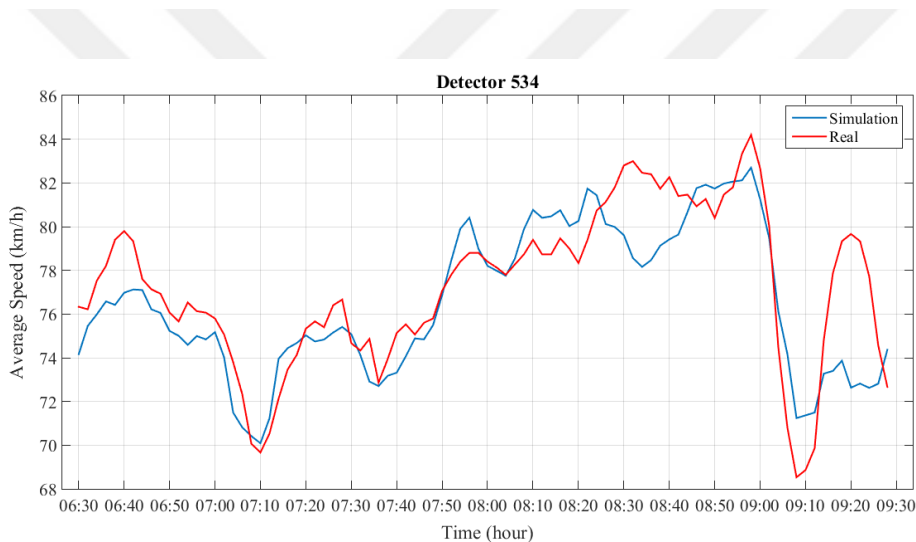


Figure 6.13: Speed time-series profiles for model validation (534-main).

6.3 Intervention via COM interface

The component Object Model (COM) interface is used to collaborate between the binary components of different programs. In this section, the COM interface components are introduced with guidelines and practical examples for using it to run VISSIM from MATLAB and utilize some control of VISSIM attributes.

6.3.1 The object model of VISSIM

The basic trigger of using COM is understanding COM-VISSIM model object hierarchy, see Figure 6.14. The presented hierarchy describes how COM-VISSIM

objects and sub-objects are leveled. The objects contain the model elements' properties as presented in Figure 6.15.

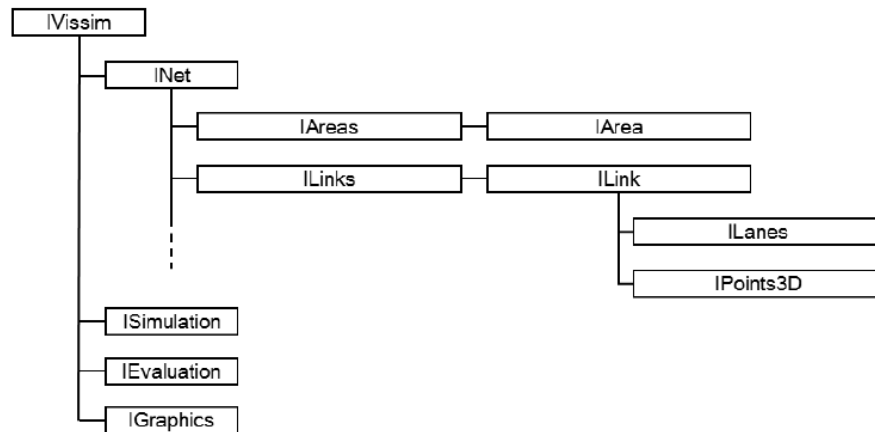


Figure 6.14: COM-VISSIM model object hierarchy (source: PTV AG, 2015).

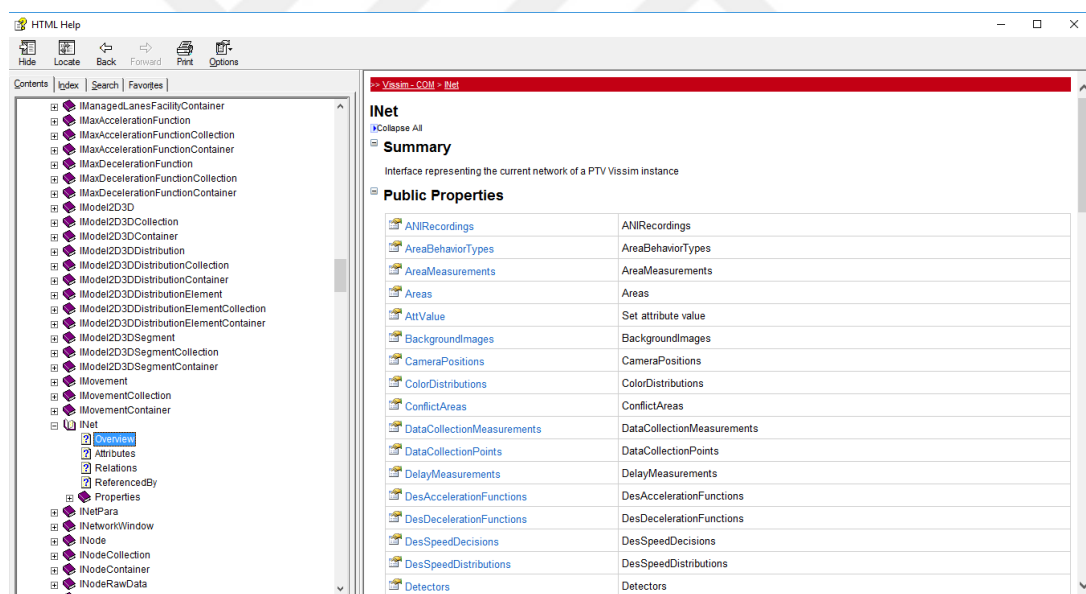


Figure 6.15: INet object properties.

6.3.2 Commands and methods

COM-interface has many important methods that allow the user to call and apply changes to any of the properties attributes. These methods present a set of commands which can be used to apply the required action from MATLAB through COM. In the following the most important commands which used in this study:

- 1) Get: requests and returns the properties of an object.
- 2) Set: allows MATLAB to define properties values of an object.

The above-mentioned commands are used to get online traffic characteristic measurements downstream of the merging area and return to the control algorithm. After the algorithm computes the required metering rate in order to utilize the downstream occupancy and convert it to a green time interval for the traffic signal, the command set is used to set these computed green time intervals to the traffic signal groups. Figure 6.16 depicts an MATLAB-COM code for setting a signal program. For more information about MATLAB-COM coding, the training examples in VISSIM documentations have a brief explanation.

```

64 % Set a signal controller program:
65 SC_number = 1; % SC = SignalController
66 SignalController = Vissim.Net.SignalControllers.ItemByKey(SC_number);
67 new_signal_programm_number = 2;
68 set(SignalController, 'AttValue', 'ProgNo', new_signal_programm_number);
69
70 % Set relative flow of a static vehicle route of a static vehicle routing decision:
71 SVRD_number = 1; % SVRD = Static Vehicle Routing Decision
72 SVR_number = 1; % SVR = Static Vehicle Route (of a specific Static Vehicle Routing Decision)
73 new_relativ_flow = 0.6;
74 set(Vissim.Net.VehicleRoutingDecisionsStatic.ItemByKey(SVRD_number).VehRoutSta.ItemByKey(SVR_number), 'AttValue', 'RelFlow(1)', new_relativ_flow);
75 % 'RelFlow(1)' means the first defined time interval; to access the third defined time interval: 'RelFlow(3)'
76
77 % Set vehicle input:
78 VI_number = 1; % VI = Vehicle Input
79 new_volume = 600; % vehicles per hour
80 set(Vissim.Net.VehicleInputs.ItemByKey(VI_number), 'AttValue', 'Volume(1)', new_volume);
81 % 'Volume(1)' means the first defined time interval
82 % Hint: The Volumes of following intervals Volume(i) i = 2...n can only be
83 % edited, if continuous is deactivated: (otherwise error: "AttValue failed: Object 2: Attribute Volume (300) is no subject to changes.")
84 set(Vissim.Net.VehicleInputs.ItemByKey(VI_number), 'AttValue', 'Cont(2)', false);
85 set(Vissim.Net.VehicleInputs.ItemByKey(VI_number), 'AttValue', 'Volume(2)', 400);
86
87 % Set vehicle composition:

```

Figure 6.16: MATLAB-COM code for signal controller program.

6.4 Experiment Set-Up

In Chapter 4 the proposed ramp metering algorithms (ALINEA and PI-ALINEA) are described briefly, where both of them share a set of parameters require to be calibrated before utilizing them. The first three parameters (downstream detector location, downstream desired occupancy, and update cycle time) are going to be determined where the last parameters K_R and K_P will be set as 70 and 120 (veh/h/%) since in the literature (Papageorgiou et al., 2008; Papageorgiou et al., 1991) they did not show any significant effects on the computed rate value.

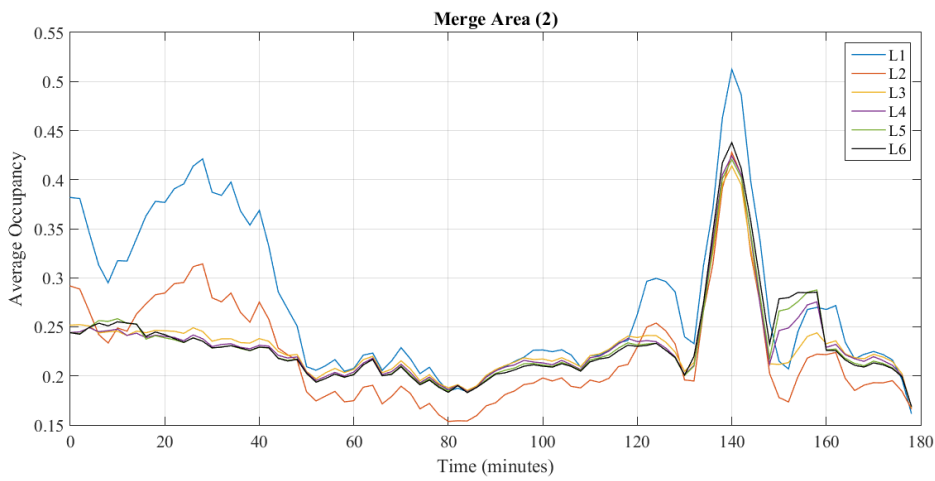
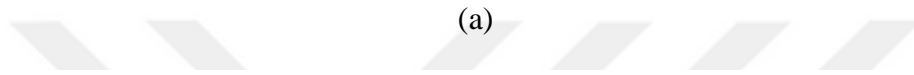
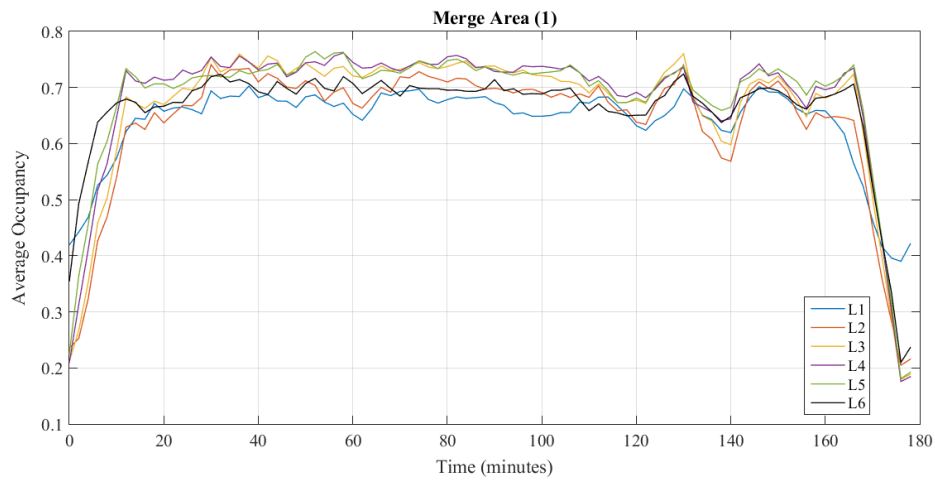
6.4.1 Downstream detector location

The Performance of both ALINEA and PI-ALINEA depends on the early detection of congestion formation, therefore the location of the downstream detector should be located in the area where congestion forms first. In this study, the freeway section has three merge areas wherein along the downstream part of each area is covered by detectors (6 groups for merge area 1, and 2, and 4 groups for merge area 3) locate 50 m apart at locations L1-L6 for the groups 1 and 2, and L1-L4 for the third group. The locations numbering starts from the ramp nose (upper end of the downstream) to the lower end of the downstream.

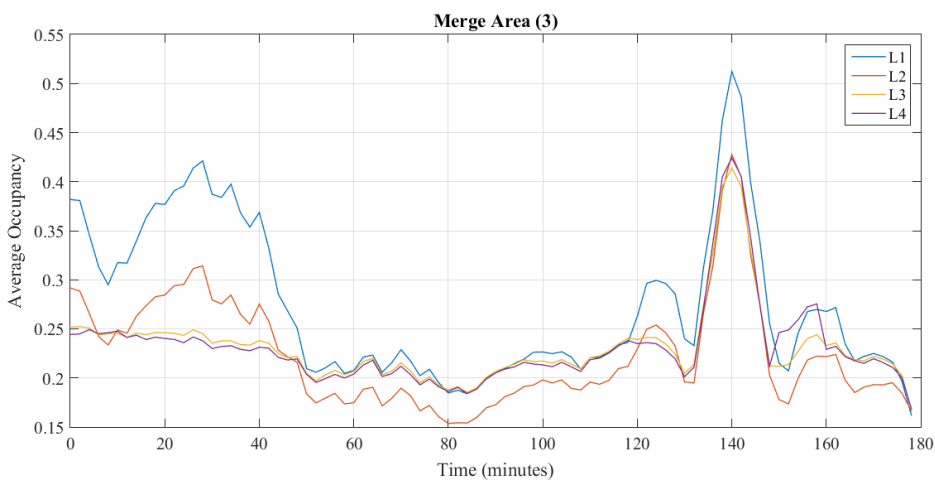
Figure 6.17a, b, and c present the occupancy time-series profiles for all groups at each location in merge areas 1, 2, and 3 respectively. According to Figure 6.17a, the traffic breaks down (occupancy increases sharply) first at L1 and L6 approximately at the same time, while the reason for breaking down at L1 because it is the on-ramp merging point with the mainstream. On the other hand, the traffic breaks down at L6 because at this locations vehicles make a lane-change maneuver in order to reach the off-ramp connector which is only 100 m further than L6. Still, L6 shows higher occupancy values more than L1, for that reason it is chosen as a downstream detector for the first merging area. Referring to Figure 6.17b and c, the traffic breaks down first at L1, the reason is for merging area 2 the relative flow in phase-2 is considerably small so the traffic breaks down because of the merging point with the on-ramp, and it is the same for the merge area-3. Table 6.5 summarized the downstream detectors' locations for each merge area.

Table 6.5: Downstream Detectors Locations.

Merge Area	Detector Location	Distance from the Ramp Nose (m)
1	L6	315
2	L1	50
3	L1	50



(b)



(c)

Figure 6.17: a, b, and c occupancy time-series profile.

6.4.2 Downstream critical occupancy

Ramp metering algorithms try to maintain a desired downstream occupancy (density) by regulating the ramp inflow. This desired occupancy (\hat{O}_{cr}) can be either equal or slightly smaller than occupancy value at the capacity threshold. Therefore, for each group, the occupancy-flow diagram is developed in order to check the occupancy of each downstream area at the capacity threshold. Stands to the reason that the first merging area shows a severe congestion during the proposed time interval (6:30 to 9:30 am), in this subsection \hat{O}_{cr} is only developed for the merge area-1. For other merge areas the same value is considered because they do not show any severe congestion, accordingly, the observed occupancy values are very far from the capacity one.

Figure 6.18 presents a scatter plot of the time occupancy ratio versus volume. The downstream part reaches its maximum volume 2190 (veh/h/lane) at occupancy rate 66.27 (%/lane), after this threshold the traffic flow breaks down reaching the minimum volume 1060 (veh/h/lane). According to the scatter plot, three desired occupancy values can be determined (28, 55, and 66 %) where it is classified in terms the link optimization level into low, medium (equilibrium phase), and highly optimized link respectively. These values are relatively higher than the one mentioned in the literature because there are different detectors' configurations and types.

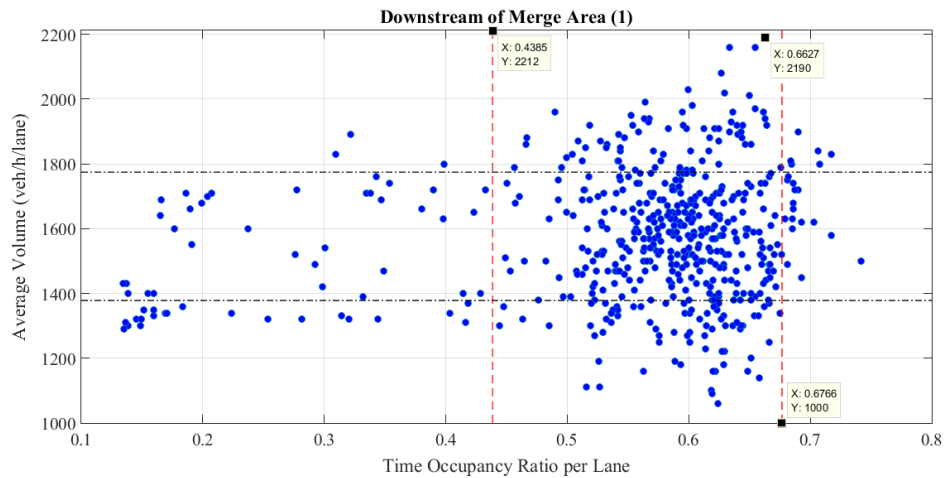


Figure 6.18: Time occupancy ratio vs volume.

6.5 Measures of Effectiveness

The evaluation criteria of a ramp metering algorithm consider the improvement in traffic characteristics and some other parameters, which they can be termed as measures of effectiveness (MOEs). Since the essential purpose of using ramp metering strategies is to improve the freeway mainline stream, especially in merge areas, six MOEs are considered in this study:

- 1) Traffic volume at downstream of the merging area, in other words the discharge rate (DR) of the merging section between the ramp and mainline.
- 2) The average speed of vehicles along the merge area section, where it is supposed to show improvement.
- 3) Total time spent in the network (TTS) presented the traveled vehicle's hours.
- 4) The improvement in the average time occupancy ratio, where the control algorithm task is to maintain the downstream occupancy as much as possible under the critical value.
- 5) Vehicles' emissions including carbon monoxide (CO), volatile organic compounds (VOC), and Nitrogen oxide (NO_x). As the TTT decreases, the emissions have to decrease also since the fuel consumption becomes lesser.
- 6) The reduction in traffic oscillations by evaluating the change in the acceleration rates.

Traffic oscillations are instigated by the instabilities in longitudinal vehicle interaction (car-following) and lane changing maneuvers (LCMs) as a response for congestion phase. (Chen et al., 2014) states that, the prominent trigger of oscillation formation is site-specific, where in some cases the LCMs is prominent, however in the other cases the CF is prominent. For merge areas such as on-ramps, drivers after they complete their merging maneuver, they delay acceleration process or further reduces the speed in order to maintain a higher safety distance from the leader vehicle. Accordingly, Slow-and-Go (SG) disturbance is amplified, leading to traffic oscillations propagation.

6.6 Simulation and Analysis

At each merge area, the above-mentioned MOEs compare the performance of ALINEA and PI-ALINEA in improving the traffic flow characteristics. As an initial

evaluation, the improvement on traffic characteristics downstream of each merge is considered to judge on the performance of ALINEA and PI-ALINEA. The evaluation criteria include the average increase of speed and volume and the average occupancy reduction at the downstream detector. The simulation results are summarized in the Tables 6.6, 6.7, and 6.8.

Table 6.6: Evaluation results (merge area-1).

Merge Area	K_R, K_P	Control Algorithm	\hat{O}_{cr} (%)	Volume (%)	Speed (%)	Occupancy (%)
1	70	ALINEA	28	-4.46	12.9	-14.9
			55	-0.06	4.13	0.07
			65	1.85	2.36	-0.36
		PI-ALINEA	28	-4.22	11.8	-14.3
			55	0.10	7.01	-2.81
			65	1.46	1.58	-0.11
	120	ALINEA	28	-3.85	11.7	-18.2
			55	-2.89	1.47	2.83
			65	-0.37	2.50	2.65
		PI-ALINEA	28	-3.65	16.5	-22.3
			55	-1.44	3.60	0.80
			65	-0.80	1.85	1.93

Table 6.7: Evaluation results (merge area-2).

Merge Area	K_R, K_P	Control Algorithm	\hat{O}_{cr} (%)	Volume (%)	Speed (%)	Occupancy (%)
2	70	ALINEA	28	-3.80	4.42	-11.6
			55	-0.12	4.37	-3.48
			65	1.70	8.54	-3.48
		PI-ALINEA	28	-3.50	3.85	-10.3
			55	0.06	4.80	-7.07
			65	1.26	5.86	-7.96
	120	ALINEA	28	-3.33	7.07	-14.1
			55	-2.50	6.38	-12.6
			65	-0.19	5.80	-9.71
		PI-ALINEA	28	-3.07	5.42	-12.3
			55	-1.19	8.90	-16.8
			65	-0.66	4.73	-8.12

Table 6.8: Evaluation results (merge area-3).

Merge Area	K_R, K_P	Control Algorithm	\hat{O}_{cr} (%)	Volume (%)	Speed (%)	Occupancy (%)
3	70	ALINEA	28	-3.00	3.84	-7.20
			55	-0.71	7.95	-9.72
			65	1.08	8.68	-10.2
		PI-ALINEA	28	-3.40	1.25	-3.90
			55	0.47	7.47	-8.88
			65	1.31	8.89	-10.7
	120	ALINEA	28	-3.02	4.98	-9.06
			55	-2.80	11.3	-16.7
			65	0.02	10.1	-13.4
		PI-ALINEA	28	-3.31	5.82	-5.84
			55	0.42	10.6	-15.2
			65	-1.24	9.01	-11.6

The evaluation criteria take two main faces: the performance of the control algorithm in case of *highly congested sections* and *low congested sections*. Starting with merge area-1 which present highly congested section, for both values of K_R and K_P , PI-ALINEA outperforms ALINEA at low and medium downstream optimization levels by having less volume reduction downstream or higher increase in the downstream discharge. On the other hand, at the high level of optimization ALINEA performs better. As noticed, the volume reduction decreases by increasing \hat{O}_{cr} and the values of K_R and K_P , this is normal since the concept behind a ramp meter is reducing the ramp inflow in order to relief congestion.

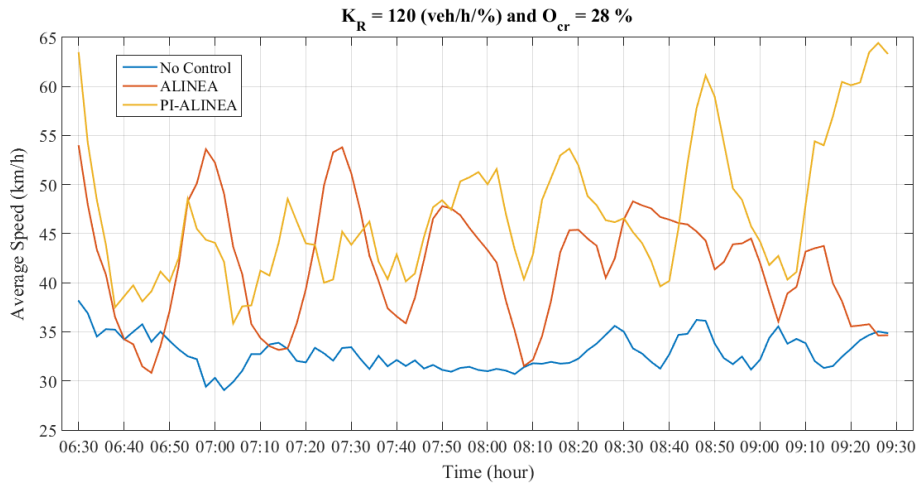
For the speed parameter, it is clear that the speed is improved in all scenarios presenting an inverse relationship with \hat{O}_{cr} . The same as volume, PI-ALINEA has a better impact of the speed increase at low and medium downstream optimization levels, while ALINEA gives better results at the high optimization level.

The downstream occupancy reduction follows the same relationship between speed and \hat{O}_{cr} whereas PI-ALINEA provided the best reduction between all scenarios at K_R and K_P values equal to 120 (veh/h/%). This can be explained as the proportional term compensates the increase or the reduction of volume that results due to the significant difference between the occupancy measures for the current and the previous control cycle.

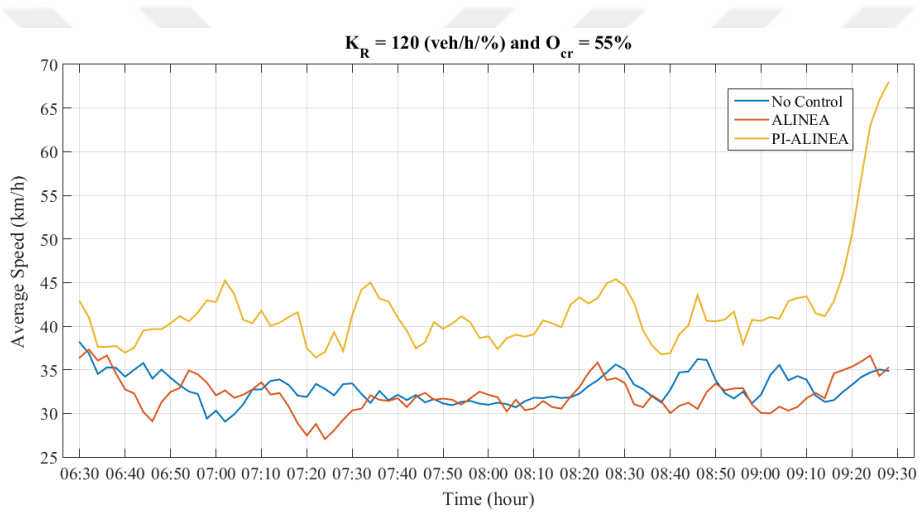
At low congested sections such as merge area 1 and 2, the downstream volume reduction decreases with the increase of $\hat{\theta}_{cr}$ and K_R and K_P , where PI-ALINEA performs better than ALINEA at all the optimization levels. However, for the other measures speed and occupancy, both strategies do not give a defined relationship between these measures and the algorithm's input parameters. For example, at merge area-2 the downstream occupancy reduction increases with increasing $\hat{\theta}_{cr}$, meanwhile, the contrast happens at merge area-3. Accordingly as mentioned in the literature, evaluating a ramp meter algorithm must be conducted on a congested section in order to get reliable results. Still, a noticeable speed increase is instigated by increasing $\hat{\theta}_{cr}$ showing a better performance of ALINEA at low and high optimization levels.

The Figures 6.19a, b, and c, and 6.20a, b, and c present the speed time-series profiles at the downstream of the merge areas 1,2, and 3 respectively. As the figures declare, PI-ALINEA performs better than ALINEA by giving the maximum speed increase in all scenarios at merge areas 1 and 2, while they perform nearly the same at merge area 3.

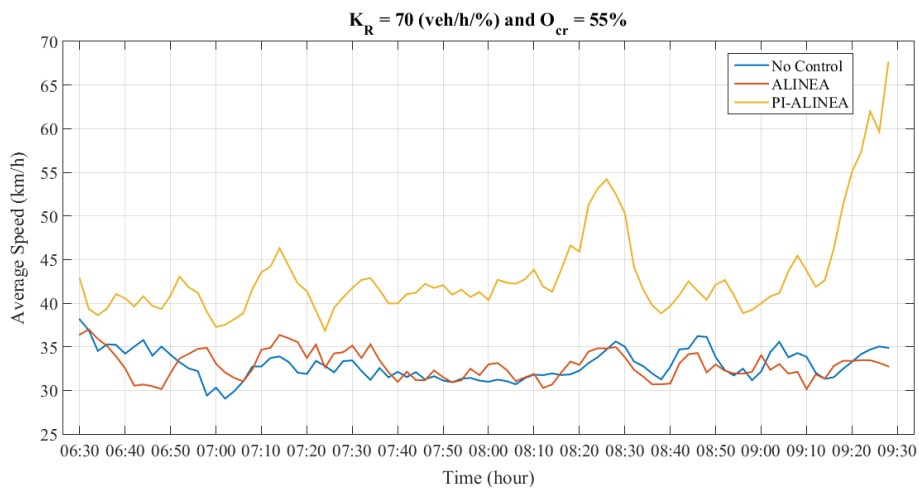
As Figure 6.19a depicts that in congested traffic the speed profile fluctuates frequently, the reason is that when the occupancy reaches the threshold value which is very strict, in this case, the control algorithm reduces the number of entering vehicles resulting in improving the speed on the mainstream. Later, once the ramp is opened, the vehicles' platoons disturb the speed profile by fluctuating up and down. For the same merge area, when the desired occupancy is relatively high the speed profile becomes smoother. Stands to the reason, vehicles in the mainstream already maintain a low speed because the downstream area is highly optimized, see Figures 6.19b and c. For other merge areas, the speed profiles are smooth because there is no a severe congestion exists so vehicles when they merge, do not disturb others' speed, see Figure 6.20a and b for the second merge area, and Figure 6.20c for the third merge area.



(a)

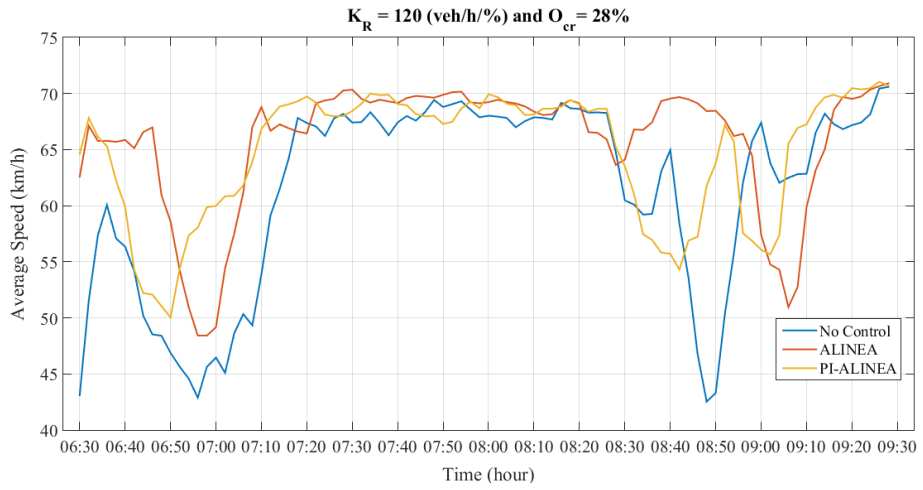


(b)

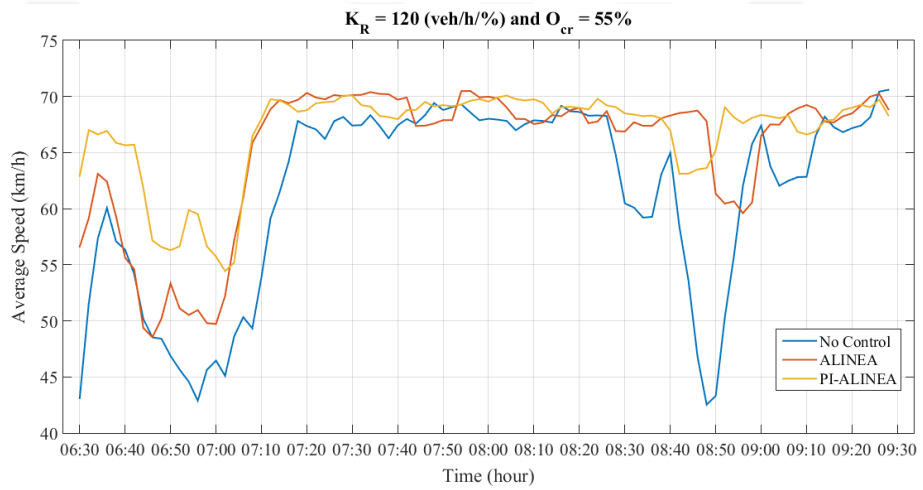


(c)

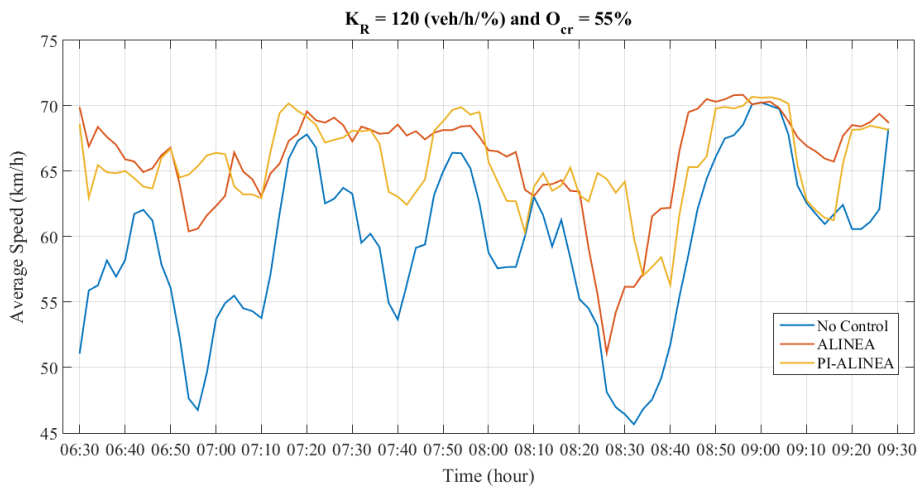
Figure 6.19: a, b, and c Time-series speed profiles at downstream of merge area-1.



(a)



(b)



(c)

Figure 6.20: Time-series speed profiles, a and b at merge-2, and c at merge-3.

Figure 6.21 a, b and c depict the time-series speed profiles at the locations of the RTMS detectors 301, 533, and 534 respectively. These profiles indicate that the improvement in the traffic characteristics in the upstream of the merge area, tells how the control algorithm prevents the speed from breaking down as much as possible, even in severe congestion conditions as in the first merge area. Also, as it is noticed the time-series speed profiles upstream of the merge area have improved in terms of showing no or fewer fluctuations, in other words, the profile is more uniform. The reason is, relieving the congestion downstream of a merge area, prevents the SG wave to propagate backward which can be considered as a good advantage of ramp metering. However, as mentioned before, the reason for this high fluctuation in the time-series speed profiles downstream of the merge area especially at a low level of optimization, vehicles merge to the mainstream in platoons causing sudden drops in the speed.

Figures 6.22, 6.23, and 6.23, a,b, and c present 3-dimensional surface plot for the occupancy distribution along the downstream of each merge area (the best scenario from the occupancy reduction perspective is presented in each case). As the Figures reveal, PI-ALINEA performs better than ALINEA in terms of the occupancy reduction, especially at the first merge area (most congested), with lesser volume reduction and higher speed increase.

Table 6.9 summarizes the reduction in the average TTS for all traveling vehicles along the mainstream line. As it is noticed, PI-ALINEA outperforms ALINEA in all scenarios, especially the TTS is increased in the case of using ALINEA at $K_R = 120$ (veh/h/%) , and critical occupancy 55% and 65%. This increase agrees with the occupancy increase for the same scenarios at merge area 1. By matching the occupancy reduction and the speed increase a proportional relationship can be developed between them and the TTS reduction.

The tables 6.10, 6.11, and 6.12 summarize the total vehicles' emissions, whereas in most of the scenarios both algorithms fail to reduce the emissions, yet they increase them. This increase can be explained by the increase of the traffic volume (some scenarios will be mentioned later) or because of the vehicles' queuing resulted from the ramp closure. Therefore, the scenario provides both volume and emissions reduction should be considered as an optimum scenario, since other parameters speed, occupancy, TTS have improved well in all scenarios.

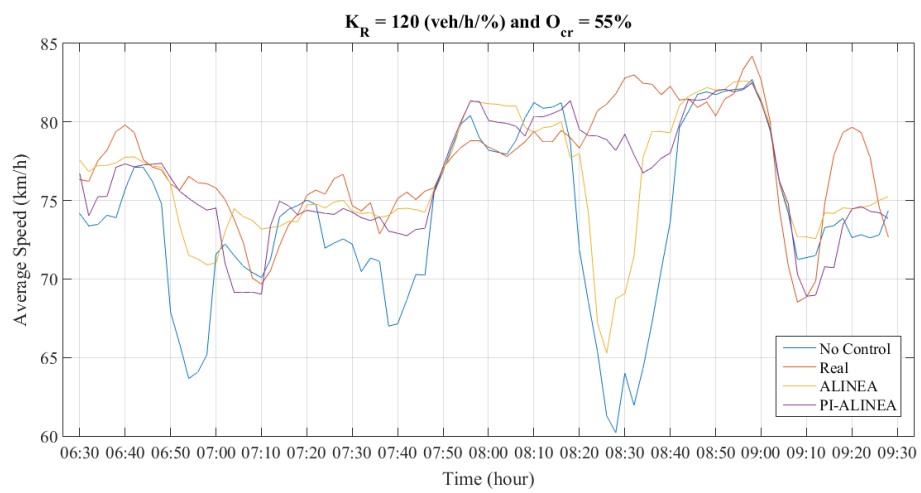
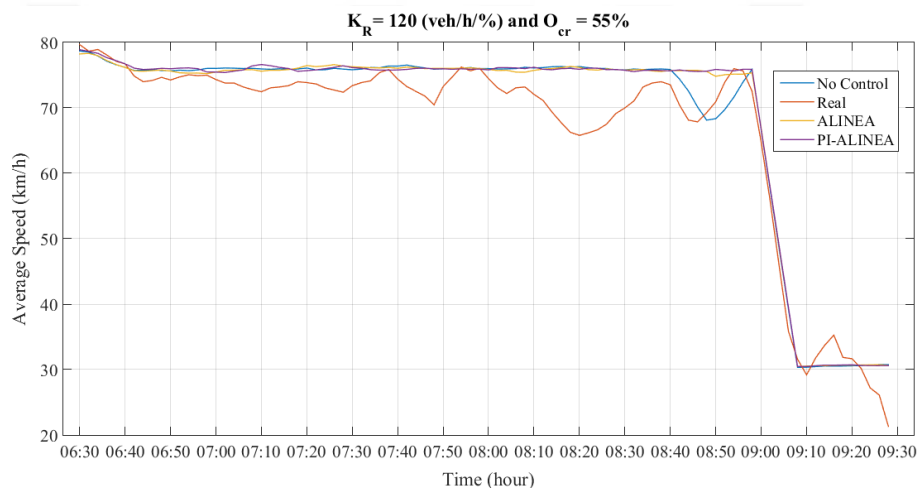
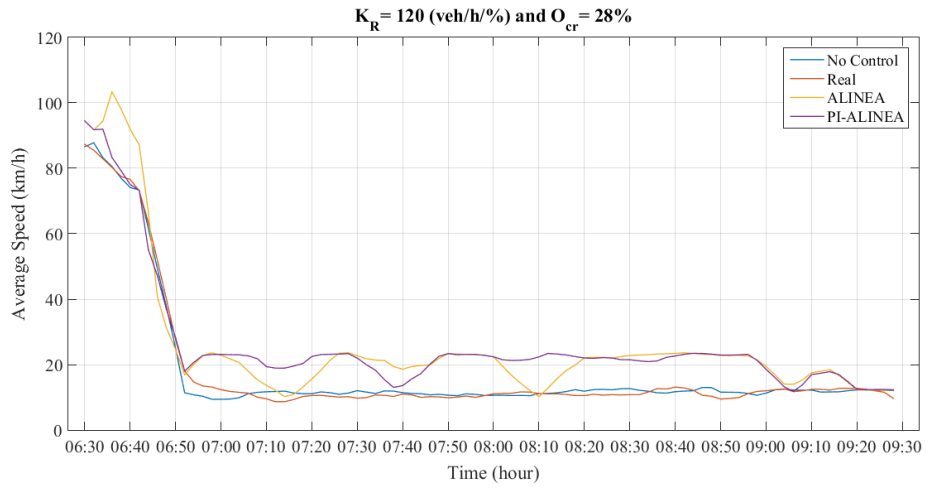
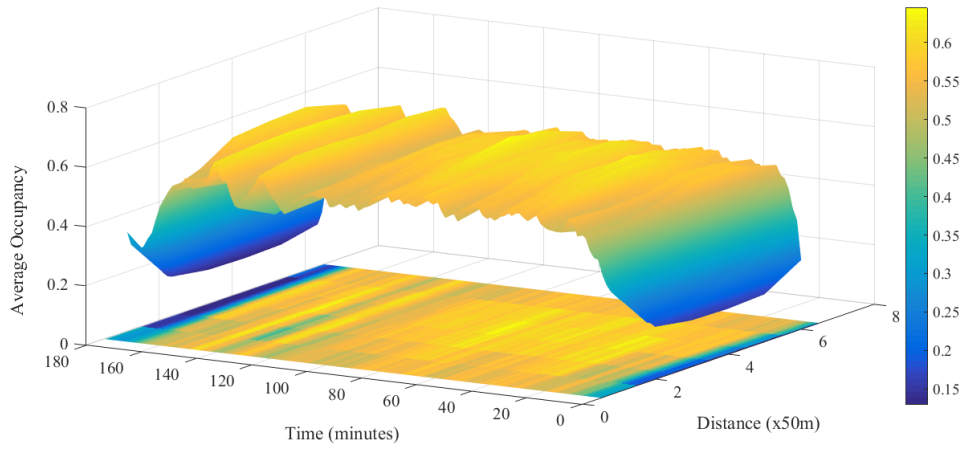
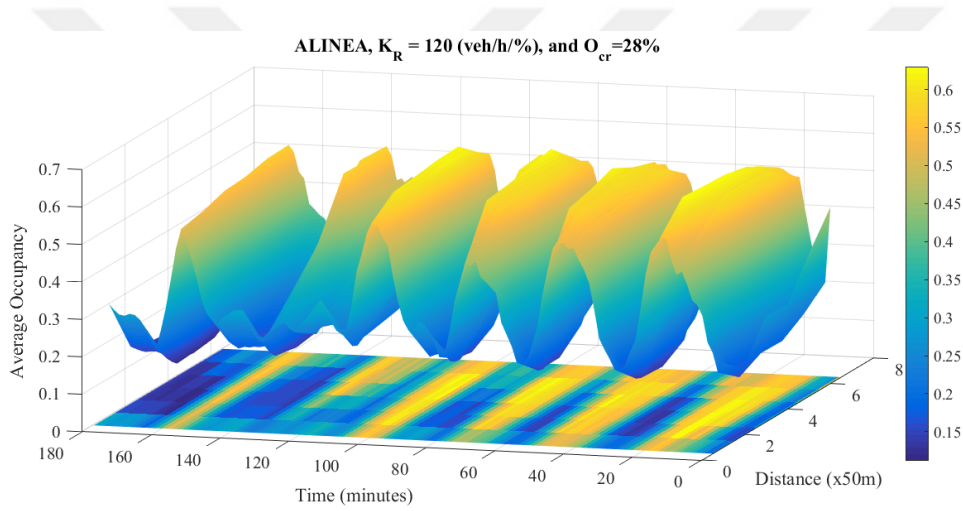


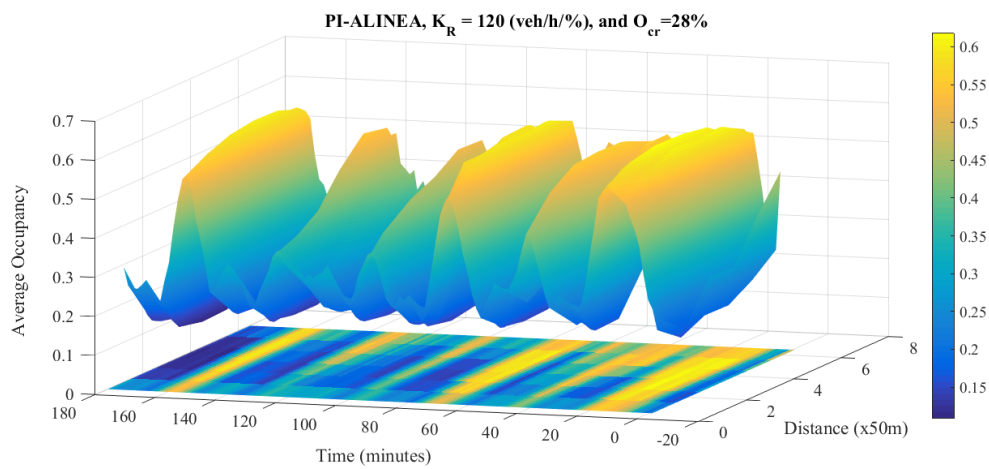
Figure 6.21: a, b, and c time-series speed profiles, at merge 1,2, and 3 respectively.



(a)

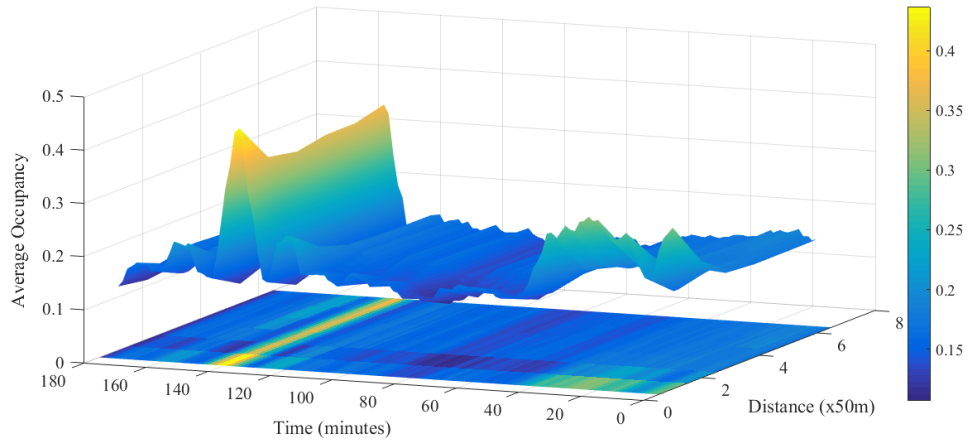


(b)

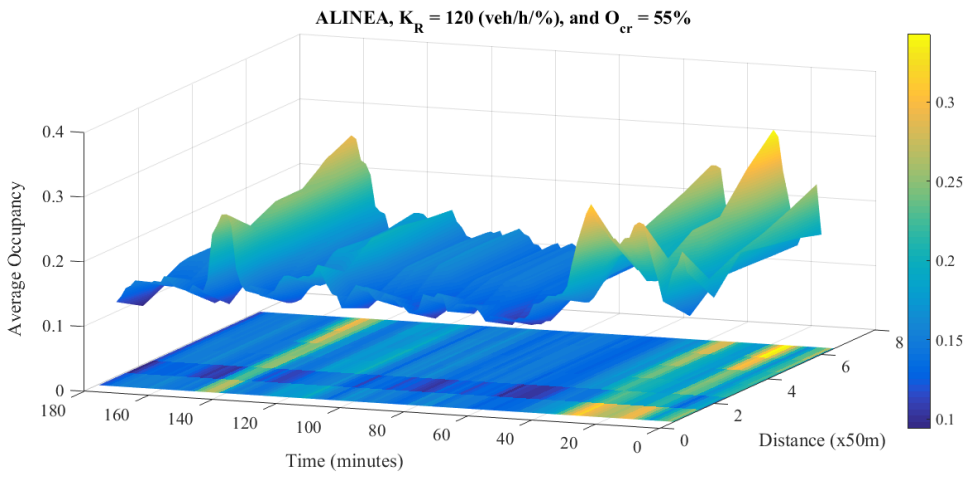


(c)

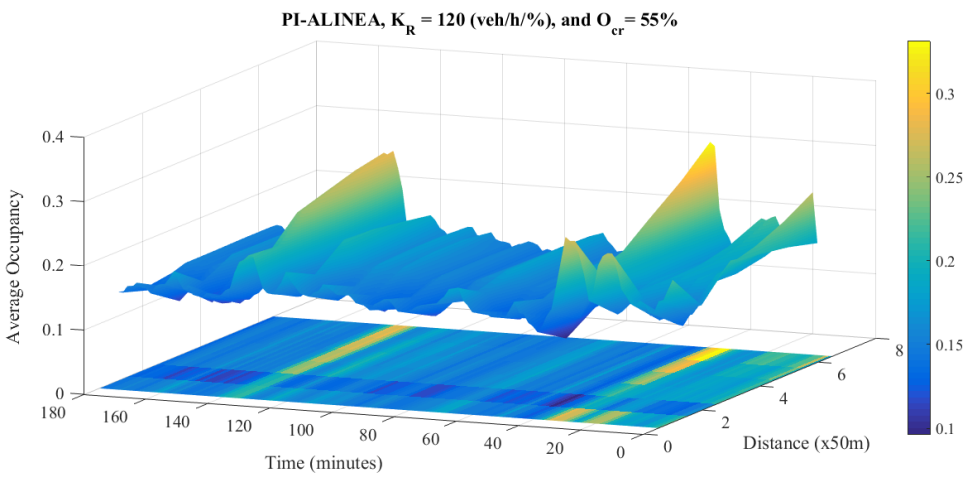
Figure 6.22: a, b, and c the occupancy 3D surface plot along the merge area-1.



(a)

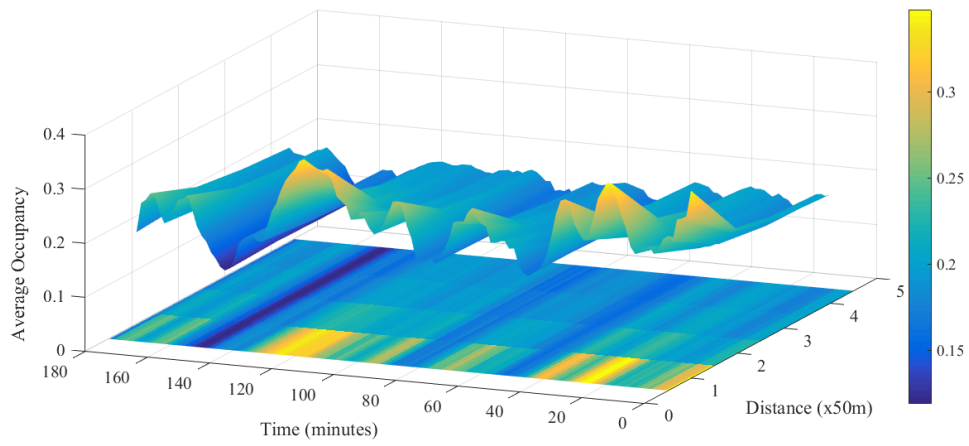


(b)



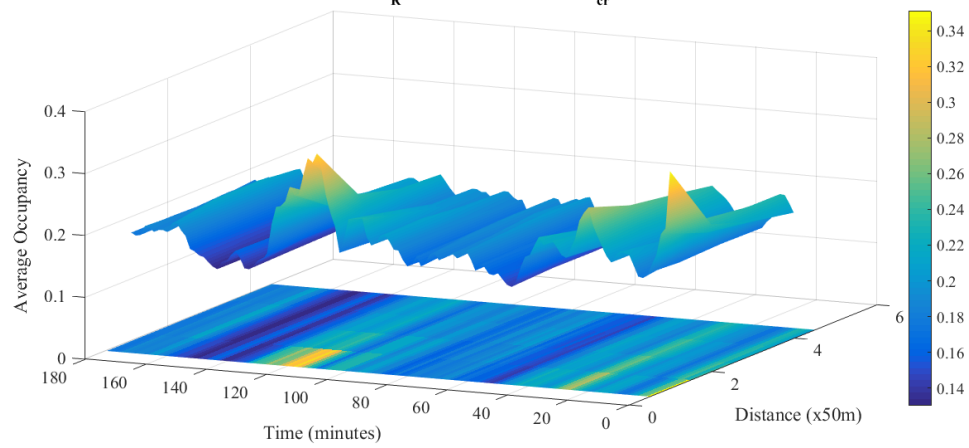
(c)

Figure 6.23: a, b, and c the occupancy 3D surface plot along the merge area-2.



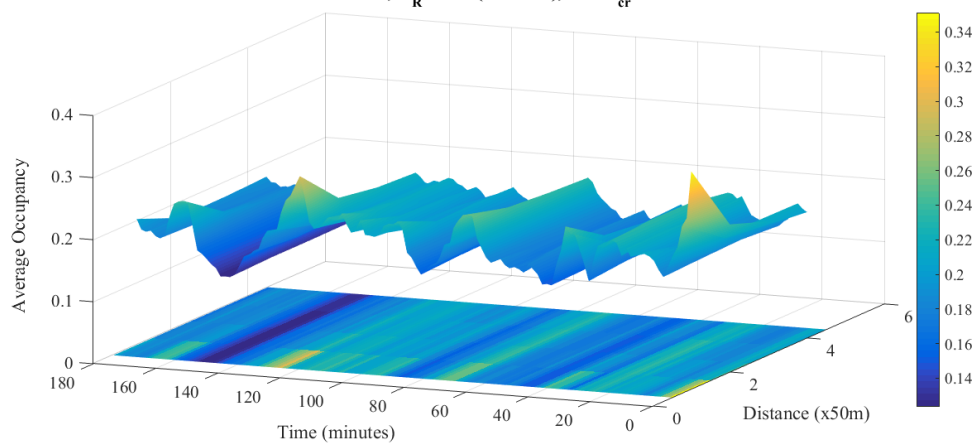
(a)

ALINEA, $K_R = 120$ (veh/h/%) and $O_{cr} = 55\%$



(b)

PI-ALINEA, $K_R = 120$ (veh/h/%) and $O_{cr} = 55\%$



(c)

Figure 6.24: a, b, and c the occupancy 3D surface plot along the merge area-3.

Table 6.9: TTS reduction summary.

	Control Algorithm	$\hat{\theta}_{cr}$ (%)	K_R, K_P	
			70	120
TTS Reduction (%)	ALINEA	28	-26.3	-29.3
		55	-3.96	2.38
		65	-2.67	6.46
	PI-ALINEA	28	-26.5	-31.0
		55	-10.3	-4.29
		65	-7.77	-1.46

Table 6.10: Vehicles' emissions summary (merge area-1).

Merge Area	K_R	$\hat{\theta}_{cr}$ (%)	Vehicle Emissions (CO, VOC, and NO _x) (%)	
			ALINEA	PI-ALINEA
1	70	28	-28.84	4.75
		55	-2.487	6.64
		65	-0.767	9.03
	120	28	-25.69	5.26
		55	8.049	7.33
		65	6.51	8.57

Table 6.11: Vehicles' emissions summary (merge area-2).

Merge Area	K_R	$\hat{\theta}_{cr}$ (%)	Vehicle Emissions (CO, VOC, and NO _x) (%)	
			ALINEA	PI-ALINEA
2	70	28	-6.321	1.362
		55	7.232	1.932
		65	-3.867	1.508
	120	28	-4.590	1.477
		55	-7.139	0.856
		65	-4.024	1.393

Table 6.12: Vehicles' emissions summary (merge area-3).

Merge Area	K_R	$\hat{\theta}_{cr}$ (%)	Vehicle Emissions (CO, VOC, and NO _x) (%)	
			ALINEA	PI-ALINEA
3	70	28	-2.348	5.912
		55	-3.763	-1.207
		65	-2.029	-3.608
	120	28	1.275	10.18
		55	-7.366	-6.303
		65	-5.047	-3.937

The values shaded by gray color refer to the scenarios succeed both volume increase and emission reduction. PI-ALINEA shows an increase in the emissions, especially at the first merge area. This increase is related to one of two reasons, either due to the volume increase, or the proportional term's regulator parameter K_P has to be lower than the assumed value.

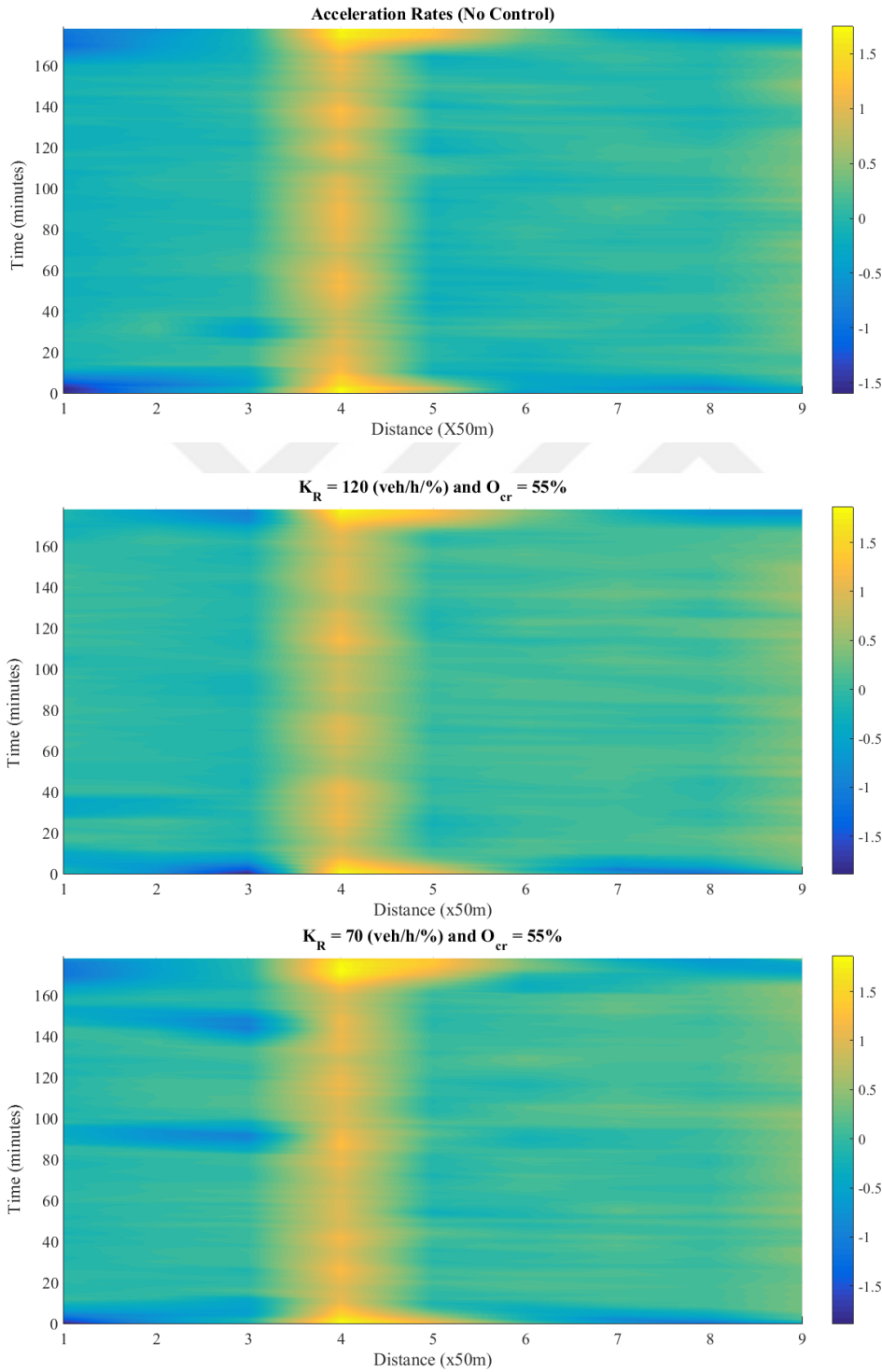


Figure 6.25: Acceleration rates image plots in case of using ALINEA at merge-1.

The Figures 6.25 and 6.26 are image plots presenting the acceleration rates along the first merge area under ALINEA and PI-ALINEA control respectively. The first merge area is chosen because it has the most congestion period leading to high acceleration rates and oscillations.

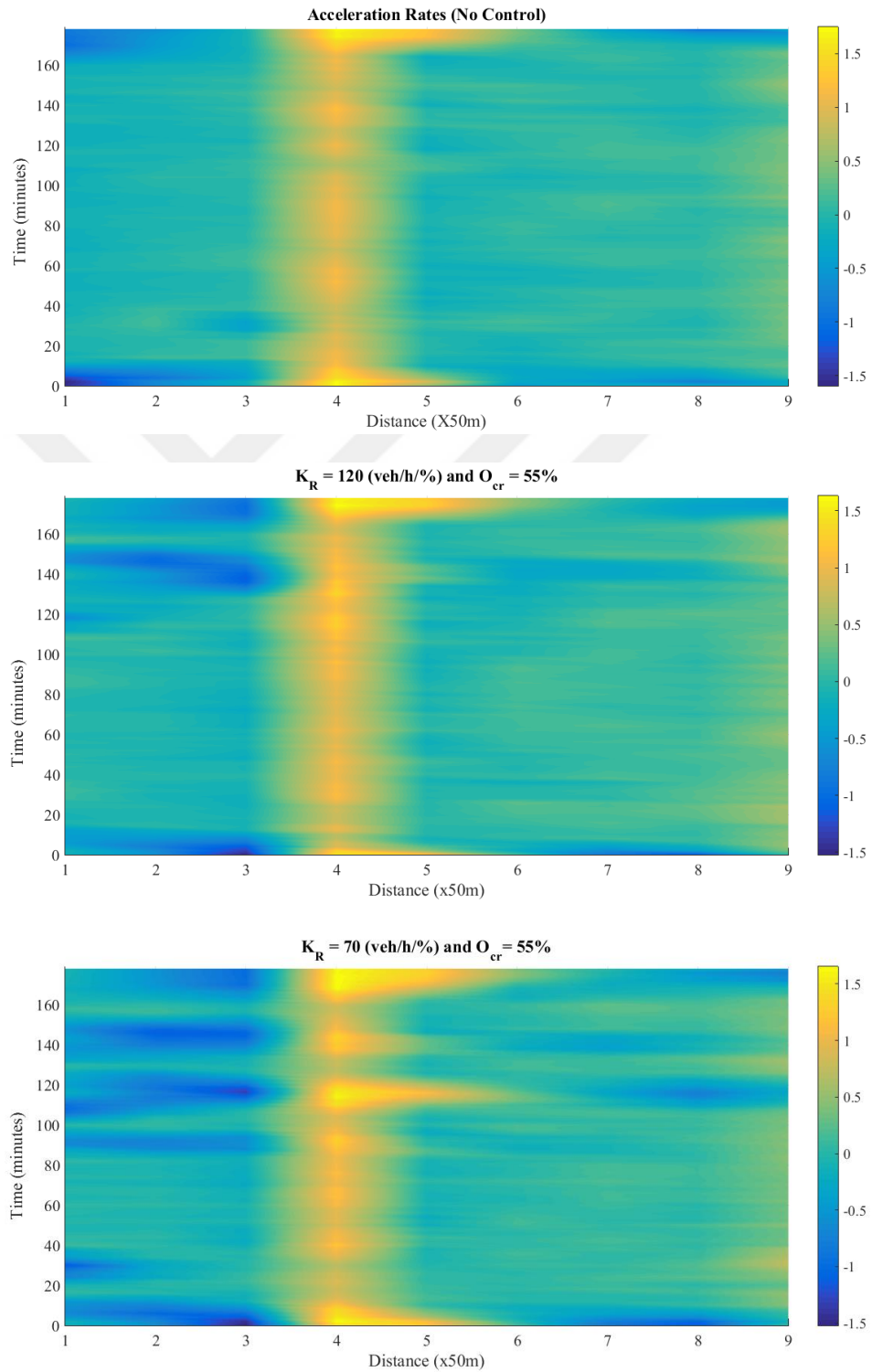


Figure 6.26: Acceleration rates image plots in case of using PI-ALINEA at merge-1.

Table 6.13 summarizes the simulation results of utilizing PI-ALINEA with different values of K_P where it is clear that there is no significant difference occurs by varying the value of K_P .

Table 6.13: Evaluation results (PI-ALINEA).

Merge Area	K_P	K_R	\hat{O}_{cr} (%)	Volume (%)	Speed (%)	Occupancy (%)	TTS Reduction (%)
1	40	70	28	-3.84	11.1	-17.5	-28.7
			55	-1.54	3.46	2.14	4.70
			65	-0.60	1.58	2.40	3.69
		120	28	-4.69	12.9	-20.9	-30.9
			55	-0.13	2.19	-0.42	-6.46
			65	0.66	3.26	-1.28	-1.54
	70	120	28	-4.78	9.19	-17.5	-30.3
			55	-0.45	2.45	-0.67	-7.33
			65	-1.02	2.09	3.78	4.63

7. CONCLUSIONS

The congestion consequences, for example, the increase in travel time and the increase of vehicles' emissions are important challenges requiring a continuous research work to find creative solutions for congestions on freeways. Ramp metering strategies have gained their position as freeway control measures to ensure an effective freeway operation. Along the previous years, various types and configurations of ramp metering strategies have been tested. The performance evaluated by either field implementation assessments, or evaluation of simulation-based studies. The current study presents a simulation-based evaluation study considering the performance of the local ramp metering algorithms ALINEA and PI-ALINEA. The study is conducted on a section of D-100 freeway, Istanbul. The followed methodology considered the calibration of VISSIM, sensitivity analysis of the control algorithms parameters, and a comparative evaluation discussion. The study findings are presented in the following section.

7.1 Findings

The utilization of ALINEA and PI-ALINEA requires the downstream detector to locate at the congestion origin point; also, the control update cycle time should allow the merging vehicles to reach the downstream detector so the traffic characteristic changes are observable.

For highly congested downstream areas, the speed in using both ALINEA and PI-ALINEA has an inverse relationship with the desired downstream occupancy. On the other hand, for low congested downstream areas, the speed increases by increasing the desired downstream occupancy.

Increasing the value of K_R and K_p does not show any significant effect on the speed increase and occupancy reduction considering highly congested areas, contrary, a

significant increase is observed in the low congested down streams especially using PI-ALINEA.

Generally, the downstream discharge decreases once ramp metering is used under a low level of optimization. However, by increasing the desired occupancy, this volume reduction is reduced ending up with volume increase at a high level of optimization. In this term, PI-ALINEA outperformed ALINEA in both cases, either with a lower volume reduction or higher volume increase.

For highly congested downstream areas, the occupancy rate increases by increasing the desired downstream occupancy, however, PI-ALINEA outperformed ALINEA in this case. In contrast, areas with a low congestion show some increase on the occupancy rate by increasing the desired occupancy especially using ALINEA.

For all the above-mentioned terms, PI-ALINEA performs better than ALINEA at low and medium levels optimization, on the other hand at a high level of optimization ALINEA performs better. PI-ALINEA can give better results at the high level of optimization if K_R and K_p are adjusted, however, the parameters are kept the same to show the general performance of both.

Eventually, it is very clear that the simulation results for the low congested areas do not have any specific trend, where it is very difficult to conduct any evaluation process for a ramp metering strategy, thus for a proper evaluation, the medium or highly congested on-ramps should be considered.

PI-ALINEA performed better than ALINEA in terms of improving the TTS reduction since the last one has increased the TTS at K_R equal to 120.

For the acceleration rates, PI-ALINEA also outperforms ALINEA by maintaining a traffic stream along the merge area with relatively maximum acceleration and deceleration rates.

Finally, PI-ALINEA shows a better performance in terms of the speed increase, occupancy decrease, and low downstream volume reduction. Still, for both ALINEA and PI-ALINEA it is very important to chose the proper values of the algorithm's parameters and differentiate between using them in a highly congested and low congested on-ramp.

7.2 Further Research Directions

Typically, the evaluation studies of ramp metering consider changing the control algorithm parameters to get the best performance, however, it should be noticed that the trigger of congestion at merges is related mainly to the driver behavior, where drivers alter the acceleration or even decelerate after joining the mainstream. Therefore, the impact of connected and autonomous vehicles must be considered also in the evaluation of any ramp metering control strategies. Using a single control approach for relieving freeways congestion is not enough, a coordinated system of ramp metering and variable speed limits system and route guidance will give better results.





REFERENCES

- Abdel-Aty, M., Dhindsa, A., and Gayah, V.** (2007). Considering Various ALINEA Ramp Metering Strategies for Crash Risk Mitigation on Freeways under Congested Regime. *Transportation research part C: emerging technologies*, Vol. 15, No. 2, pp. 113-134.
- Abuamer, I. M., Silgu, M. A., and Celikoglu, H. B.** (2016). Micro-Simulation Based Ramp Metering on Istanbul Freeways: An Evaluation Adopting ALINEA. In *Intelligent Transportation Systems (ITSC), 2016 IEEE 19th International Conference on*, pp. 695-700.
- Abuamer, I. M., and Celikoglu, H. B.,** (2017). Local Ramp Metering Strategy ALINEA: Microscopic Simulation Based Evaluation Study on Istanbul Freeways. *Transportation Research Procedia*, Vol. 22, pp. 598-606.
- Alexiadis, V., Gettman, D., and Hranac, R.** (2004). Next Generation Simulation (NGSIM): Identification Prioritization of Core Algorithm Categories. Report No. FHWA-HOP-06-008, *Federal Highway Administration, US Department of Transportation*.
- Athol, P.** (1965). Interdependence of Certain Operational Characteristics within a Moving Traffic Stream. *Highway Research Record*, No. 72, pp. 58-87.
- Banks, J. H.** (1993). Effect of Response Limitations on Traffic-Responsive Ramp Metering. *Transportation Research Record*, Vol. 1394, pp. 17-25.
- Banks, J. H., Amin, M. R., Cassidy, M., and Chung, K.** (2003). Validation of Daganzo's Behavioral Theory of Multi-Lane Traffic Flow: final report. *Institute of Transportation Studies California Partners for Advanced Transit and Highways (PATH)*.
- Bellemans, T., De Schutter, B., and De Moor, B.** (2006). Model Predictive Control for Ramp Metering of Motorway Traffic: A Case Study. *Control Engineering Practice*, Vol. 14, No. 7, pp. 757-767.
- Ben-Akiva, M. E. and Lerman, S. R.** (1985). Discrete Choice Analysis: theory and application to travel demand. Vol. 9. MIT press.
- Bhourri, N., Haj-Salem, H., and Kauppila, J.** (2013). Isolated Versus Coordinated Ramp Metering: Field Evaluation Results of Travel Time Reliability and Traffic Impact. *Transportation Research Part C: Emerging Technologies*, Vol. 28, pp. 155-167.
- Bogenberger, K., and May, A. D.** (1999). Advanced Coordinated Traffic Responsive Ramp Metering Strategies. *California Partners for Advanced Transit and Highways (PATH)*.

- Burley, M., and Gaffney, J.** (2010). Managed Freeways: Freeway Ramp Signals Handbook (No. 02631).
- Bush, B. W.** (2000). An Algorithmic Overview of TRANSIMS. Available at the TRANSIMS homepage <http://transims.tsasa.lanl.gov>.
- Chang, E. C. P., Messer, C. J., and Wang, S. H.** (1994). Development of Freeway Ramp Control Evaluation System. *Transportation Research Board*.
- Chen, D., Ahn, S., Laval, J., and Zheng, Z.** (2014). On the Periodicity of Traffic Oscillations and Capacity Drop: The Role of Driver Characteristics. *Transportation research part B: methodological*, Vol. 59, pp. 117-136.
- Chen, D., & Ahn, S.** (2015). Variable speed limit control for severe non-recurrent freeway bottlenecks. *Transportation Research Part C: Emerging Technologies*, Vol. 51, pp.210-230.
- Chen, O. J., Hotz, A. F. and Ben-Akiva, M. E.** (1997) Development and Evaluation of a Dynamic Traffic Control Model for Real-Time Freeway Operations. *Proceedings of the 8th International Federation of Automatic Control (IFAC) Symposium on Transportation Systems*. Chania, Greece, pp. 1162-1168.
- Chu, L., Liu, H. X., Recker, W., and Zhang, H. M.** (2004). Performance Evaluation of Adaptive Ramp-Metering Algorithms Using Microscopic Traffic Simulation Model. *Journal of Transportation Engineering*, Vol. 130, No. 3, pp. 330-338.
- Chu, L., Recker, W., and Yu, G.** (2009). Integrated Ramp Metering Design and Evaluation Platform with Paramics. *California Path Research Report, Institute of Transportation Studies*, University of California, Berkeley.
- Ciarallo, F. W., and Mirchandani, P. B.** (2002). RHODES-ITMS-MILOS: Ramp Metering System Test (No. FHWA-AZ02-481,). *Arizona Department of Transportation*.
- Daganzo, C. F.** (2002). A behavioral Theory of Multi-Lane Traffic Flow Part II: Merges and the Onset of Congestion. *Transportation Research Part B: Methodological*, Vol. 36, No. 2, pp. 159-169.
- Demiral, C., and Celikoglu, H. B.** (2011). Application of ALINEA Ramp Control Algorithm to Freeway Traffic Flow on Approaches to Bosphorus Strait Crossing Bridges. *Procedia-Social and Behavioral Sciences*, Vol. 20, pp. 364-371.
- Elefteriadou, L., Roess, R. P., and McShane, W. R.** (1995). Probabilistic Nature Of Breakdown at Freeway Merge Junctions. *Transportation Research Record*, No. 1484, pp. 80-89.
- Fellendorf, M., and Vortisch, P.** (2001). Validation of the Microscopic Traffic Flow Model VISSIM in Different Real-World Situations. *In transportation research board 80th annual meeting*.
- Frejo, J. R. D., Núñez, A., De Schutter, B., & Camacho, E. F.** (2014). Hybrid model predictive control for freeway traffic using discrete speed limit signals. *Transportation Research Part C: Emerging Technologies*, Vol. 146, pp.309-325.

- Garber, N. J., and Hoel, L. A.** (2014). Traffic and Highway Engineering. Cengage Learning.
- Gawron, C.** (1999). Simulation-Based Traffic Assignment: Computing User Equilibria in Large Street Networks (*Doctoral dissertation*).
- Ghods, A. H., Fu, L., and Rahimi-Kian, A.** (2010). An Efficient Optimization Approach to Real-Time Coordinated and Integrated Freeway Traffic Control. *IEEE Transactions on Intelligent Transportation Systems*, Vol. 11, No. 4, pp. 873-884.
- Greenshields, B. D.** (1935). A Study of Traffic Capacity. *Highway Research Board Proceedings*, No. 14, pp. 448-477.
- Hadj-Salem H., Davée M., Blosseville M., and Papageorgiou M.** (1988). ALINEA: Un Outil de Regulation d'Accès Isolé sur Autoroute. Report INRETS 80. Arcueil, France.
- Hegyi, A., De Schutter, B., and Hellendoorn, J.** (2005). Optimal Coordination of Variable Speed Limits to Suppress Shock Waves. *IEEE Transactions on intelligent transportation systems*, Vol. 6, No. 1, pp. 102-112.
- Hoogendoorn, S. P. and Bovy, P. H.** (2001). State-of-the-art of Vehicular Traffic Flow Modelling. *Special Issue on Road Traffic Modelling and Control of the Journal of Systems and Control Engineering*, Vol. 215, No.4, pp. 283-303.
- Ioannou, Petros A., and Jing Sun** (2012). Robust Adaptive Control. Courier Corporation.
- ITS International** (1997). Ramp up the Volume. November/December, pp. 39-41.
- Jacobson, L., Henry, K., and Mehyar, O.** (1989) Real-time Metering Algorithm for Centralized Control. *Transportation Research Record*, Vol. 1232, Transportation Research Board, National Research Council, Washington, DC, pp. 17-26.
- Jayakrishnan, R., Mahmassani, H. S., and Hu, T. Y.** (1994). An Evaluation Tool for Advanced Traffic Information and Management Systems in Urban Networks. *Transportation Research Part C: Emerging Technologies*, Vol. 2, No. 3, pp.129-147.
- Jillella, S.** (2001). A Comparative Study of Weaving Sections in TRANSIMS and Highway Capacity Manual. (*PhD dissertation, Virginia Tech*).
- Kerner, B. S.** (2007). Control of Spatiotemporal Congested Traffic Patterns at Highway Bottlenecks. *IEEE Transactions on intelligent transportation systems*, Vol. 8, No. 2, pp. 308-320.
- Kesting, A., and Treiber, M.** (2013). Traffic Flow Dynamics: Data, Models and Simulation.
- Khondaker, B., & Kattan, L.** (2015). Variable speed limit: A microscopic analysis in a connected vehicle environment. *Transportation Research Part C: Emerging Technologies*, Vol. 58, pp. 146-159.
- Klijnhout, J. J.** (1985). Motorways and Urban Networks. *Traffic Engineering and Control*, Vol. 26, No. 4, pp. 205-209.

- Koble, H. M., and Samant, V. S.** (1980). Control Strategies in Response to Freeway Incidents, Vol. 4. Federal Highway Administration, Offices of Research & Development, Traffic Systems Division.
- Kosmatopoulos, E., Papageorgiou, M., Manolis, D., Hayden, J., Higginson, R., McCabe, K., and Rayman, N.** (2006). Real-Time Estimation of Critical Occupancy for Maximum Motorway Throughput. *Transportation Research Record: Journal of the Transportation Research Board*, Vol.1959, pp. 65-76.
- Kwon, E., Nanduri, S., Lau, R., and Aswegan, J.** (2001). Comparative Analysis of Operational Algorithms for Coordinated Ramp Metering. *Transportation Research Record: Journal of the Transportation Research Board*, Vol. 1748, pp. 144-152.
- Laval, J. A. and Daganzo, C. F.** (2006). Lane Changing in Traffic Stream. *Transportation Research Part B: Methodological*, Vol. 40, No. 3, pp. 251-264.
- Lenz, H., Sollacher, R., and Lang, M.** (2001). Standing Waves and the Influence of Speed Limits. In Control Conference (ECC), European, IEEE, pp. 1228-1232.
- Leonard, D. R., Gower, P., and Taylor, N. B.** (1989). CONTRAM: Structure of the Model. Research report-Transport and Road Research Laboratory, (178).
- Lighthill, M. J. and Whitham, G. B.** (1955). On Kinematic Waves: II. A Theory of Traffic Flow on Long Crowded Roads. *In Proceedings of the Royal Society of London A: Mathematical, Physical and Engineering Sciences*, No. 1178, Vol. 229, pp. 317-345.
- Lorenz, M., and Elefteriadou, L.** (2001). Defining Freeway Capacity as Function of Breakdown Probability. *Transportation Research Record: Journal of the Transportation Research Board*, No. 1776, pp. 43-51.
- Lyles, R. W., Taylor, W. C., Lavansiri, D., and Grossklaus, J.** (2004). A Field Test and Evaluation of Variable Speed Limits in Work Zones. *In Transportation Research Board Annual Meeting (CD-ROM)*, Washington, DC.
- Mahut, M.** (2001). A multi-lane extension of the Space-Time Queue Model of Traffic Dynamics. TRISTAN IV, Azores Islands.
- Masher, D. P., Ross, D. W., Wong, P. J., Tuan, P. L., Zeidler, H. M., and Petracek, S.** (1975). Guidelines for Design and Operation of Ramp Control Systems.
- Mauch, M. and Cassidy, M. J.** (2002). Freeway Traffic Oscillations: Observations and Predictions. *Proceedings of the 15th International Symposium on Transportation and Traffic Theory*, Elsevier Science Ltd., Adelaide, Australia, pp. 653-673.
- May Jr, A. D., Athol, P., Parker, W., and Rudden, J. B.** (1963). Development and Evaluation of Congress Street Expressway Pilot Detection System. *Highway Research Record*, No 21, pp. 48-70.

- May, A. D.** (1990). *Traffic Flow Fundamentals*. Englewood Cliffs, NJ: Prentice Hall.
- Meldrum, D. R., and Taylor, C. E.** (1995). Freeway Traffic Data Prediction Using Artificial Neural Networks and Development of a Fuzzy Logic Ramp Metering Algorithm. Final Technical Report (No. Wa-Rd 365.1).
- Monsere, C. M., Bertini, R. L., Ahn, S., and Eshel, O.** (2008). Using Archived Its Data To Measure The Operational Benefits Of A System-Wide Adaptive Ramp Metering System.
- Moscowitz, K.** (1973). Motorway Surveillance and Control. *Traffic Engineering and Control*, Vol. 41, No. 1, pp. 526-528.
- Nagel, K. and Schreckenberg, M.** (1992). A Cellular Automaton Model for Freeway Traffic. *Journal de physique I*, Vol. 2, No 12, pp. 2221-2229.
- National Research Council (US)** (1998). Transportation Research Board. Committee for Guidance on Setting, and Enforcing Speed Limits. Managing speed: review of current practice for setting and enforcing speed limits. Vol. 254. *Transportation Research Board*.
- Newman, L., Dunnet, A., and Meis, G. J.** (1969). Freeway Ramp Control. What it can and Cannot Do. *Traffic Engineering*, Vol. 39, pp. 14-21.
- Oh, H., and Sisiopiku, V. P.** (2001). A Modified ALINEA Ramp Metering Model. *Transportation Research Board 80th Annual Meeting 01-3096*, National Research Council, Washington, DC.
- Owens, D., and Schonfield, M. J.** (1988). Access Control on the M6 Motorway: Evaluation of Britain's First Ramp Metering Scheme. *Traffic engineering and control*, Vol. 29, No. 12, pp.616-623.
- Papageorgiou, M.** (1980). A New Approach to Time-Of-Day Control Based on a Dynamic Freeway Traffic Model. *Transportation Research Part B: Methodological*, Vol. 14, No. 4, pp. 349-360.
- Papageorgiou, M.** (1983). Application of Automatic Control Concepts to Traffic Flow Modeling and Control. New York.
- Papageorgiou, M.** (1990). Dynamic Modeling, Assignment, and Route Guidance in Traffic Networks. *Transportation Research Part B: Methodological*, Vol. 24, No. 6, pp. 471-495.
- Papageorgiou, M., Blosseville, J. M., & Haj-Salem, H.** (1990). Modelling and Real-Time Control of Traffic Flow on the Southern Part of Boulevard Périphérique in Paris: Part II: Coordinated on-ramp metering. *Transportation Research Part A: General*, Vol. 24, No. 5, pp. 361-370.
- Papageorgiou, M., Hadj-Salem, H., and Blosseville, J. M.** (1991). ALINEA: A Local Feedback Control Law for On-Ramp Metering. *Transportation Research Record*, Vol.1320, No.1, pp. 58-67.
- Papageorgiou, M., Hadj-Salem, H., and Middelham, F.** (1997). ALINEA Local Ramp Metering: Summary of Field Results. *Transportation Research Record: Journal of the Transportation Research Board*, Vol. 1603, pp. 90-98.

- Papageorgiou, M., Kosmatopoulos, E., Papamichail, I., and Wang, Y.** (2008). A Misapplication of the Local Ramp Metering Strategy ALINEA. *IEEE Transactions on intelligent transportation systems*, Vol. 9, No. 2, pp. 360-365.
- Papamichail, I. and Papageorgiou, M.** (2008). Traffic-responsive Linked Ramp-Metering Control. *IEEE Transactions on Intelligent Transportation Systems*, Vol. 9, No. 1, pp. 111–121.
- Papamichail, I., Papageorgiou, M., Vong, V., and Gaffney, J.** (2010). Heuristic Ramp-Metering Coordination Strategy Implemented at Monash Freeway, Australia. *Transportation Research Record: Journal of the Transportation Research Board*, Vol. 2178, pp. 10-20.
- Pasquale, C., Sacone, S., Siri, S., & De Schutter, B.** (2016). A multi-class ramp metering and routing control scheme to reduce congestion and traffic emissions in freeway networks. *IFAC-Papers OnLine*, Vol. 49, No. 3, pp.329-334.
- Pipes L. A.** (1953). An operational Analysis of Traffic Dynamics. *Journal of Applied Physics*, Vol 24, No. 3, pp. 274-281.
- Poole, A., & Kotsialos, A.** (2016). Traffic Flow Model Validation Using METANET, ADOL-C and RPROP. *IFAC-PapersOnLine*, Vol. 49, No. 3, pp. 291-296.
- PTV, A.** (2018). VISSIM 8.00 User Manual. Karlsruhe, Germany.
- R Dorf, Richard C., and Robert H. Bishop** (1998). Modern Control Systems.
- Reuschel, A.** (1950). Vehicle Movements in a Platoon. *Oesterreichisches Ingenieur-Archiv*, No. 4, pp. 193-215.
- Richards, P. I.** (1956). Shockwaves on the Highway. *Operations Research*, Vol. 4, No. 1, pp. 42-51.
- Rompis, S. Y., Habtemichael, F. G., and Cetin, M.** (2014). A Methodology for Calibrating Microscopic Simulation for Modeling Traffic Flow under Incidents. *In Intelligent Transportation Systems (ITSC), 2014 IEEE 17th International Conference on*, pp. 3161-3166.
- Roncoli, C., Papamichail, I., & Papageorgiou, M.** (2016). Hierarchical model predictive control for multi-lane motorways in presence of Vehicle Automation and Communication Systems. *Transportation Research Part C: Emerging Technologies*, Vol. 62, pp. 117-132.
- Rrecaj, A. A., and Bombol, K. M.** (2015). Calibration and Validation of the VISSIM Parameters-State of the Art. *TEM JOURNAL-TECHNOLOGY EDUCATION MANAGEMENT INFORMATICS*, Vol. 4, No. 3, pp. 255-269.
- Sadat, M., and Celikoglu, H. B.** (2017). Simulation-based Variable Speed Limit Systems Modelling: An Overview and A Case Study on Istanbul Freeways. *Transportation Research Procedia*, Vol. 22, pp. 607-614.
- Scariza, J. R.** (2003). Evaluation of Coordinated and Local Ramp Metering Algorithms Using Microscopic Traffic Simulation (*Doctoral dissertation*, Massachusetts Institute of Technology).

- Sisiopiku and Virginia P.** (2001). Variable speed control: Technologies and Practice. In *Proceedings of the 11th Annual Meeting of ITS America*, pp. 1-11.
- Smaragdis, E., and Papageorgiou, M.** (2003). Series of New Local Ramp Metering Strategies: Emmanouil Smaragdis and Markos Papageorgiou. *Transportation Research Record: Journal of the Transportation Research Board*, Vol.1856, pp. 74-86.
- Smulders, S.** (1990). Control of Freeway Traffic Flow by Variable Speed Signs. *Transportation Research Part B: Methodological*, Vol. 24, No. 2, pp. 111-132.
- Stephanedes, Y. J., and Chang, K. K.** (1993). Optimal control of Freeway Corridors. *Journal of Transportation Engineering*, Vol. 119, No. 4, pp. 504-514.
- Sukthankar, R., Baluja, S., and Hancock, J.** (1997). Evolving an Intelligent Vehicle for Tactical Reasoning in Traffic. In *Robotics and Automation, Proceedings. 1997 IEEE International Conference*, Vol. 1, pp. 519-524.
- UK Highways Agency** (1996). UK Design Manual for Roads and Bridges.
- Wall, G. T. and Hounsell, N. B.** (2005). Microscopic Modelling of Motorway Diverges. *European Journal of Transport and Infrastructure Research*, Vol. 5, No. 3, pp. 139-158.
- Wang, Y., Kosmatopoulos, E. B., Papageorgiou, M., and Papamichail, I.** (2014). Local Ramp Metering In The Presence of a Distant Downstream Bottleneck: Theoretical Analysis and Simulation Study. *IEEE Transactions on Intelligent Transportation Systems*, Vol. 15, No. 5, pp. 2024-2039.
- Wardrop, J. G.** (1952). Some Theoretical Aspects of Road Traffic Research. *Proceedings of the Institution of Civil Engineers, Part II*, Vol. 1, pp. 325-362.
- Wardrop, J. G., and Charlesworth, G.** (1954). A Method of Estimating Speed and Flow of Traffic from a Moving Vehicle. *Proceedings of the Institution of Civil Engineers, Part II*, Vol. 3, No. 1, pp. 158-171.
- Wattleworth, J. A.** (1963). Peak-period Control of a Freeway System: Some theoretical considerations. Report/Expressway Surveillance Project; 9.
- Wattleworth, J. A.** (1967). Peak Period Analysis and Control of A Freeway System/With Discussion. *Highway Research Record*, No. 157, pp. 1-21.
- Wei, C. H., and Wu, K. Y.** (1996). Applying an Artificial Neural Network Model to Freeway Ramp Metering Control. *Yun shu chi hua= transportation planning journal*. Vol. 25, No. 3, pp. 335-355.
- Wiedemann, R.** (1974). Simulation des Strassenverkehrsflusses.
- Wiedemann, R.** (1991). Modelling of RTI-Elements on Multi-lane Roads. In Drive Conference (1991: Brussels, Belgium) (Vol. 2).

- Wilkie, J. K.** (1997). Using Variable Speed Limit Signs to Mitigate Speed Differentials Upstream of Reduced Flow Locations. No. SWUTC/97/72840-00003-2.
- Wu, J., McDonald, M., and Chatterjee, K.** (2007). A Detailed Evaluation of Ramp Metering Impacts on Driver Behaviour. *Transportation Research Part F: Traffic Psychology and Behaviour*, Vol. 10, No. 1, pp. 61-75.
- Yoshino, T., Sasaki, T., and Hasegawa, T.** (1995). The Traffic-Control System on the Hanshin Expressway. *Interfaces*, Vol. 25, No. 1, pp. 94-108.
- Yuan, Y.** (2008). Coordination of Ramp Metering Control in Motorway Networks. E. TU Delft, Rijkswaterstaat, Editor.
- Zhang, L., and Levinson, D. M.** (2004). Ramp Metering and the Capacity of Active Freeway Bottlenecks.
- Zhang, M., Kim, T., Nie, X., Jin, W., Chu, L., and Recker, W.** (2001). Evaluation of On-Ramp Control Algorithms. California Partners for Advanced Transit and Highways (PATH).
- Zhang, Y., & Ioannou, P. A.** (2016). Environmental Impact of Combined Variable Speed Limit and Lane Change Control: A Comparison of MOVES and CMEM Model. *IFAC-PapersOnLine*, Vol. 49, No. 3, pp. 323-328.



CURRICULUM VITAE

Name Surname: ISMAIL ABUAMER

Place of Birth: Palestine

Date of Birth: 12/ 02/ 1991

E-mail: ismailmaabuamer@itu.edu.tr



EDUCATION:

B.Sc.: 2013, University of Palestine, Palestine, Faculty of Engineering and Urban Planning, Civil Engineering Department

PUBLICATIONS ON THE THESIS:

Abuamer, I. M., Silgu, M. A., and Celikoglu, H. B. (2016). Micro-Simulation Based Ramp Metering on Istanbul Freeways: An Evaluation Adopting ALINEA. In *Intelligent Transportation Systems (ITSC), 2016 IEEE 19th International Conference on*, pp. 695-700.

Abuamer, I. M., and Celikoglu, H. B., (2017). Local Ramp Metering Strategy ALINEA: Microscopic Simulation Based Evaluation Study on Istanbul Freeways. *Transportation Research Procedia*, Vol. 22, pp. 598-606.

Sadat, M., Abuamer, I. M., Silgu, M. A., and Celikoglu, H. B. (2017) Comparative Performance Analysis of Variable Speed Limit Systems Control Methods Using Micro-Simulation: A Case Study on D100 Freeway, Istanbul, *Sixteenth International Conference on Computer Aided Systems Theory*, Las Palmas de Gran Canaria. Canary Islands, Spain, February 19 – February 24, 2017. Article accepted for Springer LNC volumes.